Stability of outfalls during installation

March 1998

E. de Jong

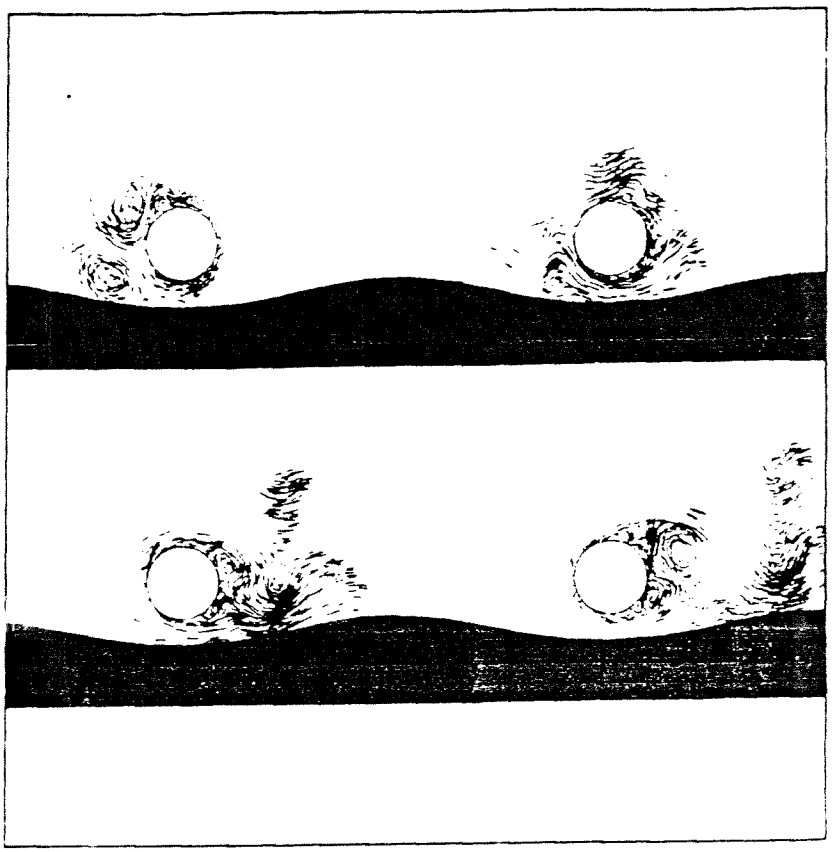

TU Delft
Technische Universiteit Delft

Faculteit der Civiele Techniek

Graduate project

'STABILITY OF OUTFALLS DURING INSTALLATION'

Main report

Cover: Flow around a marine pipeline placed over a trench during a half wave period.
(Fredsøe, J., *Hydrodynamics around cylindrical structures.* World Scientific, 1997)

Delft University of Technology
Faculty of Civil Engineering

Division of Hydraulic and Geotechnical Engineering
Hydraulic and Offshore Engineering Section

March 1998
Erwin de Jong

PREFACE

This main report 'Stability of outfalls during installation' is written within the scope of a graduate project that is part of the engineering exam at Delft University of Technology, Faculty of Civil Engineering, Hydraulic and Offshore Engineering Section.

The graduate subject has been put forward by Van Oord ACZ, Marine and Dredging Contractors, in Gorinchem. Van Oord ACZ is involved in many outfall projects around the world and I would like to thank the company for giving me the opportunity to do a graduate study on a practical problem.

At the beginning of the graduate project, a literature review on the forces on outfalls during installation has taken place. Next, a sensitivity analysis on outfall stability has been carried out. The third and final part of the graduate study was a stability analysis of an outfall under oblique wave and current attack. In the main report, this division is still found in respectively part A, B and C.

Further I owe thanks to Mr. van Elsen and Mr. Lindo of Van Oord ACZ and Mr. Schiereck and Mr. Massie of Delft University of Technology for their support. Finally, I thank Mr. van Gelder of the Section Probabilistic Methods at Delft University of Technology for the use of the computer program BestFit and the adding advises.

Bergambacht, March 1998

Erwin de Jong
402044

Coaches:

prof.ir. K. d'Angremond	TU Delft, graduate professor
ing. L.J. van Elsen	Van Oord ACZ
ir. G.J. Schiereck	TU Delft, Hydraulic and Offshore Engineering Section
W.W. Massie, MSc, P.E.	TU Delft, Offshore Technology Section

CONTENTS

EXECUTIVE SUMMARY

Introduction to outfall construction

Outfall system

An outfall is a structure extending into a body of water for the purpose of discharging sewage, storm runoff, or cooling water. The prime structure in an ocean outfall system is the outfall itself, the pipe that has been laid through surf zones and which extends from shore out a distance of normally 500 to 3000 meters. It is usual to have on shore, at the upstream end of the outfall, a plant that can have various functions. Often this is a wastewater treatment plant; in most cases it is also a pumping plant. At the end of the outfall, the pipe-diameter opening is capped off and the wastewater flow enters the sea through a series of small holes spaced along the sides of the pipe. The length of the outfall through which the effluent leaves is known as the diffuser and is typically a hundred to a thousand meters in length.

The steel for the outfall is usually of relatively high yield stress, and is selected for weldability. Almost all steel pipelines have been joined by full-penetration welds, and are protected from corrosion by inside and outside epoxy coatings. The external epoxy may be further protected from abrasion by a concrete coating. To give stability to the pipeline during installation, the line must have a net negative buoyancy. This is usually supplied by a reinforced concrete weight coating. Figure 1 gives a typical cross-section of an outfall.

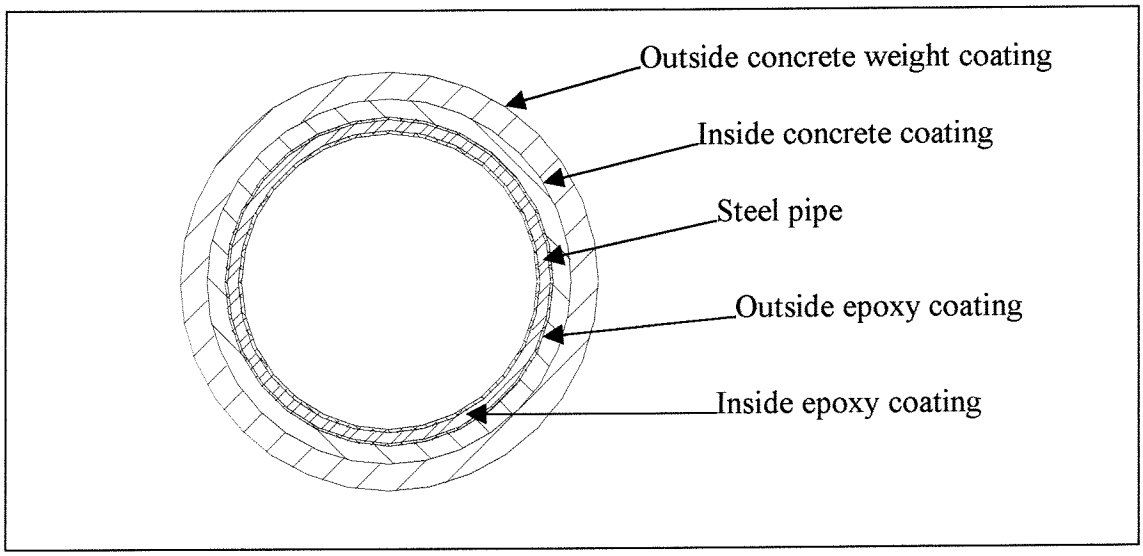

Figure 1 Outfall cross-section

Trenching and burial of outfalls

If it is not practical to apply adequate concrete coating to stabilise a large-diameter outfall on the seabed without incurring installation and manufacturing difficulties, stability can be achieved by trenching. A trench has a two-fold stabilising effect. First, it shelters the pipe, and reduces hydrodynamic forces. Second, a pipeline in a trench has a greatly enhanced lateral resistance, because it can only move by sliding up the side of the trench.

After the outfall has been approved, the trench can be filled back with dredged materials, by dumping crushed rock into the trench, or natural sedimentation. If required, an armour layer can be placed over the trench backfill. This is illustrated in figure 2. The burial of outfalls provides protection against repetitive pounding under wave action and the impact of dropped anchors and to prevent loss of fishing gear by fishermen. Burial also permits the

outfall to be designed with less net weight. The pounding referred to is especially serious in the surf zone, as well as in shallow water where vortex shedding by wave-induced currents can cause alternate raising and lowering of sections of the line. This can lead to fatigue and the rupture and break off of the concrete coating, allowing the line to rise. In the inner portion of the surf zone, direct wave impact and abrasion from moving sand and gravel may aggravate the damage.

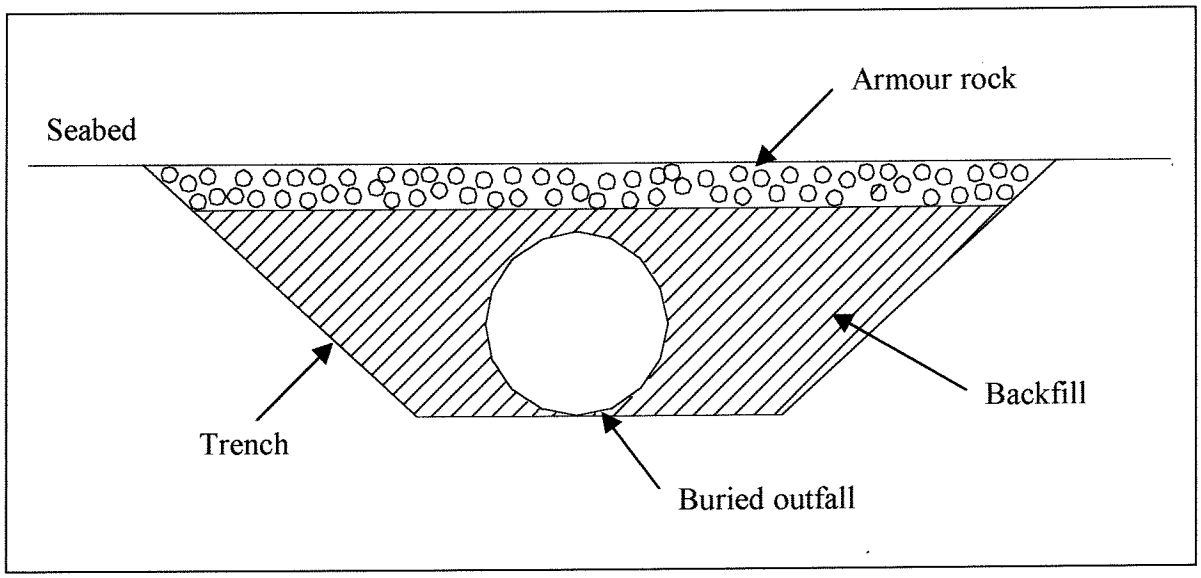

Figure 2 Trenched and buried outfall

Outfall installation with the bottom-pull method

The most commonly employed method of outfall laying is the bottom-pull method. This method has been developed and extensively used to install lines, which extend from shore out a distance of several thousand meters.

The outfall is assembled on shore in parallel segments of 25-300 m in length and a launching ramp with roller supports is constructed, leading out through the inner surf zone. The inner surf zone may be protected by a sheet pile cofferdam so that a trench will stay open. The first segment of the outfall is made up on the launching ramp, with joints welded and coated. Since the ramp is inclined, the outfall is restrained from longitudinal movement by a holdback winch at the landward end. A pull barge with a large winch installed on board, is anchored offshore. When all is ready, the first section of line is pulled out through the surf zone. When its landward end reaches the beach, pulling stops and the next pipeline is rolled sideways into the launching ramp and the joint welded and coated. The next pull is made.

The length of the pull is limited by the winch power, the allowable pipe tension, and the weight of the line. Friction on the launching ramp can be reduced by the use of rollers or small rail cars to support the pipe. The pipe here is in the air, thus having its full weight exerted on the ramp. Once underwater, the empty line has only its buoyant weight. This must be slightly negative which results in friction on the seafloor. It is this friction which the pull barge must overcome.

References

- Palmer, A.C., et al., *Stability of pipelines in trenches*, 1988.
- Gerwick, B.C., *Construction of offshore structures*, 1986.
- Grace, R.A., *Marine outfall systems, planning, design and construction*, 1978.
- Det Norske Veritas, *Rules for classification of fixed offshore installations*, 1996.

Background of the graduate project

Problem description
With increasingly stringent environmental directives, it is important to situate the end of an outfall, the diffuser, further offshore. This is possible by reducing the pipeline weight in order to decrease pull forces. Outfall weight reduction can be achieved by optimising the conservative schematisation of the offshore technology common practice of pipeline stability applied to outfalls. The conservatism is probably caused by underestimating the soil resistance by applying the Coulomb friction model and not taking into account the hydrodynamic force variation along an outfall due to oblique wave attack. This is apparent because up to now there are no problems with stability of outfalls during installation.

Objective
As a graduate project at Delft University of Technology, research has been done into a different, more specific and thus less conservative approach of calculating resultant hydrodynamic forces on outfalls during installation. This approach, which takes the hydrodynamic force variation along an outfall due to oblique wave attack into account, must offer perspectives to the construction of longer outfalls and an improved economic design in general.

Problem restriction
This graduate project concentrates on the most common situation of an outfall built in shallow water, approximately at right angles to the depth contours. Trenching and application of a heavy weight coating have to assure stability during installation. The impact forces on the outfall generated by breaking waves will not be considered because a cofferdam will provide protection within the breaking zone during installation.

Structure of the main report

A literature review on forces on outfalls during installation has been made during the first period of the graduate study and is reported in part A. Part B is a sensitivity analysis of outfall stability. This is a probability study on the extent of influence of the separate hydrodynamic variables in the equilibrium equations of outfall stability. An analysis on outfall stability under oblique wave and current attack can be found in part C.

Every part is preceded by an introduction in which the structure of the separate parts is further stated.

Previous graduate projects

The following graduate projects on pipeline stability and related subjects have been carried out at Delft University of Technology. These linking projects are inventoried to prevent overlap in the present study.

- W.T van Rossum, *Pipeline over rock bottom*, Constructive Hydraulic Engineering. June 1977.
- R. Rijper, *Experimental research on hydrodynamic coefficients and dynamics of a submarine pipeline exited by waves*, Hydraulic Engineering. June 1984.
- M. van Driel, *The behaviour of submarine pipelines in slurry transport*, Offshore Technology/MTI Holland. October 1996.

ABSTRACT

Outfalls are built for the purpose of discharging sewage, storm runoff or cooling water into the sea. During the installation, outfalls are exposed to relatively large hydrodynamic forces compared to their own weight in case of adverse weather or high currents. To resist these forces, a heavy concrete weight coating has to be applied. With increasingly stringent environmental directives, it is important to situate the end of an outfall further offshore. This is possible by optimising the conservative schematisation of the offshore technology common practice of pipeline stability applied to outfalls. This optimisation can lead to a reduction of the outfall weight coating, which offers perspectives to the construction of longer outfalls and an improved economic design in general.

Therefor, research into a less conservative approach of calculating the resultant hydrodynamic forces on outfalls has been carried out as a graduate project at Delft University of Technology. The graduate project concentrates on the most common situation of an outfall built in shallow water, approximately at right angles to the depth contours. Trenching and application of a heavy weight coating have to assure stability during installation. The impact forces on the outfall generated by breaking waves will not be considered.

Hydrodynamic forces acting on outfalls are described with the Morison equations. They are used in offshore pipeline engineering because it is the only reasonable straightforward theoretical model available. When waves and currents are acting simultaneously, the combined effect should be considered. The equations can also be applied to oblique members. Common use is to decompose the undisturbed velocity and acceleration into components normal to the cylinder axis, and then use the Morison equations with normal components of velocity and acceleration.

Wave characteristics, needed to solve the Morison equations, are described with the linear Airy wave theory. Tests indicated that horizontal water particle velocities at the bottom, calculated with this wave theory are in reasonable agreement with the measured values. For a wide variety of locations a power law formula gives a good fit to measured tidal current profiles.

The accuracy of the Morison equations depends on the accuracy of the basic formulation and the hydrodynamic force coefficients. The lack of adequate data on the hydrodynamic loading on a pipeline on the seabed, resulted in several research programs. In order to be able to select the most appropriate hydrodynamic force coefficients for outfall construction, it is recommended to do supplementary research on the backgrounds of the different model test programs.

The geotechnical interaction between an outfall and the seabed is treated as a contact governed by Coulomb friction, although tests have indicated that more resistance is available due to pipe-soil interaction. Therefor, it is recommended to do supplementary research on the geotechnical interaction between outfall and seabed.

Uncertainty analysis offers the designer insight regarding the contribution of each stochastic input parameter to the overall uncertainty of the model output. Such knowledge is essential to identify the important parameters to which more attention should be given, in order to have a better assessment to their values, and accordingly, to reduce the overall uncertainty of the output.

From the sensitivity analysis, it can be concluded that in the case of a moderate current velocity, the hydrodynamic parameter that influences the equilibrium equations of the stability of outfalls most is the wave period. This is especially true for a wave climate that is

characterised by rather high and long waves. In the case of stronger currents, the current velocity and the angle of current attack become more important. Small changes in the angle of wave attack are in any case of little significance. On the other hand, changes in the angle of current attack are of significant importance in the case of high current velocities or small outfall diameters.

A more thorough sensitivity analysis can be executed if the various hydrodynamic force coefficients are taken in consideration. Further, a more advanced computer program, which has the possibility of defining and handling correlation between basic variables is recommended.

A two-dimensional stability analysis takes the most unfavourable combination of drag, lift and inertia forces due to wave and current attack on a segment of an outfall into account. For all phase angles of the wave profile, the hydrodynamic forces acting on an outfall segment are calculated and the matching safety factor is determined. The decisive safety factor is taken as the minimum occurring. The submerged weight of the outfall segment is adjusted until the decisive safety factor meets the requirements. This stability calculation and the resulting weight are performed at several locations along the outfall length.

A three-dimensional stability analysis is taking into account the wave-induced bottom velocity and acceleration variation, due to oblique wave attack, in the direction of the outfall axis along the length of an on this axis projected wave length. By integrating the equations for the drag, lift and inertia forces over a defined part of an outfall at one moment in time, the resultant hydrodynamic forces acting on the considered outfall length and the matching safety factor can be determined. The submerged weight of the defined outfall length is adjusted until the decisive safety factor meets the requirements.

The resultant forces calculated with this three-dimensional method are in the order of 10% lower than if determined with the two-dimensional stability analysis.

When applying the three-dimensional stability analysis, it is recommended to consider the variation of the hydrodynamic forces along the length of an outfall equal to half a projected wave length. Further, the decisive phase angle of the two-dimensional stability analysis has to be taken as the centre of the defined part.

PART A

FORCES ON OUTFALLS DURING INSTALLATION

A literature review

INTRODUCTION

As a preamble and exploration of the graduate project 'Stability of outfalls during installation', a literature review on forces on outfalls during installation has been made during the first period of the graduate study.

For a cost-effective construction of outfalls, an engineer requires a precise knowledge of the forces induced by oscillatory and steady state currents on a cylindrical pipe resting on a plane seabed. Hydraulic institutes have carried out much research to supplement the state of the art information of this subject.[17] The researches mainly deal with the choice of the hydrodynamic coefficients. These coefficients are highly controversial because major investigations indicate different values. A point to note is that the most parameter ranges covered in the tests differ from sea state conditions during outfall installation. Drawback of the field measurements is the wide scatter of the results and so far no conclusive settlement of the hydrodynamic coefficients has been established.

After general information about hydrodynamic aspects in chapter 1, the results of several researches on hydrodynamic coefficients are presented in chapter 2. The model test program conducted by A.C. Palmer and Hydraulic Research Ltd., whose results are used by Van Oord ACZ as a design guide, is described in paragraph 2.2. Chapter 3 presents a different approach concerning the maximum occurring wave forces. Some reflections on the force distribution on an outfall in unsteady flow are presented in chapter 4, while chapter 5 considers the lateral resistance of an outfall. The conclusions and recommendations are presented in chapter 6. Finally, in Appendix I a comparison of hydrodynamic parameters is documented.

LIST OF SYMBOLS

H	wave height
λ	wave length
T	wave period
k	wave number
ω	circular frequency
h	water depth
η	instantaneous elevation of the water surface relative to still water level (SWL)
g	acceleration due to gravity
t	time
x	horizontal co-ordinate
z	vertical co-ordinate
u_x	horizontal water particle velocity
u_z	vertical water particle velocity
a_x	horizontal water particle acceleration
a_z	vertical water particle acceleration
ξ	horizontal water particle displacement
ζ	vertical water particle displacement
θ	angle of wave attack
$u_{c(z)}$	speed of the tidal current at the height z above the seabed
$\bar{u}_c$	depth-averaged speed of the tidal current
$u_{c(0.5D)}$	speed of the tidal current at the height 0.5D above the seabed
$u_{c(y_m)}$	measured tidal current speed at height y_m above the seabed
F_x	horizontal force per unit length of pipeline
F_y	vertical force per unit length of pipeline
F_D	drag force
F_M	inertia force
F_L	lift force
C_D	drag coefficient
C_M	inertia coefficient
C_L	lift coefficient
a	semi-orbit length of the oscillating flow at the bed
a'	relative equivalent amplitude displacement
α	current ratio
ρ	density of water
υ	cinematic water viscosity
D	diameter outfall
V	volume of the pipeline
A	cross-sectional area of the pipeline
W_S	total submerged pipeline weight
y_t	trench depth
α_t	side slope of trench
r_c	Coulomb friction factor
c	undrained shear strength
γ	submerged unit weight of the soil

1 HYDRODYNAMIC ASPECTS

1.1 Wave characteristics

Outfalls are build in shallow water and installed during a wave climate within the operating conditions. With these water depth and wave height conditions, the Stokes 2nd order wave theory is valid for the description of the wave mechanics. This wave theory predicts a wave form that is unsymmetrical about the still water level (SWL) but still symmetrical about the vertical line through the crest and has water particle orbits that are open. It can be shown that, for second-order theories, expressions for wave celerity and wave length are identical to those obtained by linear theory. Therefore, and for the sake of simplicity, the generally most useful theory for describing waves, the linear Airy wave theory, is adopted. Linear theory applies to a wave that is symmetrical about SWL and has water particles that move in closed orbits.[1]

Airy presented a wave theory in which he simplified the wave profile to a linear sinusoidal wave form. His theory provides equations for the most important properties of surface gravity waves, and predicts these properties within useful limits in most practical conditions, even though real water waves are not sinusoidal.[3] His definition sketch of a progressive, oscillatory surface gravity wave is presented in figure 1.1.

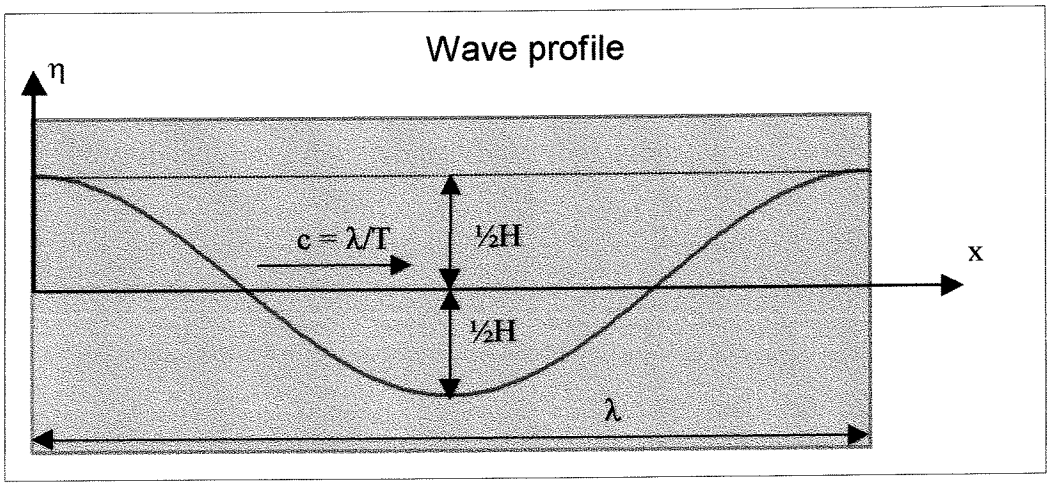

Figure 1.1 Definition sketch of a sinusoidal surface wave

This wave has the following characteristics (first order approximation): [1]

- wave profile:

$$\eta = \frac{H}{2} \cos (kx - \omega t)$$

where:

η	instantaneous elevation of the water surface relative to SWL
H	wave height
k	wave number = $2\pi/\lambda$
λ	wave length
x	horizontal co-ordinate
ω	circular frequency = $2\pi/T$

T wave period
t time

- wave celerity:

$$c = \frac{\lambda}{T} = \frac{\omega}{k} = \frac{gT}{2\pi} \tanh kh$$

where:

g acceleration due to gravity
h water depth

- wave length:

$$\lambda = cT = \frac{gT^2}{2\pi} \tanh kh$$

- instantaneously wave-induced water particle velocity components:

$$u_x = \frac{\omega H}{2} \frac{\cosh k(z+h)}{\sinh kh} \cos(kx - \omega t)$$

$$u_z = \frac{\omega H}{2} \frac{\sinh k(z+h)}{\sinh kh} \sin(kx - \omega t)$$

where:

u_x horizontal water particle velocity
u_z vertical water particle velocity
z vertical co-ordinate measured from the still water level

- instantaneously wave-induced water particle acceleration components:

$$a_x = \frac{\omega^2 H}{2} \frac{\cosh k(z+h)}{\sinh kh} \sin(kx - \omega t)$$

$$a_z = \frac{\omega^2 H}{2} \frac{\sinh k(z+h)}{\sinh kh} \cos(kx - \omega t)$$

where:

a_x horizontal water particle acceleration
a_z vertical water particle acceleration

- instantaneously wave-induced water particle displacement components:

$$\xi = \frac{-H}{2} \frac{\cosh k(z+h)}{\sinh kh} \sin(kx - \omega t)$$

$$\zeta = \frac{H}{2} \frac{\sinh k(z+h)}{\sinh kh} \cos(kx - \omega t)$$

where:

ξ horizontal water particle displacement
ζ vertical water particle displacement

Figure 1.2 shows the relation between the direction of the velocity and the acceleration of water particle at certain phases in the wave period. The water particle displacement is shown in figure 1.3 for a shallow and a deep water wave.

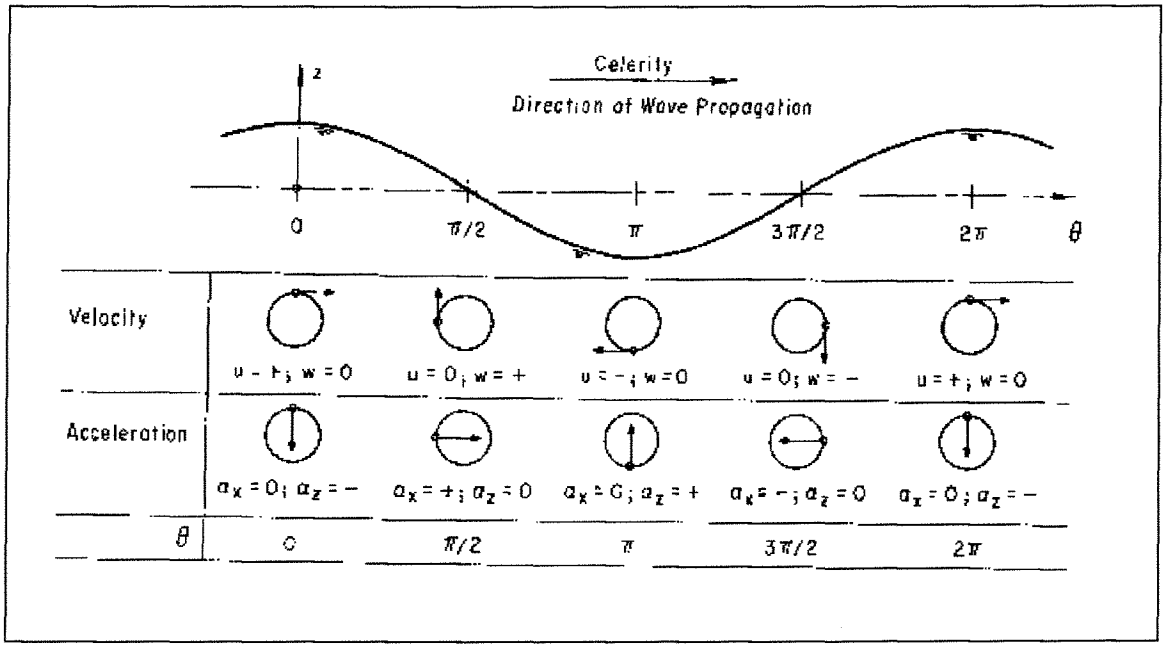

Figure 1.2 Local fluid velocities and accelerations [1]

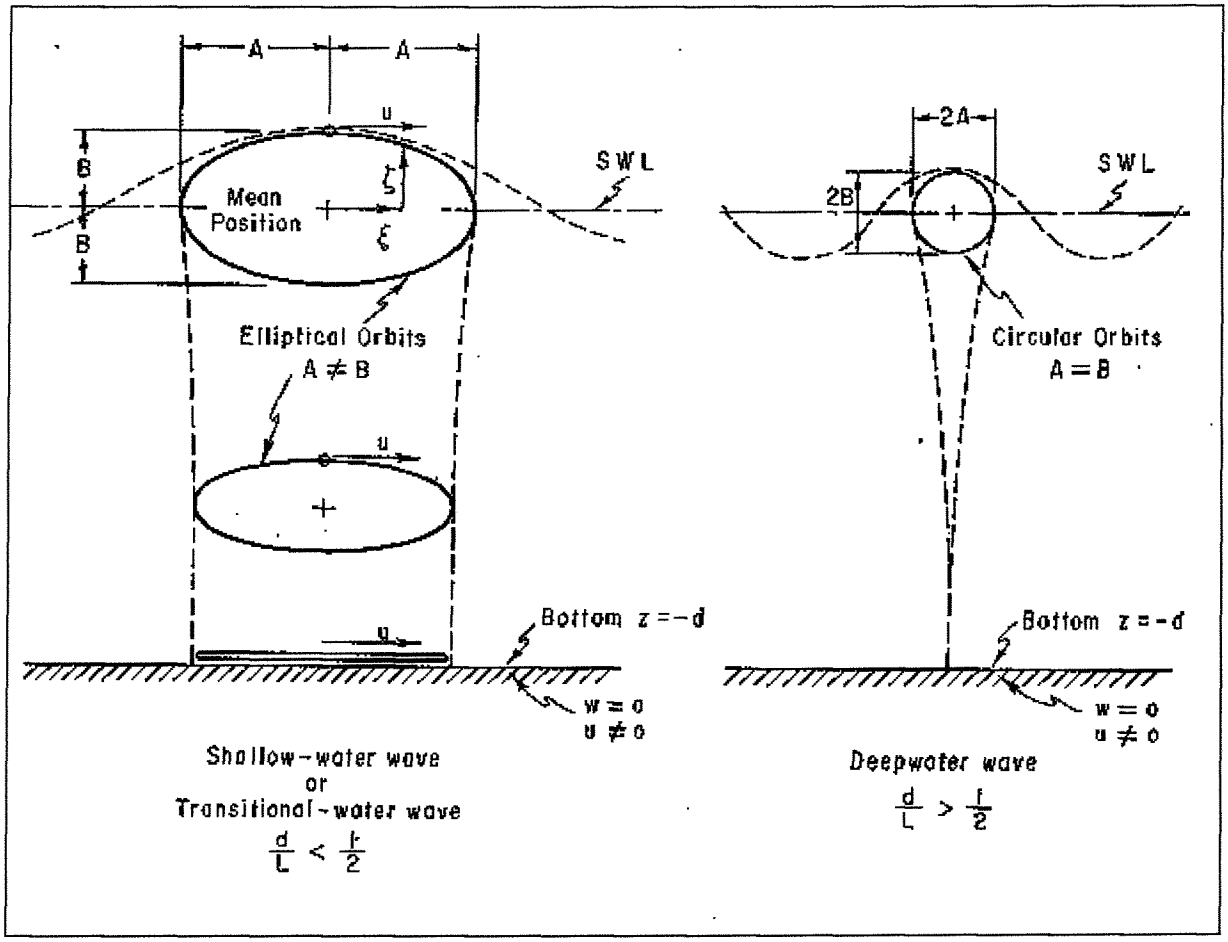

Figure 1.3 Orbital motion under a shallow water wave and a deep water wave [1]

Figure 1.2 indicates that the fluid under the crest moves in the direction of wave propagation and returns during passage of the trough. Linear theory does not predict any mass transport; hence, the sketch shows only an oscillatory fluid motion.[1]

Figure 1.3 shows that in deep water the effect of the waves does not extend down to the bed; in shallow water the water makes an oscillating movement over the entire depth. Near the surface the water particles describe an elliptical path, near the bottom the water particles make an horizontal oscillating movement.[3]

The linear wave theory is not exact, because of the approximation of the boundary condition at the free surface, and the errors become more significant as the water depth increases.[1]

Le Mehaute (1968) has carried out a measurement program in which distributions over depth of horizontal water particle velocities were measured under the crest phase position of fairly high waves in the shallow and transitional depth ranges. For a number of cases the measured water particle velocity distributions were compared to various wave theories. The Stream function theory was included by Dean (1974). The tests indicated that horizontal water particle velocities at the bottom, calculated with the linear wave theory, are in reasonable agreement with the measured values.[6]

1.2 Current characteristics [11]

The quasi-steady current at any location and time is the vector sum of tidal and non-tidal, i.e. residual components. The regular and predictable tidal current is the largest component of the quasi-steady current.[2] The maximum tidal current is associated with the highest or lowest astronomical tide. Residual currents are irregular but at most locations the largest residual to be considered is likely to be the extreme storm surge current. Other residuals include short period currents and long period, or 'mean', currents.

Over most of the water depth, the speed of the tidal current varies by less than ± 25% from the depth-averaged value. For a wide variety of locations the following power law formulae give a good fit to measured tidal current profiles:

$$u_{c(z)} = \left(\frac{z}{0.32\,h}\right)^{\frac{1}{7}} \cdot \bar{u}_c \qquad \text{for} \quad 0 \le z \le 0.5\,h$$

$$u_{c(z)} = 1.07 \cdot \bar{u}_c \qquad \text{for} \quad 0.5\,h \le z \le h$$

where:

$u_{c(z)}$	speed of the tidal current at the height z above the seabed
$\bar{u}_c$	depth-averaged speed of the tidal current
z	height above the seabed of $u_{c(z)}$
h	total water depth

A method to calculate, for the case of an outfall in a trench, the speed of the tidal current at the height of the outfall centre is:

$$u_{c(0.5D)} = \left(\frac{y_m}{h}\right)^{\frac{1}{7}} \left(\frac{h}{h + y_t}\right) \left(\frac{0.5D}{h + y_t}\right)^{\frac{1}{7}} u_{c(y_m)}$$

where:

$u_{c(0.5D)}$	speed of the tidal current at the height 0.5D above the seabed
$u_{c(y_m)}$	measured tidal current speed at height y_m above the seabed
D	outside diameter of the outfall
y_t	trench depth
h	total water depth

Results from using these formulae are usually accurate to within ± 15% but they are less accurate very near the sea bed, in deep water and in areas of weak tidal currents.[8]

Where a more accurate tidal current profile is needed in the neighbourhood of the sea bed, the following logarithmic formulae are preferable:

$$u_{c(z)} = \frac{\bar{u}_c \ln\left(\frac{z}{z_{ob}}\right)}{\ln\left(\frac{\delta}{2\,z_{ob}}\right) - \frac{\delta}{2h}} \qquad \text{for} \quad z_{ob} \le z \le 0.5\,\delta$$

$$u_{c(z)} = \frac{\bar{u}_c \ln\left(\frac{\delta}{2z_{ob}}\right)}{\ln\left(\frac{\delta}{2\,z_{ob}}\right) - \frac{\delta}{2h}} \qquad \text{for} \quad 0.5\,\delta \le z \le h$$

where:

z_{ob}	sea bed roughness length, determined by the nature of the sea bed – see Table 1
δ	thickness of the boundary layer

In coastal regions shallower than 20m, δ should be assumed to be equal to the water depth.

Table 1

Typical values of seabed roughness length, z_{ob}, for different bottom types

Bottom type	Z_{ob} (m) $*10^{-3}$
Mud	0.2
Mud/sand	0.7
Silt/sand	0.05
Sand (unrippled)	0.4
Sand (rippled)	6
Sand/shell	0.3
Sand/gravel	0.3
Mud/sand/gravel	0.3
Gravel	3

1.3 Forces on a horizontal cylinder in regular waves

A cylinder subject to an oscillatory flow may experience two kinds of forces: the in-line force and the lift force.[10]

1.3.1 In-line force in oscillatory flow [10]

Flow around a cylinder will exert a resultant force on the cylinder, due to pressure and friction. In steady current, this force acting in the in-line direction is given by:

$$F_X = \frac{1}{2} \rho \, C_D \, D \, u \, |u|$$

where:

F_X	horizontal force per unit length of pipeline
ρ	density of water
C_D	drag coefficient
u	instantaneous horizontal velocity of the water

The velocity-squared term is written in the form of $u|u|$ to ensure that the drag force is always in the direction of the velocity.

In the case of oscillatory flow, there will be two additional contributions to the total in-line force:

$$F_X = \frac{1}{2} \rho \, C_D \, D \, u \, |u| + m' \frac{du}{dt} + \rho V \frac{du}{dt}$$

in which:

$m' \frac{du}{dt}$	hydrodynamic-mass force
$\rho V \frac{du}{dt}$	Froude-Krylov force

where:

m'	hydrodynamic mass
V	volume of the pipeline

The horizontal acceleration $\frac{du}{dt}$ in a plane flow is strictly given by

$$\frac{du}{dt} = \frac{\partial u}{\partial t} + u \frac{\partial u}{\partial x} + v \frac{\partial u}{\partial y}$$

where:

x	horizontal co-ordinate
y	vertical co-ordinate
u	instantaneous horizontal velocity of the water
v	instantaneous vertical velocity of the water

In applications, it is usual to ignore the convective terms $u \frac{\partial u}{\partial x} + v \frac{\partial u}{\partial y}$.[5]

The hydrodynamic mass can be illustrated by reference to the following example. Suppose that a thin, long plate is immersed in still water and that it is impulsively moved from rest. When the plate is moved in its own plane, it will experience almost no resistance. Whereas, when it is moved in a direction perpendicular to its plane, there will be a tremendous resistance against the movement. The reason why this resistance is so large is that it is not only the plate but also the fluid in the immediate neighbourhood of the plate, which has to be accelerated in this case due to the pressure from the plate.

The hydrodynamic mass is defined as the mass of the fluid around the body that is accelerated with the movement of the body due to action of pressure.

Traditionally, the hydrodynamic mass is written as:

$$m' = \rho C_m A$$

where:

A	cross-sectional area of the pipeline
C_m	hydrodynamic-mass coefficient

When the body is moved with an acceleration in still water, there will be a force on the body, namely the hydrodynamic-mass force. When the body is held stationary and the water is moved with an acceleration, however, there will be two effects. First, the water will be accelerated in the immediate neighbourhood of the body in the same way as in the previous case. Therefore, the mentioned hydrodynamic-mass will be present. The second effect will be that the accelerated motion of the fluid in the outer-flow region will generate a pressure gradient according to:

$$\frac{\partial p}{\partial x} = - \rho \frac{du}{dt}$$ where u is the velocity far from the cylinder.

This pressure gradient in turn will produce an additional force on the cylinder, which is termed the Froude-Krylov force. For a cylinder with the cross–sectional area A and with unit length, this force will be:

$$\rho A \frac{du}{dt}$$

Now the total in-line force can be formulated for an accelerated environment where the cylinder is held stationary:

$$F_X = \frac{1}{2} \rho C_D D u |u| + \rho C_m A \frac{du}{dt} + \rho A \frac{du}{dt}$$

$$= \frac{1}{2} \rho C_D D u |u| + \rho (C_m + 1) A \frac{du}{dt}$$

By defining a new coefficient, the inertia coefficient $C_M = C_m + 1$, the equation will read as follows:

$$F_X = \frac{1}{2} \rho C_D D u |u| + \rho C_M A \frac{du}{dt}$$

in which:

$\rho C_M A \frac{du}{dt}$ inertia force

1.3.2 Lift force in oscillatory flow [10]

When a cylinder is exposed to an oscillatory flow, it may undergo a lift force perpendicular to the drag and inertia force, caused by a lower pressure at the top of the pipeline produced by the contraction of the water streamlines.[3]

The lift force is written as:

$$F_Y = \frac{1}{2} \rho C_L D u^2$$

where:

F_Y vertical force per unit length of pipeline
C_L lift coefficient

1.3.3 Morison equations [5]

The formulas describing the in-line and lift forces on a slender fixed cylinder due to an oscillatory flow, as described in the previous sections, are:

$$F_X = \frac{1}{2} \rho C_D D u |u| + \rho C_M A \frac{du}{dt}$$

$$F_Y = \frac{1}{2} \rho C_L D u^2$$

These equations are known as the Morison equations. They are not known to be a good representation of the forces on slender bodies in unsteady flow, but are widely used in offshore pipeline engineering because it is the only reasonable straightforward theoretical model available

1.3.4 Morison equations: waves and currents [17]

When waves and currents are acting simultaneously, the combined effect should be considered. Common use is to add vectorially the wave-induced velocity and the current velocity in the velocity terms of the Morison equations. One should be aware that the force coefficients C_D, C_M, and C_L are also influenced by the presence of the current.

1.3.5 Morison equations: oblique members

The Morison equations can also be applied to oblique members. Common use is to decompose the undisturbed velocity and acceleration into components normal to the cylinder axis, and then use the Morison equations with normal components of velocity and

acceleration. The force direction will be perpendicular to the cylinder axis.[16] Tests have shown that the force coefficients C_D, C_M, and C_L decrease slightly when the flow does not cross the outfall at right angles. It is therefore conservative to apply the Morison equations with the perpendicular velocity and acceleration components and the same coefficients as for perpendicular flow.[13]

1.3.6 Morison equations: influencing parameters [2]

The accuracy of the Morison equations depends on the accuracy of the basic formulation and the force coefficients C_D, C_M, and C_L. The force coefficients are in fact functions of numerous parameters, including:

- the Keulegan-Carpenter number, defined by:

$$KC = \frac{u_w T}{D}$$

where:

u_w	maximum bottom velocity in regular waves
T	period of the flow oscillation
D	diameter outfall

The KC-number is a measure of the ratio between the distance moved by a water particle between its extreme positions in oscillating flow and the diameter of the pipeline. It is generally agreed that the force coefficients depend primarily on the KC-number.

- the relative contributions of the oscillatory wave velocity and the steady current velocity.
- the Reynolds number, which describes the ratio of the inertial to viscous forces, defined by:

$$Re = \frac{u_w D}{\upsilon}$$

where:

ν	cinematic viscosity of water.

- the ratio of the gap under the pipeline to the pipeline diameter.
- the surface roughness of the pipeline, often written in dimensionless form as the ratio of the typical surface roughness height to the pipeline diameter.

2 HYDRODYNAMIC FORCE ANALYSIS BASED ON THE MORISON EQUATIONS

The Morison equations are semi-empirical, in that they are based on a theoretical understanding of the fluid mechanics, but require empirical force coefficients, which incorporate all flow effects, to provide a realistic match to actual data. The main limitation in the use of the Morison equation lies in the selection of appropriate coefficients.[2] Much research has been carried out to find the right coefficients for different situations. This chapter describes some of the tests and their results.

2.1 Morison coefficients derived from model tests on a flat seabed by Bryndum [18]

2.1.1 Model test program

The Danish Hydraulic Institute has performed an extensive model test program on the hydrodynamic forces on a submarine pipeline, exposed on a flat seabed, for the American Gas Association, in the period 1983-1986. The test program comprised approximately 500 individual tests, covering the following environmental conditions:

- steady current
- regular waves
- regular waves and steady current
- irregular waves
- irregular waves and steady current.

The influence of the most significant non-dimensional parameters, i.e. the KC-number, the current ratio α (the ratio of the steady current velocity to the maximum wave-induced bottom velocity), and the pipe roughness ratio (the ratio of the hydraulic roughness of the pipe to the pipe diameter), on the hydrodynamic forces has been determined from these tests. Parameters, which have secondary influence on the hydrodynamic forces, such as the seabed roughness ratio (the ratio of the seabed roughness to the pipe diameter) and the wave irregularity in natural wave trains, have also been investigated.

2.1.2 Testing technique and instrumentation

The testing technique applied is the so-called carriage technique, which combines the advantages and flexibility of a medium size facility with the capability of carrying out tests at full scale or near full scale. The model as such is composed of the model pipe itself and a part of the seabed, i.e. a flat plate sufficiently long to allow a correct oscillatory boundary layer to develop. The model is suspended vertically from a carriage, which runs on rails mounted on top of the flume walls. The carriage can be driven with any prescribed oscillatory motion and can thus move the model relative to the water, reproducing the near seabed wave-induced horizontal water particle motions. A return flow in the flume reproduces a steady current.

The seabed and both model pipes were provided with surface roughness which was varied during the course of the test program.

The hydrodynamic forces on the instrumented pipe segment were measured directly in the in-line and cross flow directions using a two component shear force transducer. The near seabed undisturbed wave-induced particle velocities and accelerations, which were produced

by the carriage motions, were measured directly by means of a tachometer and an accelerometer mounted on the carriage. In addition to these basic measurements, the steady current in the flume was measured using a reference current meter placed upstream of the pipe in the centreline of the flume, and a flow meter mounted in the flume re-circulation system.

2.1.3 Method of analysis

The objective of the applied program was to establish non-dimensional force coefficients. The coefficients were found through a Least-Squares-Fit method between the measured force components and those predicted by Morison type of equations for both in-line and lift forces.

The equations used are written as:

$$F_X = \frac{1}{2} \rho \, C_D \, D \, u(t) \, |u(t)| + \frac{\pi}{4} \rho D^2 \, C_M \, a(t)$$

$$F_Y = \frac{1}{2} \rho \, C_L \, D \, u^2(t)$$

where:

u(t)	total water particle velocity
a(t)	water particle acceleration

However, no firm established method for combining the drag, inertia and lift forces exists. In many design procedures the inertia force is neglected since it is considered 90° out of phase with the drag and lift forces. For irregular wave motion this is certainly not always the case, particularly if a steady current is present. For large diameter pipelines with small KC-numbers, the inertia force may be dominant. In some design procedures the concept of a wave being a regular sinusoidal function is taken one step further, and inline an lift force are computed for various wave phase angles in order to find the most critical combination. This method, however, cannot be simply applied for irregular waves.[4]

2.1.4 Test results

The drag, inertia and lift coefficients in combination with the Morison type formulae for in-line and lift force yield reasonable predictions for the in-line force, whereas the lift force in most cases is poorly described for both regular waves with and without steady current superimposed.

The parameter ranges covered in the tests are:

- KC-number: 3-160
- current ratio α: 0-1.6

The results of all regular wave tests without superimposed steady current are shown in figure 2.1. The force components are plotted against the wave parameter KC. Two sets of coefficients are presented. The hydrodynamic force coefficients are shown for three different values of pipe surface roughness (left side graphs) and for three different values of the seabed roughness (right side graphs). The full lines in the two sets of graphs represent the same test series. As indicated on the graphs, the variation with the KC-number is very similar for all values of the pipe surface and bed roughness.

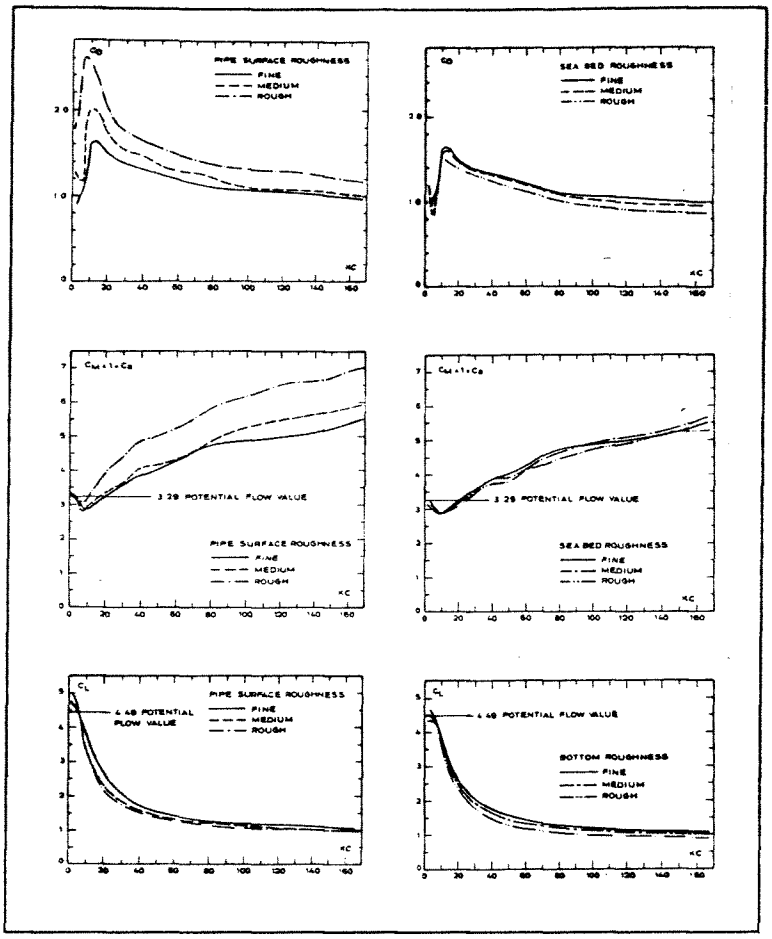

Figure 2.1 Force coefficients C_D, C_M, C_L for regular waves [18]

Figure 2.2 shows the effect in combined wave and current action (the current ratio α is plotted out on the horizontal axis). The presence of a steady current leads in all cases to reduction of the force coefficients. The drag coefficient approaches the value found in steady current for increasing α-values. It is characteristic that the steady current value is found for lower α-values the larger the KC-number. The inertia coefficient decreases with increasing α. The lift coefficient decreases with increasing α and the effect of a steady current can be compared to the effect of increasing the KC-number in case of pure wave action. This effect of the steady current is most pronounced for small KC-numbers. The decrease in the lift and drag force coefficients appearing when a steady current is superimposed on the wave motion is partly due to an increase in the effective KC-number and partly due to a decrease in the total average velocity over the pipe diameter caused by the combined wave and current boundary layer.[4]

Effect of pipe surface roughness

It can be observed that the drag and inertia coefficients increase substantially with the surface roughness whereas a slight decrease can be seen for the lift coefficient. Expressed in hydrodynamic forces, the in-line force increases whereas the lift force remains unchanged or decreases slightly. The observed influence in the pure wave case becomes more significant when a steady current is superimposed. Both the increase in drag force and the decrease in lift force are relatively stronger.

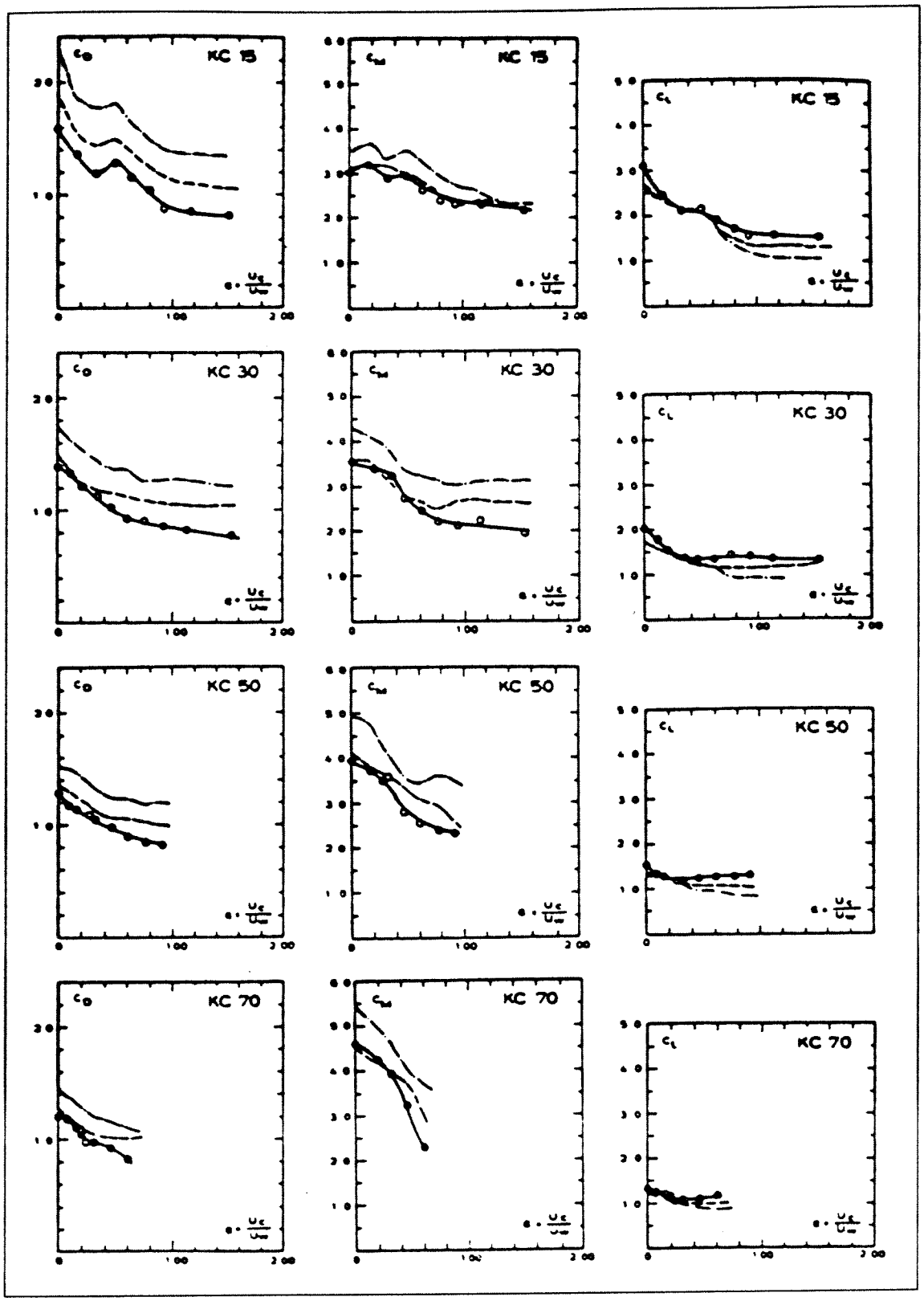

Figure 2.2 **Force coefficients C_D, C_M, C_L for regular waves and current [18]**

Effect of seabed roughness

Under oscillatory flow conditions the seabed roughness gives rise to the formation of a thin unsteady boundary layer. The effect of this boundary layer on the hydrodynamic forces has been investigated by conducting tests in which the seabed was provided with roughness

having three different values from relatively smooth to rough conditions. Increasing roughness leads to reduced drag and lift coefficients whereas the inertia coefficient is insignificantly influenced.

Effect of 3-D wave kinematics [4]
Using the force coefficients determined under 2-dimensional flow conditions may imply conservative estimates of the hydrodynamic loading on longer pipeline spans considering the 3-dimensionality of natural seas.

2.2 Morison coefficients derived from model tests on a flat seabed and in a trench by Palmer [5]

2.2.1 Model test program

The lack of adequate data on the hydrodynamic loading on a trenched pipeline, faced by British Petroleum and Woodside Petroleum, resulted in a research program. Hydraulic Research Ltd. was commissioned to carry out model tests to obtain the data.

2.2.2 Testing technique and instrumentation

The tests were carried out in a pulsating water tunnel which can produce oscillating flow of variable period and orbit length. A unidirectional current can be superimposed on the oscillatory flow. Trench sections were obtained by constructing a false floor in the tunnel. The model pipeline was mounted horizontally across the tunnel at the floor level at the midpoint of the working section. An inductive transducer measured the vertical and horizontal deflections, which are linearly proportional to the corresponding forces.

2.2.3 Method of analysis

The data analysis is based on the Morison equation for forces on slender bodies in unsteady flow. A decision to express the results in terms of Morison coefficients has the advantage that it allows straightforward comparison with measured coefficients for untrenched pipelines.

The Morison equation used is:

$$F_X = \frac{1}{2} \rho \, C_D \, D \, u \, |u| + \frac{\pi}{4} \rho D^2 \, C_M \, a$$

$$F_Y = \frac{1}{2} \rho \, C_L \, D \, u^2$$

The values of C_D and C_M were determined by comparing the coefficients of the first harmonic of a Fourier series decomposition of the Morion equation with those of the data, which were non-dimensionalised and passed through an Fast Fourier Transform harmonic analysis. The values of C_L were evaluated from the extreme values of the lift data.

The calculated values of C_D, C_M and C_L are plotted as functions of the semi-orbital movement of the water, denoted a, divided by the diameter D. The ratio a/D is a measure of the development of the wake structure. It can be seen that $2\pi a/D$ is equal to the KC-number. [17]

When a superimposed steady current v was present, the results were plotted against an relative equivalent amplitude displacement a' defined by:

$$a' = a\left(1 + \frac{v}{a\omega}\right)^2$$

The KC-number and the ratio a'/D are compared to one another in Appendix I.

By using the current ratio α, the a'/D ratio (waves and current) can be related to the KC-number (waves only). This is represented by the following expression (see Appendix I):

$$\frac{a'}{D} = KC\left(\frac{1}{2\pi} + \frac{\alpha}{\pi} + \frac{\alpha^2}{2\pi}\right)$$

2.2.4 Test results

Other research indicated that embedment of a pipe can result in a reduction of hydrodynamic coefficients, directly related to penetration depth.[19] Therefore, different embedment configurations were analysed, varying from a pipe on the bottom to a trenched outfall.

As would be expected, the forces on a pipe partially buried in the seabed are smaller than those on an unburied pipe. A trench shelters a pipeline and reduces hydrodynamic forces, and the presence of spoil mound creates a small further reduction. If there is a gap under a pipe in a trench, the top of the pipe extends further above the bottom, which tends to increase the drag, but water can pass under the pipe, which tends to reduce the drag. The net effect on the drag and lift coefficient is relatively small, but the inertia coefficient falls towards its free-stream potential theory value of 2.

The results for the pipe on the seabed, as represented in figure 2.3, can be compared with other research. Differences occur because of different experimental techniques, because of different levels of surface roughness, and because of different methods of extracting the coefficients from the data.

There is a broad agreement in the dependence on the KC-number, but the present work gives slightly lower values.

From figure 2.3, it can be seen that there is some scatter in the experimental results. This is invariably found in hydrodynamic experiments in oscillatory flow, and can be attributed to the irregular formation of large vortices in the wake as the water is swept back and forth across the pipe.

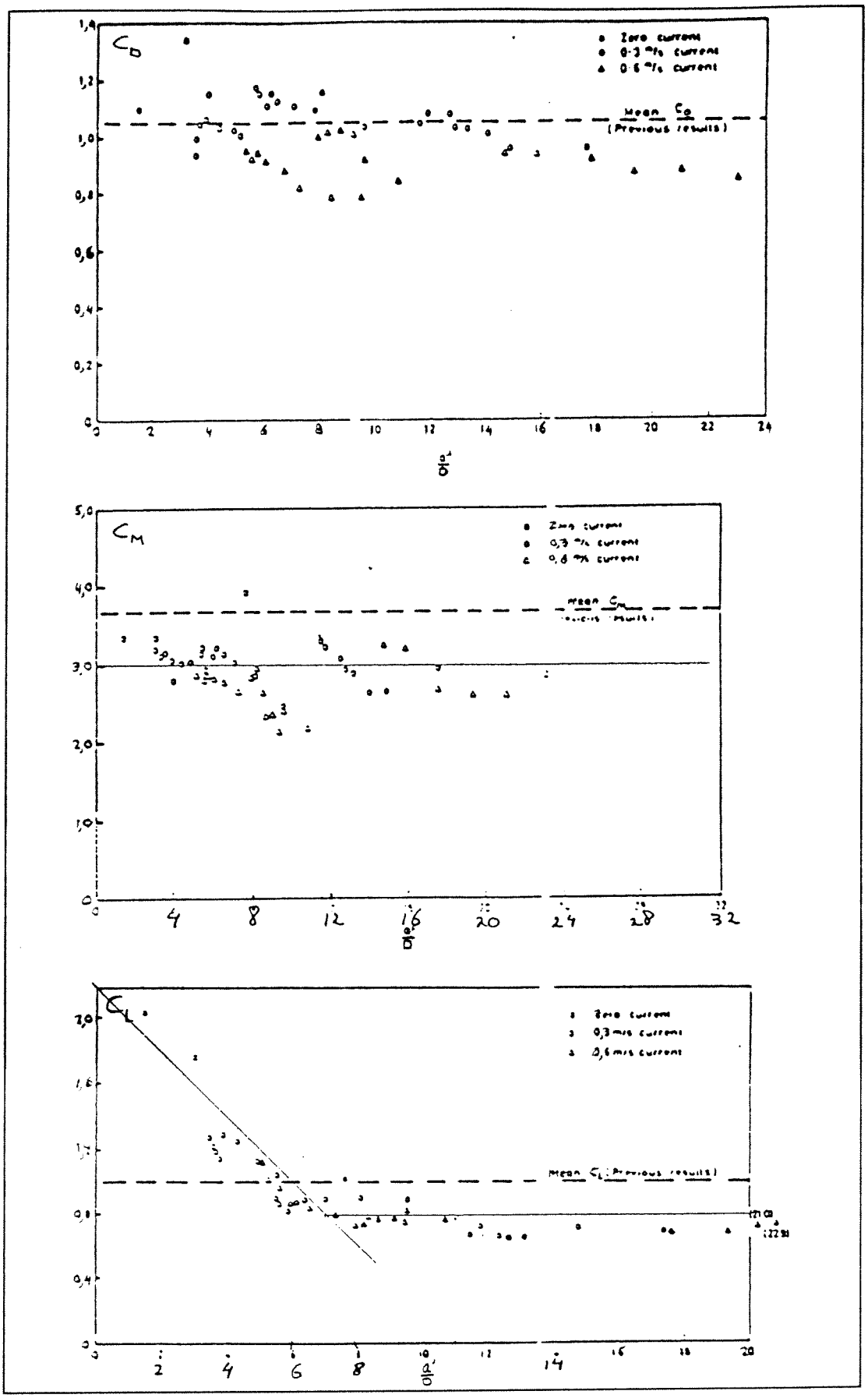

Figure 2.3 Hydrodynamic coefficients for a pipe on the seabed [5]

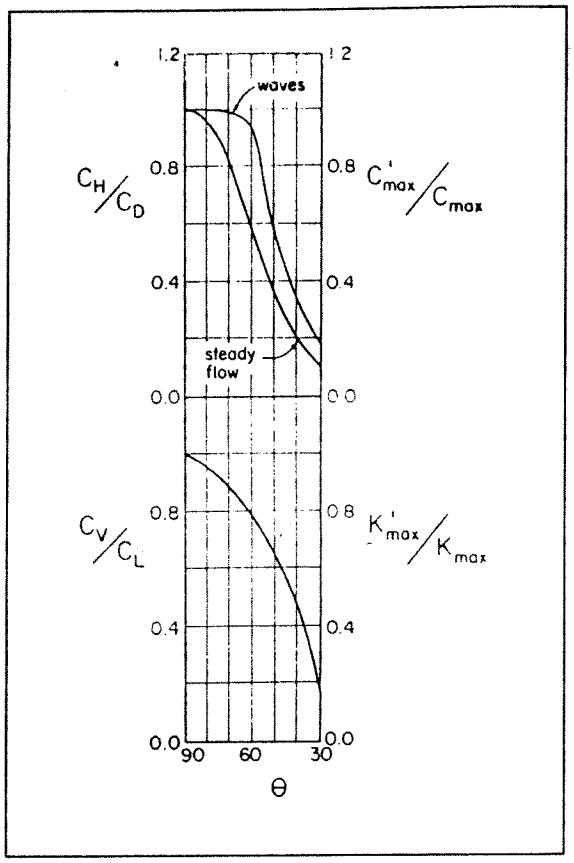

Figure 3.1 Design curve for outfalls of any clearance, angled to currents or wave fronts [11]

3.1.3 Wave forces: outfall parallel to wave fronts

Let the total wave-induced horizontal force on a pipe set parallel to the wave fronts (thus perpendicular to the water motion) be represented by F. The Morison equation is written as:

$$F = F_D + F_I$$

where F_D is the drag force encountered earlier and F_I is an inertia force. The equation for the drag force in the case of waves is:

$$F_D = \frac{1}{2} \rho C_D A u |u|$$

The product of the flow speed and its absolute value preserves the proper sign of the applied force (that would be lost by squaring the speed). The peak value of u is u_{max}. The equation for the inertia force is:

$$F_I = \frac{\pi}{4} \rho D^2 l_* C_I \frac{du}{dt}$$

where du/dt is the actual flow acceleration. Thus the inertia force is an acceleration-dependent term. Since accelerations are very much a part of wave-induced water motion, such a term is an indispensable inclusion in the general wave force case. C_I is an function of the relative clearance of a pipe from a boundary.

3 HYDRODYNAMIC FORCE ANALYSIS BASED ON MAXIMUM FORCE COEFFICIENTS

Some research workers concerned with waves on pipelines, have preferred a different approach which only gives the maximum wave forces. It cannot describe the variations in force during a cycle, or identify the most unfavourable combination of drag and lift.[2]

3.1 Maximum force coefficient model by Grace [11]

3.1.1 Current forces: current perpendicular to outfall

A flowing liquid exerts a force on an object immersed to it. The component of such a force acting in the line of the velocity vector of the approach flow is called the drag force. The equation used to determine this force (F_D) for a liquid of density ρ and approach flow v_c is:

$$F_D = \frac{1}{2} \rho C_D A v_c^2$$

where C_D is the drag coefficient and A is the projected area of the object as seen by the approaching flow. For a cylinder or pipe of diameter D and length l_* at right angles to the flow, $A = Dl_*$.

An asymmetrical body or one close to a boundary experiences a steady lift force F_L perpendicular to the incident velocity vectors. The equation for this force is written as:

$$F_L = \frac{1}{2} \rho C_L A v_c^2$$

where C_L is a lift coefficient. Grace considered design values of $C_D = 1$ and $C_L = 1$ valid for pipes on the seabed, perpendicular to a steady current.

3.1.2 Current forces: outfall at angle to current

When a steady flow approaches a pipe at some angle (θ) other than the perpendicular (θ=90°), it is convenient to think of the horizontal force on the pipe perpendicular to its line rather than the drag force. Let this force be:

$$F_H = \frac{1}{2} \rho C_H D l_* v_c^2$$

The area being used is still Dl_* and the flow speed employed is that of the flow rather than the component perpendicular to the pipe. The lift force for the angled pipe can be written as:

$$F_V = \frac{1}{2} \rho C_V D l_* v_c^2$$

The ratios C_H/C_D and C_V/C_L have been plotted in figure 3.1. Grace (1973), using data from several sources, derived these curves. The reference values $C_D = 1$ and $C_L = 1$ are outlined earlier.

Grace states that there is an apparently better way to predict the maximum wave-induced horizontal and vertical forces exerted on a pipe during the passage of a prescribed design wave. Let:

$$F_{H,\,max} = \frac{1}{2} \rho\, C_{max}\, D\, l_e\, \beta_1\, u^2_{max}$$

$$F_{V,\,max} = \frac{1}{2} \rho\, K_{max}\, D\, l_e\, \beta_1\, u^2_{max}$$

where β_1 is a correction factor, to be taken as 1.08. The variation of C_{max} and K_{max} with ψ is shown in figure 3.2.

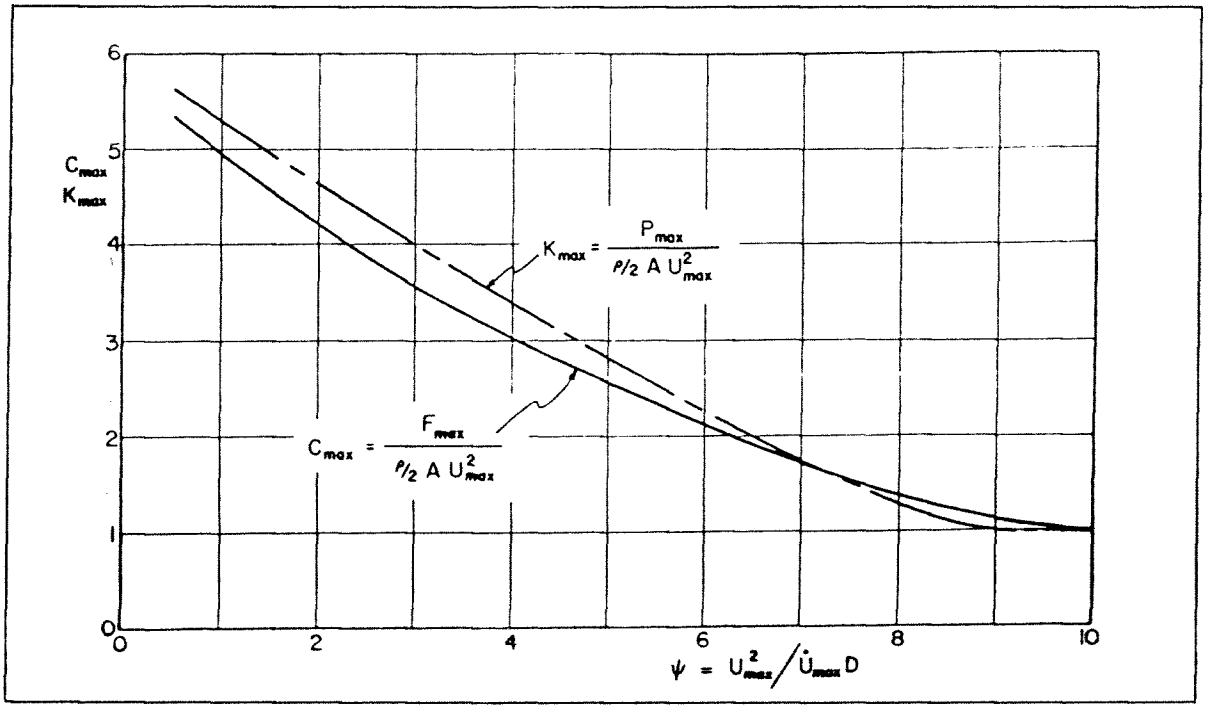

Figure 3.2 Design curve for outfalls at any clearance, parallel to wave fronts [11]

The parameter ψ chosen reflects both the velocity and acceleration aspects of the flow and is defined by:

$$\psi = \beta_3 \left[\frac{u^2_{max}}{\left(\frac{du_{max}}{dt} \cdot D \right)} \right]$$

where β_3 is an empirical factor, to be taken as 0.86.

For those cases where the value of the parameter ψ is below 0.5, the peak horizontal wave force can be computed from the expression:

$$F_{H,\,max} = \frac{\pi}{4} \rho D^2\, l_e\, C_I\, \frac{du_{max}}{dt}$$

For small ψ the inertia force contribution to the total is dominant. For large ψ, the drag force is all-important.

3.1.4 Wave forces: outfall at angle of attack

The general approach followed for steady flow force coefficients in the perpendicular flow and angled flow cases will also be used here. The peak horizontal and vertical forces are computed using the approach outlined in the preceding section, then adjusted using the curves of figure 3.1.

The outfall itself must resist the flexural stresses caused by the alternating directions of wave-induced loading over its length. The following is a suggested approach towards deriving a reasonable loading diagram for the pipe for a specific design wave characterised by its period and deep water wave height. The first step is to derive a refraction diagram for the design wave. At any station along the outfall the depth is known. The variation of wave height can be plotted against outfall station. The Airy theory can be used to give first estimates of the peak velocities and accelerations. After determining C_{max}, K_{max} and θ, figure 3.1 can be entered, deriving the altered maximum wave force coefficients. The forces can than be computed as:

$$F'_{H,\,max} = \frac{1}{2} \rho\, C'_{max}\, D\, l_*\, \beta_1\, u^2_{max}$$

$$F'_{V,\,max} = \frac{1}{2} \rho\, K'_{max}\, D\, l_*\, \beta_1\, u^2_{max}$$

where the horizontal force F'_{max} is perpendicular to the pipe.

The resulting diagram in no way represents the distribution of wave-induced force along the exposed outfall at any time; it assumes that a crest is located all along the pipe.

The design involves taking various pipe stations separated along the pipe by distances:

$$\bar{\lambda} \;/\; \sin \bar{\theta}$$

where $\bar{\lambda}$ and $\bar{\theta}$ correspond to average wave lengths and angles of attack between the offshore crest point and the onshore crest point.

As an adequate design procedure, the variation of applied forces between two adjacent wave crest stations can be represented by roughing in an approximate cosine function. The resulting force distribution all along the pipe can than be used in a flexural stress analysis for the pipe. Other locations for the crests than the first set should be used in order to find that particular situation that gives rise to the most serious stresses.

3.2 Alternative maximum force coefficient model by Hydraulics Research Ltd. [17]

3.2.1 Model test program

Hydraulics Research has carried out an experimental program for British Petroleum, which measured forces on pipes in a sinusoidal oscillating flow in a pulsating water tunnel. The

forces are related to an alternative theoretical maximum force coefficient model. The objective of the experiments was to measure the forces in an accurately-controlled experimental situation, where water is driven backwards and forwards across a pipe, by a piston in a closed water tunnel. The results could then be related to theoretical predictive models, and to field measurements on pipelines in the sea.

3.2.2 Testing technique and instrumentation

The tests were carried out in a pulsating water tunnel which can produce oscillating flow of variable period and orbit length. A unidirectional current can be superimposed on the oscillatory flow. The drag and lift forces on a cylinder in the flow were measured simultaneously with strain gauges. The total flow velocity (oscillating plus unidirectional) in the working section was measured at some distance from the cylinder by a miniature propeller meter.

3.2.3 Method of analysis

Independent physical parameters, besides instrumentation dependent geometric parameters, which characterise the flow around and the forces acting on the cylinder during the experiments are:

- D diameter of cylinder
- ω angular frequency of the oscillating flow
- a semi-orbit length of the oscillating flow at the bed
- v steady current velocity
- ρ water density
- υ cinematic water viscosity

where:

$$a = \frac{u_{max} - v}{\omega}$$

$u_{max} - v = u_w$

u_{max} maximum total flow velocity

v steady current velocity

u_w maximum bottom velocity in regular waves

The dependent physical variables considered in the analysis are:

- F_{md} maximum drag force per unit length of cylinder
- F_{ml} maximum lift force per unit length of cylinder.

Besides geometric ratios, the independent variables can be reduced to the following dimensionless parameters:

$$a/D,\ v/a\omega,\ a\omega D/\nu$$

and hence, taking $\rho D^3\omega^2$ as a scale of force/unit length, the maximum forces can be represented by a relation of the form:

$$\frac{F}{\rho D^3 \omega^2} = f\left(\frac{a}{D}, \frac{v}{a\omega}, \frac{a\omega D}{\nu}, \text{geometric ratios}\right)$$

In order to reduce the number of parameters, the flow (a, ω, v) was replaced by an equivalent (with respect to the maximum forces) purely oscillatory flow (a', ω') where:

$$a'\omega' = v + a\omega$$
$$a'\omega'^2 = a\omega^2$$

that is:

$$a' = a\left(1 + \frac{v}{a\omega}\right)^2 \quad \text{and} \quad \omega' = \omega\left(1 + \frac{v}{a\omega}\right)^{-1}$$

Because of blockage in the water tunnel, the local velocities and hence the semi-orbit length are increased. Therefore, a blockage correction, defined as $a'' = k_b\, a'$, is applied. Hence the original non dimensional variables are reduced to two:

- $F_D = f_D(a''/D, Re)$
- $F_L = f_L(a''/D, Re)$

where:

$$F_D = \frac{F_{md}}{\rho D^3 \omega^2}$$
$$F_L = \frac{F_{ml}}{\rho D^3 \omega^2}$$

As the Reynolds numbers of the experiments was very similar to prototype, it was expected that the dominant parameter would be a''/D. Hence the non-dimensional maximum forces F_D and F_L were plotted against a''/D. The aim was then to fit curves to this data.

3.2.4 Test results

The curve fitting resulted, for the case of the pipe lying on the bed, in the following recommended maximum force formulas:

$$F_{md} = \rho D^3 \omega^2 \left\{ 4.22 + 0.52 \cdot \left(\frac{a}{D}\right)^2 \right\} \qquad \text{for} \quad \frac{a}{D} \geq 2.85$$

$$= 2.96 \cdot \rho D^2 a \omega^2 \qquad \text{for} \quad \frac{a}{D} \leq 2.85$$

$$F_{ml} = 1.41 \cdot \rho D^3 \omega^2 \left(\frac{a}{D}\right)^{1.7}$$

Should it be necessary to allow for the superposition of a bottom current v upon the design wave with bottom characteristics a and ω this may be accounted for by setting:

$$a' = a\left(1 + \frac{v}{a\omega}\right)^2 \quad \text{and} \quad \omega' = \omega\left(1 + \frac{v}{a\omega}\right)^{-1}$$

and substituting a' for a and ω' for ω in the above formulas.

4 FORCE DISTRIBUTION ON AN OUTFALL IN UNSTEADY FLOW

Unsteady flow occurs under waves, where an outfall is in oscillatory wave-induced current, superimposed on a steady current associated with tide, storm and ocean circulation.[13]

4.1 Distribution due to wave cycles

A pipeline installed on the seabed is influenced by hydrodynamic lift and drag forces resulting from wave induced water particle velocities and steady state currents, and by inertia forces resulting from water particle accelerations. This is illustrated in figure 4.1.

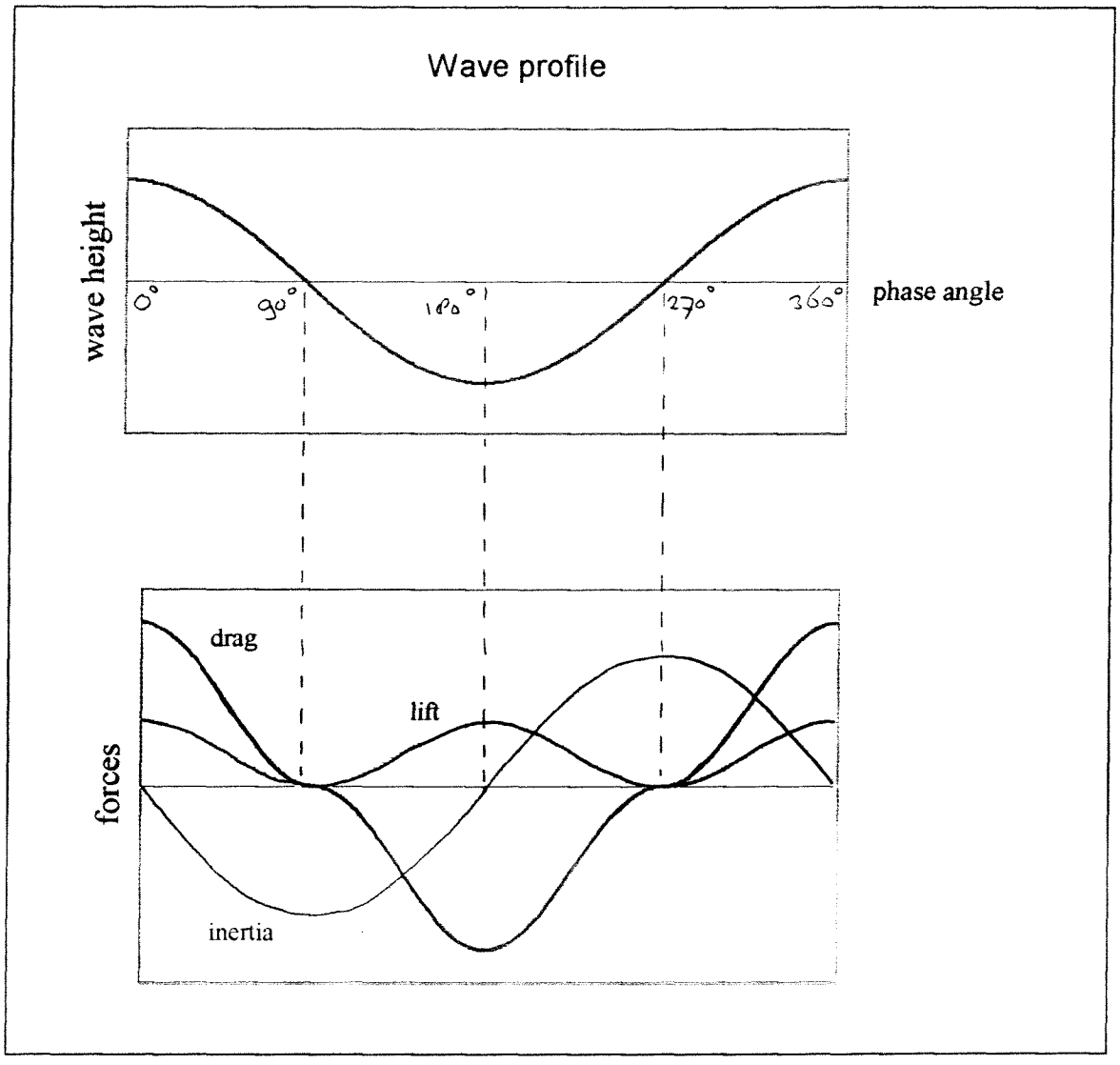

Figure 4.1 Drag, inertia and lift forces on a pipe in unsteady flow [13]

The wave induced water particle velocity is 90° out of phase with the water particle acceleration. The maximum combined force acting on the pipeline is therefore a function of the magnitudes of each of the force components at a critical phase angle.[12]

4.2 Distribution due to short-crested waves

The surface of the sea in any sea state comprises a confused, irregular pattern of waves, and has no resemblance to a singular regular wave. This non-monochromatic irregular pattern is formed by wave trains propagating from a number of directions, and hence the crest length in any particular wave is of finite length. It is therefore important to establish the crest length to wave length ratio: the wave length is measured in the direction of propagation, and the crest length (defined as the trough-to-trough distance) transversely to it, as illustrated in figure 4.2.

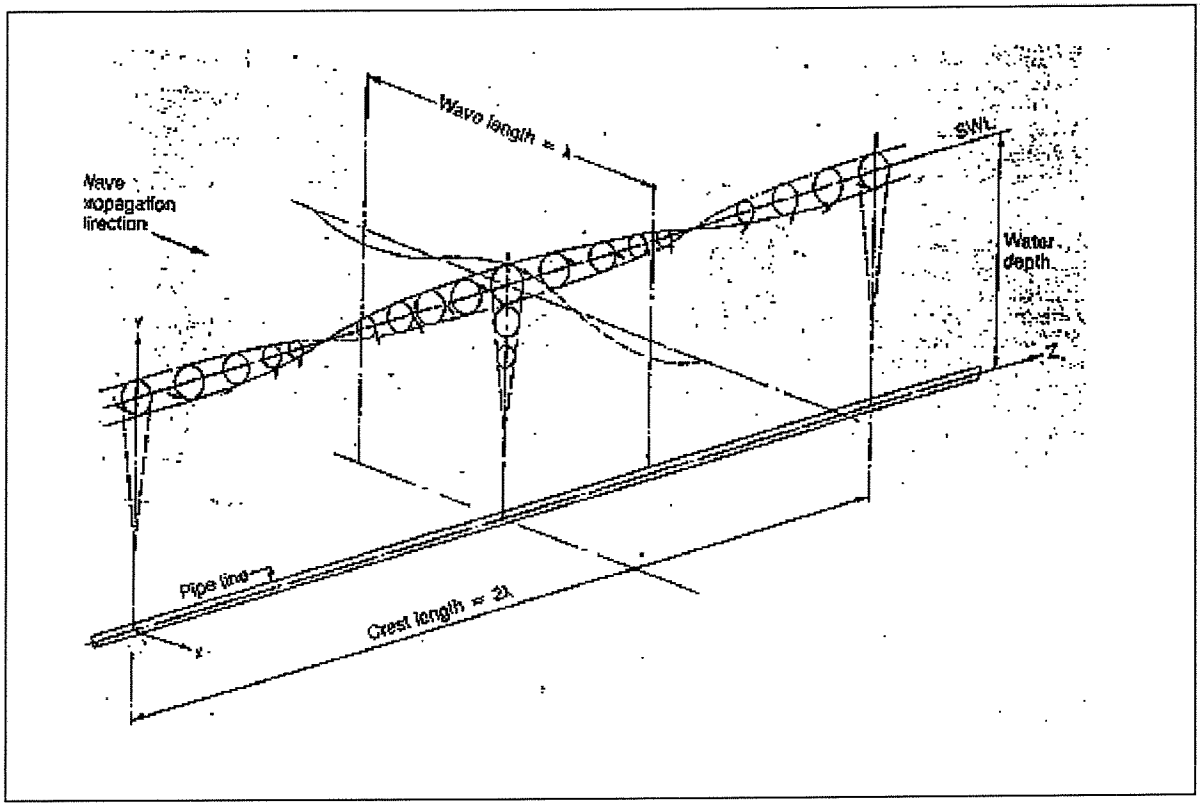

Figure 4.2 Definition sketch of wave and crest length [12]

Using standard sea state spectra, it has been established that a ratio of average crest length to average wave length (in a wave driven wave field in deep water) varies between 1.5 and 1.7. Using a wave energy spreading function, a crest length to wave length ratio 2.24 can be derived. The actual ratio is dependent on water depth, bathymetry and geographical location. At the peak position of the crest of the maximum wave, the combined force on the pipeline will be maximum. At the trough points, the wave induced velocity will be 180° out of phase with the steady state current, resulting in lesser force.

4.3 Distribution due to oblique current approach

The analysis so far has treated the problem as two dimensional, as if the transverse current were uniform along the length of the outfall. In reality, waves are short-crested, as mentioned in the previous section, and approach an outfall obliquely. In shallow water, where the outfall is approximately at right angles to the depth contours, wave refraction brings the wave propagation velocity into approximately the same direction as the outfall. The wave-induced bottom currents are not in phase along the length of the line, and vary in amplitude. These effects therefore reduce the resultant force on the outfall.[13]

5 LATERAL RESISTANCE OF AN EXPOSED OUTFALL[13]

If an outfall is exposed on the seabed, it must resist lateral movement under the hydrodynamic forces induced by waves and currents. Figure 5.1 shows the forces on a cross-section of an unburied outfall, which resists lateral movement by its own weight.

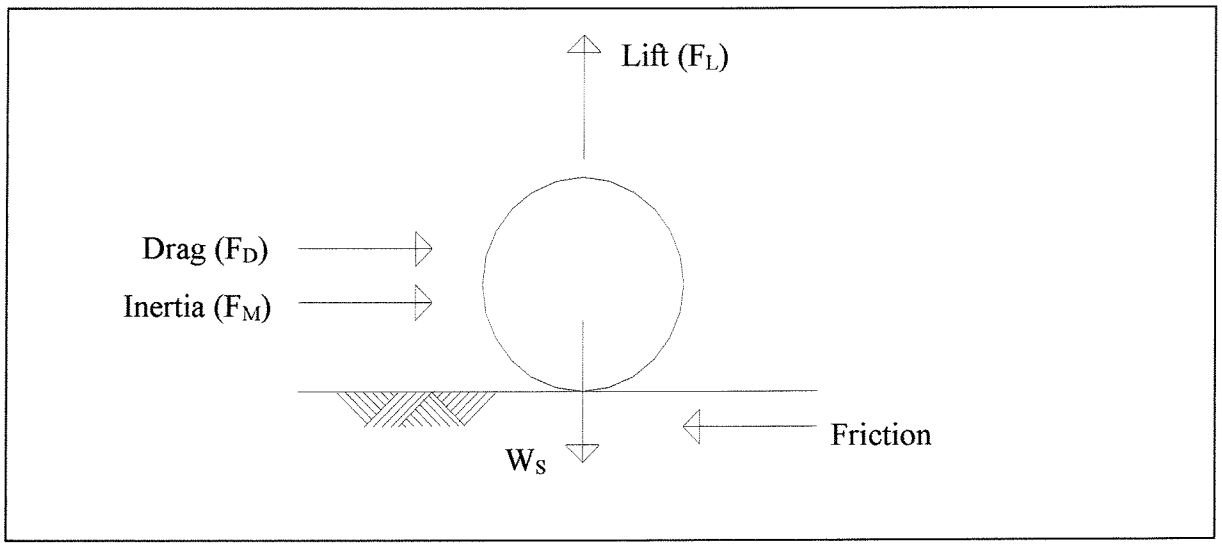

Figure 5.1 Forces on an outfall [13]

Although tests have indicated that more resistance is available due to pipe-soil interaction, it is traditional to adopt an extremely simple idealisation of the geotechnical interaction between a pipeline and the seabed, and to treat it as a contact governed by Coulomb friction.[5]

From figure 5.1 it can be shown that for the pipeline to remain stable:

$$W_S \geq \left(\frac{F_D + F_M}{r_c} \right) + F_L$$

where:

W_S	total submerged pipeline weight
F_D	drag force due to waves and currents
F_M	inertia force due to waves and currents
F_L	lift force due to waves and currents
r_c	Coulomb friction factor

The outfall stability is sensitive to the pipe weight W_S. The total pipe weight should therefore include all internal and external coatings and wraps.

The choice of r_c is largely based on experience, and on a small number of experiments. From experiments carried out on sand, it is found that small movements begin at quite small values of r_c, but that threshold of large movements correspond to a r_c value of about 0.7. Behaviour on clay is more complicated. The value r_c is small if the pipe is light enough not to sink into the clay significantly, but a heavier pipe sinks, causing r_c and the lateral resistance to increase. In outfall design it is rare to encounter a combination of high currents and a soft clay bottom, because high currents will erode the clay.[14]

A partially-buried pipeline has a much increased resistance to lateral movement, which can be estimated by conventional geotechnical methods. To become unstable the pipe must either slide up the side of the trench or deform the soil on either side. In the first case, the coefficient r_c is increased to r_c':

$$r_c' = \tan (\alpha_t + \arctan r_c)$$

where:

α_t side slope of trench

In most instances, r_c' is much larger than r_c.

Even a very small shear strength is enough to prevent the pipeline moving sideways by deforming the trench sides. If the trench sides are composed of a soil which can be treated as an ideal plastic material, the force F_R per unit length required to deform the trench sides is approximately:

$$F_R = c\, y_t \left[\frac{8}{\sqrt{3}} + \frac{\left(\frac{\gamma y_t}{c} \right)}{2\sqrt{3}} \right]$$

where:

c undrained shear strength
y_t trench depth
γ submerged unit weight of the soil [5]

Full scale pipe-soil interaction tests have shown that:

- pipe penetration is the most important soil resistance parameter. From tests on both sand and clay it was apparent that an increase/decrease in pipe penetration was directly reflected in a corresponding increase/decrease in soil resistance.
- any load condition causing an increase in pipe penetration, increases soil resistance. In both sand and clay, an increase in pipe weight increases pipe penetration and thereby leading to greater soil resistance. Furthermore, increasing the number of oscillations and/or increasing oscillatory amplitude will increase pipe penetration and soil resistance as long as no breakout occurs.
- soil resistance is in general greater in loose/soft soils than in dense/stiff soils. This is due to greater pipe embedments in loose/soft soils where the bearing capacity is relatively low.[20]

6 CONCLUSIONS AND RECOMMENDATIONS

6.1 Conclusions

The hydrodynamic forces on outfalls during installation are described with the Morison equations. To solve these equations, the wave characteristics are described with the linear Airy wave theory. The main limitation in the use of the Morison equations lies in the selection of appropriate hydrodynamic force coefficients. Hydrodynamic force analysis based on the Morison equations, derived by Bryndum (pipeline on a flat seabed) and Palmer (pipeline on a flat seabed and in a trench) can be used in outfall construction. Hydrodynamic force analysis based on maximum force coefficients are less useful, because they cannot describe the hydrodynamic force variations during a wave cycle.

The hydrodynamic forces on outfalls are divided into lift and drag forces (resulting from wave-induced water particle velocities and steady state currents), and inertia forces (resulting from water particle accelerations). The maximum combined force acting on the outfall is a function of the magnitudes of each of the force components at a critical phase angle. Because waves are short-crested and approach an outfall obliquely, the wave-induced bottom currents are not in phase along the length of pipeline, and vary in amplitude. These effects reduce the resultant forces on the outfall.

The geotechnical interaction between an outfall and the seabed is treated as a contact governed by Coulomb friction, although tests have indicated that more resistance is available due to pipe-soil interaction.

6.2 Recommendations

The researches on the hydrodynamic force coefficients are highly controversial because major investigations indicate different values. Another point to note is that the most parameter ranges covered in the tests differ from sea state conditions during outfall installation. Therefor, it is recommended to do supplementary research on the backgrounds of the different model test programs in order to be able to select the most appropriate hydrodynamic force coefficients for outfall construction.

Another recommendation is to do supplementary research on the geotechnical interaction between outfall and seabed.

REFERENCES

[1] Coastal Engineering Research Center, *Shore Protection Manual.*
Department of the army, Missisippi, 1984.

[2] Palmer, A.C., *Marine pipelines.*
Notes, Faculty of Civil Engineering, Delft University of Technology, 1997.

[3] Velden, van der, E.T.J.M., *Coastal engineering.*
Notes on f7, Faculty of Civil Engineering, Delft University of Technology, 1989.

[4] Bryndum, M.B., et al, *Hydrodynamic forces from wave and current loads on marine pipelines.*
Offshore Technology Conference 4454, 1983.

[5] Palmer, A.C., et al., *Stability of pipelines in trenches.*
Proc Offshore Oil Gas Pipeline Technology Seminar. Stavanger, 1988.

[6] Dean, R.G., *Evaluation and development of water wave theories for engineering application.*
US Army, Corps of Engineers, Coastal Engineering Research Center, Fort Belvoir.
Special report no.1, 1974.

[7] Gerwick, B.C., *Construction of offshore structures.*
Wiley series of practical construction guides, 1986.

[8] Department of Energy, Health and Safety Executive, *Offshore Installations: guidance on design, construction and certification.*
HMSO, London, 1993.

[9] Det Norske Veritas, *Rules for classification of mobile offshore units.*
Norske Veritas, Høvik, 1996.

[10] Fredsøe, J., Mutlu Sumer, B., *Hydrodynamics around cylindrical structures.*
World Scientific, Advanced series on ocean engineering - volume12, 1997.

[11] Grace, R.A., *Marine outfall systems, planning, design and construction.*
Prentice-Hall, Inc., New Jersey, 1978.

[12] Corbishley, T., *How to stabilize subsea pipelines*
Pipe Line Industry, 1982.

[13] Veritas Offshore Technology and Services A/S, *On-bottom stability design of submarine pipelines.* Recommended practice: volume E, RP E305.
Veritec, Høvik, 1988.

[14] Lyons, C.G., *Soil resistance to lateral sliding of marine pipelines.*
Offshore Technology Conference, 1973.

[15] Det Norske Veritas, *Rules for classification of fixed offshore installations.* Norske Veritas, Høvik, 1996.

[16] Faltinsen, O.M., *Sea loads on ships and offshore structures.* Cambridge Ocean Technology Series, 1990.

[17] Wilkinson, R.H., et al, *Wave forces on submarine pipelines.* Proc Int Conf on Offshore Mech and Arctic Eng. Houston, 1988.

[18] Bryndum, M.B., et al, *Hydrodynamic forces on pipelines: model tests.* Proc Int Conf on Offshore Mech and Arctic Eng. Houston, 1988.

[19] Jacobsen, V., et al, *Submarine pipeline on-bottom stability: recent AGA research* Offshore Technology Conference 6055, 1989.

[20] Brennodden, H., et al, *An energy-based pipe-soil interaction model* Offshore Technology Conference 6057, 1989.

PART B

SENSITIVITY ANALYSIS OF OUTFALL STABILITY

A research report

INTRODUCTION

After the literature review on forces on outfalls during installation, the graduate project 'Stability of outfalls during installation' was continued with a sensitivity analysis of outfall stability.

In the sensitivity analysis, the extent of influence of the separate hydrodynamic variables in the equilibrium equations of outfall stability is analysed. This results in insight regarding the contribution of each hydrodynamic variable to the overall uncertainty of outfall stability. Such knowledge is essential to identify the important parameters to which more attention should be given, in order to have a better assessment to their values, and accordingly, to reduce the overall uncertainty of the output.

Only the hydrodynamic variables are considered in the sensitivity analysis. The various hydrodynamic force coefficients are left out of consideration and are taken as values used in the common practice of outfall construction. This is done because the literature review shows that major investigations on hydrodynamic force coefficients use different testing techniques, instrumentation and methods of analysis. The result is different used parameters and found values. A just comparison of these investigations can not be made because the backgrounds of the researches are not highlighted enough in the published articles.

The theoretical background of uncertainty and reliability analysis is given in chapter 1. In chapter 2 the computer programs VaP, which evaluates the influence of variables, and BestFit, which fits curves to input data, are described. With the help of these programs, two practice cases and a theoretical case are analysed in order to make the researches. The results of the analysis of these cases are reported in chapter 3. In Chapter 4 the conclusions and recommendations can be found. Finally, in Appendix II, III, IV, V and VI the preliminary calculations, wave climate studies, and computer program input and output are documented.

LIST OF SYMBOLS

G	stochastic quantity
W_S	submerged pipeline weight per unit length of outfall
F_D	drag force due to waves and currents per unit length of outfall
F_M	inertia force due to waves and currents per unit length of outfall
F_L	lift force due to waves and currents per unit length of outfall
C_D	drag coefficient
C_M	inertia coefficient
C_L	lift coefficient
D	outside diameter of the pipeline
f	Coulomb friction factor
ρ	density of water
u_N	instantaneous horizontal water particle velocity normal to outfall
a_N	instantaneous horizontal water particle acceleration normal to outfall
H	wave height
T	wave period
L	wave length
h	total water depth
θ_{WO}	angle between waves and outfall
θ_{CO}	angle between current and outfall
V_C	current velocity averaged over outfall diameter
φ	phase angle
μ	mean value
σ	standard deviation
α	sensitivity factor

1 UNCERTAINTY AND RELIABILITY ANALYSIS

The extent of influence of the separate hydrodynamic variables in the equilibrium equations of outfall stability is analysed with the help of the computer program VaP. In this chapter, the used statistical methods in VaP are described, and the theoretical backgrounds of uncertainty and reliability analysis in general are reviewed.

1.1 Introduction

1.1.1 Uncertainties in hydraulic engineering

In the analysis and design of hydraulic-engineering systems, uncertainties arise in various aspects. Uncertainty could be defined as the occurrence of events that are beyond our control. Uncertainties attribute mainly to our lack of a perfect understanding concerning the processes involved, and a perfect knowledge of how to determine parameter values for processes that are fairly well understood.

In general, uncertainty due to inherent randomness of physical processes cannot be eliminated. Other uncertainties such as those associated with the lack of complete knowledge of the process, models, parameters, and data can be reduced through research, data collection, and careful manufacture.

The existence of uncertainties is the main contributor to potential failure of hydraulic structures. Knowledge of statistical information describing the uncertainties is essential in reliability analysis. Therefore, uncertainty analysis is a prerequisite for reliability analysis.

The most complete description of uncertainty is the probability density function of the quantity subject to uncertainty. However, in most practical problems such a probability function cannot be derived precisely. Another measure of the uncertainty of a quantity is to express it in terms of a confidence interval. A useful alternative is to use the statistical moments associated with a quantity subject to uncertainty. In particular, the second-order moment is a measure of the dispersion of a random variable.

The main objective of uncertainty analysis is to identify the statistical properties of a model output as a function of stochastic input parameters. Uncertainty analysis provides a framework to quantify the uncertainty associated with model output. Furthermore, it offers the designer insight regarding the contribution of each stochastic input parameter to the overall uncertainty of the model output. Such knowledge is essential to identify the important parameters to which more attention should be given, in order to have a better assessment to their values, and accordingly, to reduce the overall uncertainty of the output.

1.1.2 Reliability of hydraulic engineering

Hydraulic-engineering structures placed in a natural environment are subject to various external stresses. The resistance or strength of the structure is its ability to accomplish the intended mission satisfactorily, without failure, when subject to load of demands or external stresses. Failure occurs when the load exceeds the resistance of the system.

The reliability of a hydraulic-engineering structure is the probability of safety p_s that the load does not exceed the resistance of the structure,

$p_s = P\ [L \leq R]$; where p [ ] denotes probability.

Conversely, the failure probability p_f can be expressed as:

$$p_f = P[L > R] = 1 - p_s$$

Failure of hydraulic-engineering structures can be classified as structural failure and performance failure. Structural failure involves damage or change of the structure, hindering its ability to function as desired. On the other hand, performance failure does not necessarily involve structural damages, but the performance limit of the structure is exceeded and undesirable consequences occur.

A common practice for measuring the reliability of a hydraulic-engineering structure is the return period or recurrence interval. Two other types of reliability measures are frequently used in engineering practice to consider the relative magnitudes of resistance and anticipated load (called the design load) One measure is the safety margin (SM) defined as the difference between the resistance and the anticipated load, that is,

$$SM = R - L.$$

The other measure is the safety factor (SF) which is the ratio of resistance to load as:

$$SF = \frac{R}{L}$$

There are two major steps in reliability analysis:
- identify and analyse the uncertainties of each of the contributing factors;
- combine the uncertainties of the stochastic factors to determine the overall reliability of the structure.

1.2 Review of relevant statistical theories

1.2.1 Stochastic variables and their distributions

A stochastic variable is the real-valued outcome of an experiment, and can be discrete or continuous. A stochastic variable X can be described by its cumulative distribution function or simply distribution function, defined as:

$$F(x) = P(X \leq x)$$

The distribution function is a non-decreasing function of its argument. Furthermore, $\lim_{x\to-\infty}F(x) = 0$, and $\lim_{x\to+\infty}F(x) = 1$. For a continuous stochastic variable, the probability density function f(x) is defined as:

$$f(x) = \frac{dF(x)}{dx}$$

It follows that:

$$P(x < X \leq x + dx) = P(X \leq x + dx) - P(X \leq x) = F(x + dx) - F(x) = f(x)dx$$

The probability density function multiplied with an infinitesimal interval width gives the chance that the stochastic variable takes a value within that interval.

1.2.2 Statistical properties of stochastic variables

Descriptors that are commonly used to assess statistical properties of a stochastic variable are those showing the central tendency, dispersion, and asymmetry of a distribution. These descriptors are related to the statistical moments of the variable.

The central tendency of a variable is commonly measured by the expectation, the first-order central moment, which is defined as:

$$E[X] = \mu = \int_{-\infty}^{\infty} xf(x)\,dx$$

This expectation is known as the mean of a stochastic variable.

The variability of a variable is measured by the variance, the second-order central moment, which is defined as:

$$Var[X] = \sigma^2 = E\left[(X - \mu)^2\right] = \int_{-\infty}^{\infty} (x - \mu)^2 f(x)\,dx$$

The positive square root of variance is called the standard deviation, which is often used as the measure of the degree of uncertainty associated with a stochastic variable.

The asymmetry of the probability density function of a stochastic variable is measured by the skew coefficient γ, defined as:

$$\gamma = \frac{E\left[(X - \mu)^3\right]}{\sigma^3}$$

The skew coefficient is dimensionless and is related to the third central moment. Skewed distributions have more values to one side of the peak or most likely value – one tail is much longer than the other. The higher the skew coefficient, the more skewed the distribution.

1.2.3 Probability distributions

Normal distribution

One of the most used distribution types is the normal or Gauss distribution. A normal stochastic variable having the mean μ and variance σ^2 has the probability density function:

$$f(x|\mu,\sigma^2) = \frac{1}{\sqrt{2\pi}}\frac{1}{\sigma}\exp\left\{-\frac{(x - \mu)^2}{2\sigma^2}\right\} \qquad \text{for} \quad -\infty < x < \infty$$

The normal distribution is bell-shaped and symmetric with respect to $x = \mu$.

The distribution of the sum of a number of independent stochastic variables, regardless of their individual distribution, can be approximated by a normal distribution as long as none of the variables has a dominant effect on the sum. This is known as the central limit theorem.

Probability computations for normal distributed variables are made by first transforming to a standardised variable Z as:

$$Z = \frac{X - \mu}{\sigma}$$ in which Z has a mean of zero and a variance of one.

The probability density function of Z, called the standard normal distribution, is:

$$\phi(z) = \frac{1}{\sqrt{2\pi}} \exp\left\{-\frac{z^2}{2}\right\} \quad \text{for} \quad -\infty < z < \infty$$

Computations of probability for a normal stochastic variable can be made as:

$$P(X \le x) = P\left[\frac{(X - \mu)}{\sigma} \le \frac{(x - \mu)}{\sigma}\right] = P[Z \le z] = \Phi(z)$$

where $\Phi(z)$ is the cumulative distribution function of the standard normal distributed variable. A table of standard normal probability is available.

Lognormal distribution

The lognormal distribution is a commonly used continuous distribution when variables cannot be negative-valued. A stochastic variable X is lognormally distributed if its logarithmic transform Y = ln(X) has a normal distribution with mean $\mu_{\ln X}$ and variance $\sigma^2_{\ln X}$. The probability density function of a lognormal distributed variable is:

$$f\left(x \middle| \mu_{\ln X}, \sigma^2_{\ln X}\right) = \frac{1}{\sqrt{2\pi}} \frac{1}{\sigma_{\ln X}\, x} \exp\left\{-\frac{1}{2}\left(\frac{\ln(x) - \mu_{\ln X}}{\sigma_{\ln X}}\right)^2\right\} \quad x > 0$$

Statistical properties of a lognormal variable on the original scale can be computed from those of the log-transformed variable.

Since the sum of normal variables is normally distributed, the product of independent lognormal variables is also lognormally distributed.

Gamma distribution

The gamma distribution is an example of an extreme value distribution. The two-parameter gamma distribution has the probability density function defined as:

$$f\left(x \middle| \alpha, \beta\right) = \frac{\beta}{\Gamma(\alpha)} (\beta x)^{\alpha - 1} \exp(-\beta x) \qquad \text{for} \quad x > 0$$

in which $\alpha > 0$ and $\beta > 0$ are parameters and $\Gamma(\,)$ is a gamma function.

1.2.4 Multiple stochastic variables

When problems involve multiple stochastic variables, the joint distribution is used. For the purpose of illustration, the discussions are limited to problems involving two continuous stochastic variables. For discrete stochastic variables, one simply replaces the integrals by summations.

The joint probability density function of two continuous stochastic variables X and Y is denoted as $f_{X,Y}(x,y)$ and the corresponding cumulative distribution function is:

$$F_{X,Y}(x,y) = \int_{-\infty}^{x} \int_{-\infty}^{y} f_{X,Y}(x,y)\, dx\, dy$$

Two stochastic variables X and Y are statistically independent only if $f_{X,Y}(x,y) = f_X(x)f_Y(y)$ and $F_{X,Y}(x,y) = F_X(x)F_Y(y)$.

When a problem involves two dependent stochastic variables, the degree of linear dependence between the two can be measured by the correlation coefficient $\rho(X,Y)$ which is defined as:

$$\rho(X,Y) = \frac{\mathrm{cov}(X,Y)}{\sigma_X \sigma_Y}$$

where cov(X,Y) is the covariance between stochastic variables X and Y defined as:

$$\mathrm{cov}(X,Y) = E\left[(X - \mu_X)(Y - \mu_Y)\right] = E(XY) - \mu_X\mu_Y$$

1.3 First-order variance estimation method for uncertainty analysis

The methods applicable for uncertainty analysis are dictated by the information available on the stochastic variables involved and the functional relationships among the variables. In principle, it would be ideal to derive the exact probability distribution of the model output as a function of those of the stochastic variables. However, most of the models used in hydraulic engineering are non-linear and highly complex. This basically limits analytical derivation of the statistical properties of model output. Therefore, engineers frequently have to resort to methods that yield approximations to the statistical properties of uncertain model output.

The first-order variance estimation method estimates uncertainty in terms of the variance of system output, which is evaluated on the basis of statistical properties of the system's stochastic variables. The method approximates the function involving stochastic variables by the Taylor series expansion.

Consider a design quantity W is related to N stochastic variables X as:

$$W = g(X) = g(X_1, X_2, \ldots, X_N)$$

where X is an N-dimensional column vector of stochastic variables. The Taylor series expansion of the function g(X) with respect to a selected point $X = x_0$ can be expressed as:

$$W = g(x_0) + \sum_{i=1}^{N}\left(\frac{\partial g}{\partial X_i}\right)_{x_0}(X_i - x_{i0}) + \frac{1}{2}\sum_{i=1}^{N}\sum_{j=1}^{N}\left(\frac{\partial^2 g}{\partial X_i \partial X_j}\right)_{x_0}(X_i - x_{i0})^2 + \varepsilon$$

in which ε represents the higher-order terms. The partial derivative terms are called the sensitivity coefficients, each represents the rate of change of model output W with respect to a unit change of each variable around x_0. Dropping the second- and higher-order terms, the preceding equation can be expressed, in matrix/vector form, as:

$$W \approx g(x_0) + s_0^T(X - x_0)$$

in which s_0 is the vector of sensitivity coefficients evaluated at $X = x_0$. The mean and variance of W, by the first-order approximation, can be expressed, respectively, as:

$E[W] \approx g(x_0) + s_0^T(\mu - x_0)$ in which μ is the vector of means

and

$\mathrm{Var}[W] \approx s_0^T C(X) s_0$ in which C(X) is the covariance matrix

The common practice of the first-order variance method is to take the expansion point $x_0 = \mu$ and the mean and variance of W can be estimated as:

$$E[W] \approx g(\mu)$$

and

$$Var[W] \approx s^T C(X) s$$

in which s is an N-dimensional vector of sensitivity coefficients evaluated at $x_0 = \mu$. When all the stochastic variables are independent, the variance of model output W can be approximated as:

$$Var[W] \approx s^T D s = \sum_{i=1}^{N} s_i^2 \sigma_i^2$$ in which D is a diagonal matrix of variances

The ratio $s_i^2\sigma_i^2/var[W]$ indicates the proportion of overall uncertainty in the model output contributed by the uncertainty associated with variables X_i.

The first-order variance estimation method does not require knowledge of the probability density function of stochastic variables which simplifies the analysis. However, this advantage is also a disadvantage of the method because it is insensitive to the distributions of stochastic variables in the uncertainty analysis.

1.4 Load-resistance interference reliability analysis

Failure of an engineering system occurs when the load L on the system exceeds the resistance R of the system. The definitions of reliability and failure probability are applicable to component reliability, as well as total system reliability. Resistance and load are frequently functions of a number of stochastic variables, that is, $L = g(X_L)$ and $R = h(X_R)$. Accordingly, the reliability is a function of the stochastic variables involved as:

$$p_s = P[g(X_L) \leq h(X_R)]$$

Computations of reliability using this function do not consider the time-dependence of loads. This is referred to as the static reliability model, which is generally applied when the performance of the system subject to a single worst load event is of concern.

1.4.1 Reliability performance measures

In reliability analysis, the equation:

$$p_s = P[g(X_L) \leq h(X_R)]$$

is often expressed in terms of a performance function $W(X) = W(X_L,X_R)$ as:

$$p_s = P[W(X_L,X_R) \geq 0] = P[W(X) \geq 0]$$

In reliability analysis, the system state is divided into a safe set defined by $W(X) \geq 0$ and a failure set defined by $W(X) < 0$. The boundary that seperates the safe set and failure set is a surface defined by $W(X) = 0$ and this surface is called the failure surface or limit-state surface. Since the performance function W(X) defines the condition of the system, it is sometimes called the system state function.

The performance function W(X) can be expressed as:

$$W(X) = R - L = h(X_R) - g(X_L)$$

which is identical to the notion of safety margin.

The reliability index $\beta = \mu_W/\sigma_W$ is another frequently used reliability indicator, which is defined as the reciprocal of the coefficient of variation of the performance function W(X). In the definition of β, μ_W and σ_W are the mean and standard deviation of the performance function, respectively. The reliability, assuming an appropriate probability density function, can then be computed as:

$$p_S = 1 - F_W(0) = 1 - F_{W'}(-\beta)$$

in which $F_{W'}$ is the cumulative density function of the performance variable W and W' is the standardised performance variable defined as $W' = (W - \mu_W)/\sigma_W$. In practice, the normal distribution is commonly used for W(X), in which case the reliability can be computed as:

$$p_S = 1 - \Phi(-\beta) = \Phi(\beta)$$

in which $\Phi()$ is the standard normal cumulative density function.

1.4.2 Mean-value first-order second moment (MFOSM) method

The MFOSM method for reliability analysis employs the FOVE method to estimate the statistical moments of the performance function W(X). Once the mean and standard deviation of W(X) are obtained, the reliability index β_{MFOSM} is computed as:

$$\beta_{MFOSM} = \frac{W(\mu)}{\sqrt{s^T C(X)\, s}}$$

from which the reliability is computed according to $p_S = \Phi(\beta)$.

The application of the MFOSM method is simple and straightforward. However, it possesses certain weaknesses:

- Provided that $p_S < 0.99$, reliability is not greatly influenced by the choice of distribution for W, and the assumption of a normal distribution is quite satisfactory. For reliability higher than this value, accurate assessment of the distribution of W (X) should be made.
- Inappropriate choice of the expansion point: in reliability computation, one should be concerned with those points in the parameter space that fall on the limit-state surface.
- Poor estimation of the mean and variance of highly non-linear functions: this because the first-order approximation of a highly non-linear function is not accurate.
- Sensitivity of the computed failure probability to the formulation of the performance function W.
- Inability to incorporate available information on of the stochastic variables affecting the load and resistance.

From these arguments, the general rule of thumb is not to rely on the result of the MFOSM method if any of the following conditions exist:

- high accuracy requirements for the estimated reliability
- high non-linearity of the performance function
- many skewed stochastic variables are involved in the performance function.

1.4.3 Advanced first-order second moment (AFOSM) method

The main thrust of the AFOSM method is to reduce the error of the MFOSM method associated with the non-linearity and non-invariability of the performance function, while keeping the simplicity of the first-order approximation. In the AFOSM method, the expansion point $x_* = (x_L^*, x_R^*)$ is located on the failure surface defined by the limit-state equation $W(x) = 0$ which defines the boundary that separates the system performance from being unsafe or being safe, that is:

$$W(x) \begin{cases} > 0 & \text{safe region} \\ = 0 & \text{failure surface} \\ < 0 & \text{failure region} \end{cases}$$

Among all the possible values of x that fall on the limit-state surface $W(x) = 0$, one is more concerned with the combination of stochastic variables that would yield the lowest reliability or highest risk. The point on the failure surface with the lowest reliability is the one having the shortest distance to the point where the means of the stochastic variables are located. This point is called the design point by Hasofer and Lind or the most probable failure point.

Refer to the first-order approximation of the performance function W(X). Taking the expansion point $x_0 = x_*$, the expected value and variance of the performance function W(X) can be approximated as:

$$\mu_W \approx s_*^T (\mu - x_*)$$

$$\sigma_W^2 \approx s_*^T C(X) s_*$$

in which $s_* = (s_{1*}, s_{2*}, \ldots, s_{N*})^T$ is a vector of sensitivity coefficients of the performance function W(X) evaluated at x_*; and μ and C(X) are the mean vector and covariance matrix of the stochastic variables, respectively. The standard deviation of the performance function W(X) can alternatively be expressed in terms of the directional derivatives, with uncorrelated stochastic variables, as:

$$\sigma_W = \sum_{i=1}^{N} \alpha_{i*} s_{i*} \sigma_i$$

where α_{i*} is the directional derivative for the i-th stochastic variable at the expansion point x_*:

$$\alpha_{i*} = \frac{s_{i*}\sigma_i}{\sum_{j=1}^{N} s_{j*}\sigma_j}$$

Figure 1.1 shows the design point and an unit vector α_* emanating from this point. The elements of α_*, α_{i*}, are called the directional derivatives.

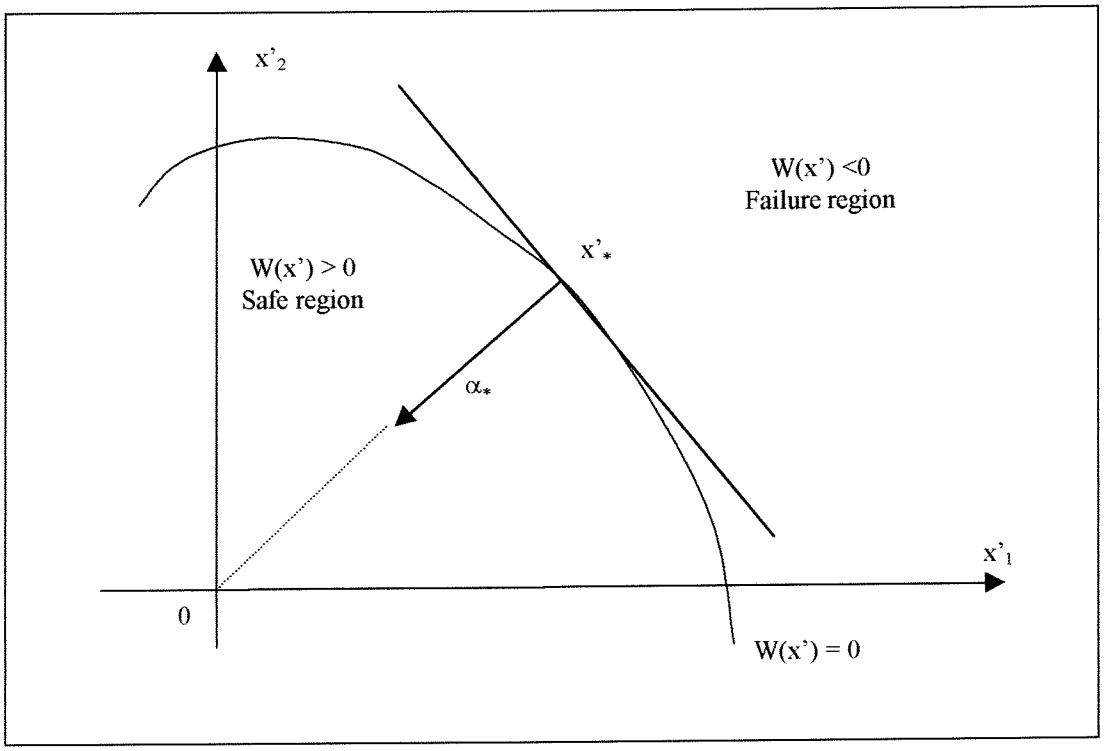

Figure 1.1 Characteristics of design point in standardized spaces

With the mean and standard deviation of the performance function W(x) computed at x_*, the AFOSM reliability index β_{AFOSM} can be determined as:

$$\beta_{AFOSM} = \frac{\mu_W}{\sigma_W} = \frac{\sum_{i=1}^{N} s_{i*}(\mu_i - x_{i*})}{\sum_{i=1}^{N} \alpha_{i*} s_{i*} \sigma_i}$$

This equation indicates that the AFOSM reliability index β_{AFOSM} is identical to the shortest distance from the origin to the design point in the standardised parameter space. β_{AFOSM} is also called the Hasofer-Lind reliability index.

Once β_{AFOSM} is computed, the reliability can be estimated as $p_S=\Phi(\beta_{AFOSM})$. The rate of change in β_{AFOSM} due to a one standard deviation change in stochastic variable X_i is represented by $-\alpha_{i*}$.

Due to the nature of non-linear optimisation, the algorithm AFOSM-HL does not necessarily converge to the true design point associated with the minimum reliability index. Therefore, different initial trial points have to be used and the smallest reliability index has to be selected to compute the reliability.

A procedure for finding the true design point, is to make a new estimation of the first design point, with:

$$x_{i*} = \mu_{i*} - \alpha_{i*}\beta_*\sigma_i \qquad \text{for } i = 1,2,\ldots,N$$

However, the values of the directional derivatives were determined in the old design point.

Therefore, an iteration is necessary until a stable value of the design point that is the true design point, has been found.

When non-normal stochastic variables are involved, it is advisable to transform them into equivalent normal variables. An approach is to transform a non-normal distribution into an equivalent normal distribution, so that the value of the cumulative distribution function of the transformed equivalent normal distribution is the same as that of the original non-normal distribution at the failure point x_*, that is:

$$F_i(x_{i*}) = \Phi\left(\frac{x_{i*} - \mu_{i*N}}{\sigma_{i*N}}\right)$$

in which $F_i(x_{i*})$ is the cumulative density function of the stochastic variable X_i having a value at x_{i*}; and μ_{i*N} and σ_{i*N} are the mean and standard deviation of normal equivalent for the i-th stochastic variable at $X_i = x_{i*}$. From this expression, the following equations can be obtained:

$$\mu_{i*N} = x_{i*} - z_{i*}\sigma_{i*N}$$

$$\sigma_{i*N} = \frac{\Phi(z_{i*})}{f_i(x_{i*})}$$ in which $z_{i*} = \Phi^{-1}[F_i(x_{i*})]$ is the standard normal quantile.

To incorporate the normal transformation for non-normal but uncorrelated stochastic variables, the iterative algorithm for the AFOSM method has to be modified. The directional derivatives are computed by substituting the σ_{i*N}'s for the corresponding standard deviations of non-normal stochastic variables σ_i's. Then, β and α_{iN} are used to revise the location of the expansion point $x_{(r+1)}$ according to:

$$x_{i*} = \mu_{i*} - \alpha_{i*}\beta_*\sigma_i \qquad \text{for } i = 1,2,\ldots,N$$

2 SOFTWARE USED

With the used software the extent of influence of the separate hydrodynamic variables in the equilibrium equations of outfall stability is analysed. In this chapter, the computer programs VaP and BestFit, the considered equilibrium equations, the used distribution types and the methods of analysis are described.

2.1 VaP

2.1.1 Program information

VaP 1.5 for Windows, student version, not for commercial use.
Copy licensed to Delft Technical University, Department of Civil Engineering.
Created by Dr. M. Petschacher.
Copyright © Institute of Structural Engineering IBK
Eidgenössische Technische Hochschule Zürich.

2.1.2 Function and purpose

The Variables Processor (VaP) enables the user of the program to deal with stochastic quantities, so-called variables, in some given mathematical expression. In view of one of the applications of the program, this expression is called a Limit State Function. The program lends itself to the evaluation of influence of variables. Disadvantage of VaP 1.5 is that there is no possibility of defining and handling correlation between basic variables. This implies a complex expression for the limit state function.

2.1.3 Derivation of Limit State Function

If an outfall is exposed on the sea bed, it must resist lateral movement under the hydrodynamic forces induced by waves and currents. The hydrodynamic forces are calculated with the Morison equations. They are widely used in offshore pipeline engineering because it is the only reasonable straightforward theoretical model available. Figure 2.1 shows the forces on a cross-section of an unburied outfall, which resists lateral movement by its own weight.

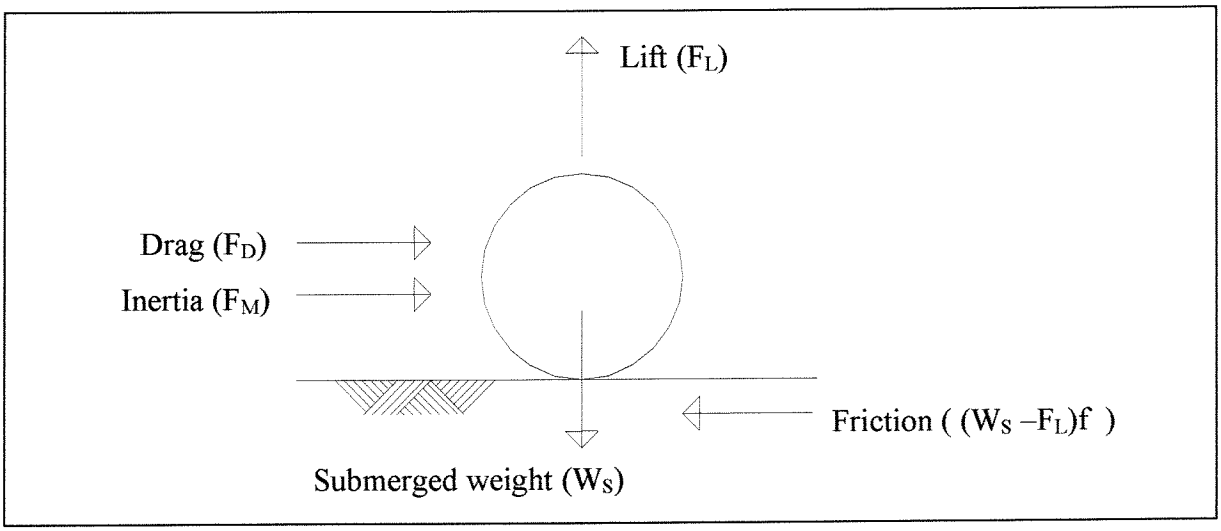

Figure 2.1 Hydrodynamic forces on an outfall segment

From figure 2.1 it can be shown that for the pipeline to remain stable:

$$W_S \geq \left(\frac{F_D + F_M}{f} \right) + F_L$$

where:

W_S	submerged pipeline weight per unit length of outfall
F_D	drag force due to waves and currents per unit length of outfall
F_M	inertia force due to waves and currents per unit length of outfall
F_L	lift force due to waves and currents per unit length of outfall
f	Coulomb friction factor

It is traditional to adopt an extremely simple idealisation of the geotechnical interaction between a pipeline and the sea bed, and to treat it as a contact governed by Coulomb friction.

The Limit State Function in VaP (Appendix V) is defined as:

$$G = (W_S - F_L)f - F_D - F_M$$

where:

G	stochastic quantity

F_L, F_D, F_M are defined as:

$$F_D = \frac{1}{2} \rho \, C_D \, D \, u_N |u_N|$$

$$F_M = \rho \, C_M \, \frac{1}{4} \pi D^2 \, a_N$$

$$F_L = \frac{1}{2} \rho \, C_L \, D \, u_N^2$$

where:

C_D	drag coefficient
C_M	inertia coefficient
C_L	lift coefficient
D	outside diameter of the pipeline
ρ	density of water
u_N	instantaneous horizontal water particle velocity normal to outfall
a_N	instantaneous horizontal water particle acceleration normal to outfall

The horizontal water particle velocity and acceleration components normal to the outfall are defined as:

$$u_N = V_C \sin \theta_{CO} + \left[\frac{\pi H}{T} \frac{\cosh\left(\frac{\pi D}{L}\right)}{\sinh\left(\frac{2 \pi h}{L}\right)} \cos \varphi \right] \sin \theta_{WO}$$

$$a_N = \left[\frac{2\pi^2 H}{T^2} \frac{\cosh\left(\frac{\pi D}{L}\right)}{\sinh\left(\frac{2\pi h}{L}\right)} \sin\varphi \right] \sin\theta_{WO}$$

where:

H	wave height
T	wave period
L	wave length
h	total water depth
θ_{WO}	angle between waves and outfall
V_C	current velocity averaged over outfall diameter
θ_{CO}	angle between current and outfall
φ	phase angle

The Limit State Function is written as an algebraic expression and is checked automatically for correct syntax and consistency.

2.1.4 Definition of variables

Each variable in the Limit State Function is assigned a distribution type with corresponding parameters (Appendix V). The following distribution types will be used:

- Deterministic (DT)
- Normal (N):
  One of the most used distribution types is the normal or Gauss distribution. The density function is given by:

$$f_X(\xi) = \frac{1}{\sqrt{2\pi}} \frac{1}{\sigma} \exp\left\{ -\frac{(\xi - \mu)^2}{2\sigma^2} \right\}$$

  where:

  μ = mean value
  σ = standard deviation (>0)

- Lognormal (LN):
  If x is lognormal distributed, then y = ln x is normal distributed, or x = exp y with y normal distributed. The lognormal distribution can be derived from the normal distribution with a non-linear transformation. The density function is given by:

$$f_X(\xi) = \frac{1}{\sqrt{2\pi}} \frac{1}{\sigma_Y} \frac{1}{\xi} \exp\left\{ -\frac{(\ln\xi - \mu_Y)^2}{2\sigma_Y^2} \right\}$$

- Gamma (G):
  The Gamma distribution is an example of an extreme value distribution. The density function is given by:

$$f_X(\xi) = \frac{1}{a\,\Gamma(k)} \left(\frac{\xi}{a}\right)^{k-1} \exp\left(\frac{-\xi}{a}\right) \qquad \text{with gamma function } \Gamma(k)$$

2.1.5 Methods of analysis

Different methods of analysis are implemented in VaP. It calculates the moments $E[G(X)^n]$ of the stochastic quantity G, and/or the probability of failure, defined as $p_f = P[G(X) \leq 0]$. Therefore, approximation methods (e.g. First Order Reliability Method), simulation methods (e.g. Crude Monte Carlo Method), or numerical integration methods (e.g. Evans) can be chosen.

The results of the FORM are the so called Hasofer/Lind index (also known as the geometrical β-value), the sensitivity factors α and the design values of the non-deterministic variables. It appeared that FORM had difficulties with user defined variables, due to the particular shape of the corresponding histograms. This problem was solved by using the computer program BestFit, that fits curves to the histograms (Appendix IV).

In this report, the sensitivity factors α have been used to analyse the extent of the influence of each of the hydrodynamic variables in the equilibrium equations of the stability of outfalls. This results in insight regarding the contribution of the separate hydrodynamic variables to the overall uncertainty of an outfall stability analysis. The various force coefficients are left out of consideration in this sensitivity analysis, because their theoretical and empirical backgrounds are not clear enough.

2.2 BestFit

2.2.1 Program information

BestFit 1.0
Copyright (c) 1993
Palisade Corporation
Palisade and BestFit are registered trademarks of Palisade Corporation.

2.2.2 Function and purpose

As stated, the First Order Reliability Method in VaP has difficulties with the user defined variables, due to the particular shape of the corresponding histograms. To avoid this problem, the histograms in the Aveiro case and the Northumbrian case, describing the distribution of wave height, period and length, are curve-fitted with the computer program BestFit.

The goal of BestFit is to find the distribution that best fits the input data. BestFit does not produce an absolute answer, it just identifies the distribution that is most likely to have produced the data. The results of a best fit calculation are only a best estimate, as it is nearly impossible to find an exact distribution to fit the data. Therefore the BestFit results are evaluated quantitatively and qualitatively, examining both the comparison graphs and statistics prior to using a result.

3 CASE STUDIES

For the researches into the influence of hydrodynamic variables in the equilibrium equations of the stability of outfalls, two practice cases and a theoretical case are analysed. The wave climate data of the practice cases in Aveiro (Portugal) and Northumbrian(England) is supplied by Van Oord ACZ. In this chapter, the VaP input and output is shown, processed and evaluated.

3.1 Aveiro – Portugal case

The wave climate in Aveiro is characterised by rather high and long waves. Van Oord ACZ is involved here in a sand reclamation project. Because outfall installation is taking place during the summer period, when the wave climate is more moderate, only the months July, August and September of the wave climate data are taken into account (Appendix III).

Distribution types and values of the parameters
With the values of a default situation as starting-point, the parameters that change in three other situations are:

- Situation A: smaller water depth (which also influences the wave length)
- Situation B: higher current velocity
- Situation C: smaller outfall diameter

In table 3.1, the parameters which distribution type and values are not changed in situation A, B or C are presented.

Table 3.1 Invariable parameters (Aveiro case)

Parameter	Type		Value	Unit
wave height (H)	G	μ	1.597	m
		σ	0.975	m
wave period (T)	LN	μ	6.293	s
		σ	2.120	s
angle of wave attack (θ_{wo})	N	μ	25	deg
		σ	5	deg
angle of current attack (θ_{co})	N	μ	70	deg
		σ	20	deg
Coulomb friction factor (f)	D		0.7	-
density of water (ρ)	D		1024	kg/m^3

In table 3.2, the parameters which distribution type and values are changed in situation A, B or C are presented.

Table 3.2 Variable parameters (Aveiro case)

Parameter	Type		Default situation	Situation A	Situation B	Situation C	Unit
wave length L	LN	μ	56.996	*51.094*	56.996	56.996	m
		σ	29.719	*23.707*	29.719	29.719	m
current velocity V_C	N	μ	1.028	1.028	*2.056*	1.028	m/s
		σ	0.156	0.156	*0.156*	0.156	m/s

water depth h	DT	15	*10*	15	15	m
phase angle φ	DT	60	60	*50*	*50*	deg
outfall diameter D	DT	1.5	1.5	1.5	*0.9*	m
submerged weight W_S	DT	2950	*3932*	*7993*	*1460*	N/m
current ratio		7.11	4.38	14.22	7.12	-
KC-number		0.57	0.93	0.57	0.95	-
a'/D-ratio		5.97	4.26	21.01	9.96	-
drag coefficient C_D	DT	1.05	1.05	1.05	1.05	-
inertia coefficient C_M	DT	3.00	3.00	3.00	3.00	-
lift coefficient C_L	DT	1.00	*1.30*	*0.80*	*0.80*	-

Adding remark regarding the wave length

The mean value μ and standard deviation σ of L is determined by calculating L with the minimum, mean and maximum value of T. The calculation uses the linear wave theory. Because of the lognormal distribution of T, L is also regarded lognormal distributed.

Adding remark regarding the current velocity

The value of the current velocity V_C, denoted in knot (nautical mile per hour; 0.514 m/s), is read from nautical cards. This implies an accuracy of half a knot. The common practice is to determine the stability of outfalls is with a minimum V_C of 2 knots.

V_C is regarded normal distributed. The distribution function of the normal distribution is not known in analytical form, but has to be looked up in a table. For small chances the following approximation can be used:

$$P(u < a) = \Phi_N(\nu) = \frac{1}{-\nu\sqrt{2\pi}} \exp\left(-\frac{\nu^2}{2}\right)$$

The approximation is valid for $\nu < -2$

assume: $V_C = 2$ knots $= 1.029$ m/s

demand: $P(V_C < 0.772) = 0.05$

$\Rightarrow$ $\phi_N(-1.65) = 0.05$

$P(u < -1.65)$

$P(1.028 + \sigma \cdot u < 0.772)$

$\sigma \cdot u < -0.258$

$u < -0.258/\sigma = -1.65$

$\rightarrow$ $\sigma = 0.156$

check: $P(V_C < 1.286) = 0.95$

$P(1.028 + 0.1564 \cdot u < 1.286)$

$P(u < 1.64)$

$\Rightarrow$ $\phi_N(1.64) = 1 - \phi_N(-1.64) = 1 - 0.05 = 0.95$

thus: $V_C = n$ knots $\Rightarrow$ $\mu = n \cdot 0.514$ m/s

$\sigma = 0.156$ m/s

The cases are calculated with a default mean and standard deviation of V_C of 1.028 m/s and 0.156 m/s. In situation B the mean of V_C is changed to 2.056 m/s, with the same standard deviation of 0.156 m/s.

Sensitivity factors of the hydrodynamic variables

The sensitivity factors of the hydrodynamic variables in the Aveiro case, found with VaP, are presented in table 3.3 and in figure 3.1.

Table 3.3 Sensitivity factors of the hydrodynamic variables (Aveiro case)

	Sensitivity factors α			
	Default situation	Situation A	Situation B	Situation C
H (wave height)	0,19	0,28	0,10	0,16
L (wave lenght)	0,40	0,31	0,21	0,34
T (wave period)	0,16	0,23	0,06	0,11
V_c (current velocity)	0,14	0,09	0,19	0,23
θ_{CO} (angle of current attack)	0,09	0,06	0,43	0,14
θ_{WO} (angle of wave attack)	0,02	0,02	0,01	0,01

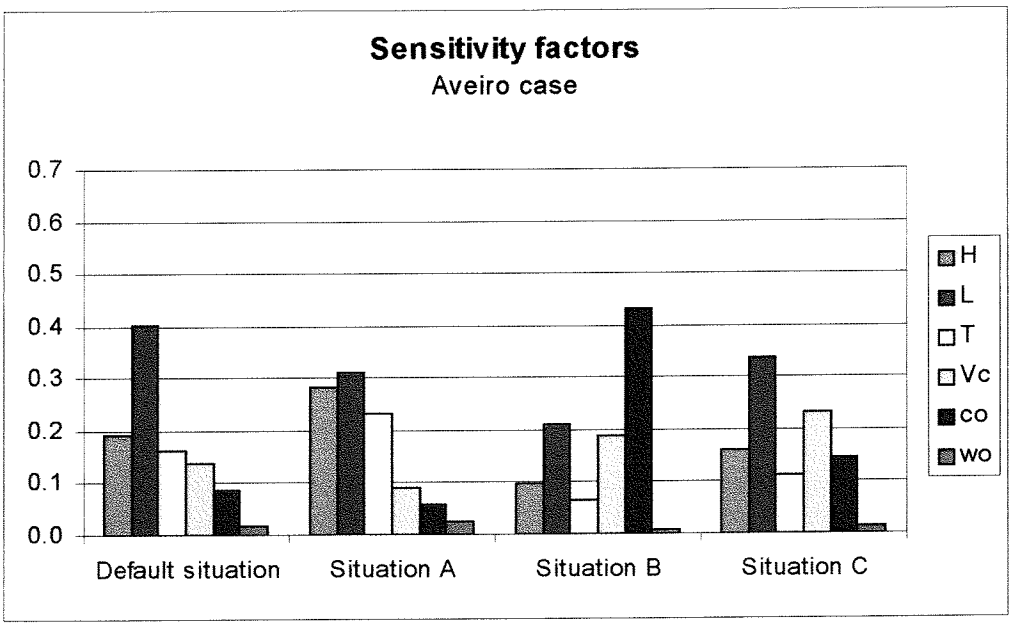

Figure 3.1 Sensitivity factors of the hydrodynamic variables (Aveiro case)

3.2 Northumbrian – England case

The wave climate in Northumbrian is moderate. Van Oord ACZ is involved here in an outfall project. Because the wave climate data were given annually, only the yearly distributions are taken into account (Appendix III).

Distribution types and values of the parameters

With the values of a default situation as starting-point, the parameters that change in three other situations are:

- Situation A: smaller water depth (which also influences the wave length)
- Situation B: higher current velocity
- Situation C: smaller outfall diameter

In table 3.4, the parameters which distribution type and values are not changed in situation A, B or C are presented.

Table 3.4 Invariable parameters (Northumbrian case)

Parameter	Type		Value	Unit
wave height (H)	G	μ	0.945	m
		σ	0.999	m
wave period (T)	LN	μ	5.099	s
		σ	1.409	s
angle of wave attack (θ_{wo})	N	μ	25	deg
		σ	5	deg
angle of current attack (θ_{co})	N	μ	70	deg
		σ	20	deg
Coulomb friction factor (f)	D		0.7	-
density of water (ρ)	D		1024	kg/m^3

In table 3.5, the parameters which distribution type and values are changed in situation A, B or C are presented.

Table 3.5 Variable parameters (Northumbrian case)

Parameter	Type		Default situation	Situation A	Situation B	Situation C	Unit
wave length L	LN	μ	40.052	*37.494*	40.052	40.052	m
		σ	19.850	*15.902*	19.850	19.850	m
current velocity V_C	N	μ	1.028	1.028	*2.056*	1.028	m/s
		σ	0.156	0.156	*0.156*	0.156	m/s
water depth h	DT		15	*10*	15	15	m
phase angle φ	DT		70	70	*50*	*50*	deg
outfall diameter D	DT		1.5	1.5	1.5	*0.9*	m
submerged weight W_S	DT		2131	*2703*	*7152*	*1179*	N/m
current ratio			20.53	9.91	41.06	20.62	-
KC-number			0.16	0.33	0.16	0.27	-
a'/D-ratio			11.80	6.28	45.03	19.75	-
drag coefficient C_D	DT		1.05	1.05	1.05	1.05	-
inertia coefficient C_M	DT		3.00	3.00	3.00	3.00	-
lift coefficient C_L	DT		0.80	*0.90*	*0.80*	*0.80*	-

Sensitivity factors of the hydrodynamic variables

The sensitivity factors of the hydrodynamic variables in the Northumbrian case, found with VaP, are presented in table 3.6 and in figure 3.2

Table 3.6 Sensitivity factors of the hydrodynamic variables (Northumbrian case)

	Sensitivity factors α			
	Default situation	Situation A	Situation B	Situation C
H (wave height)	0,13	0,33	0,02	0,06
L (wave length)	0,23	0,24	0,04	0,11
T (wave period)	0,04	0,12	0,01	0,02
V_c (current velocity)	0,38	0,18	0,29	0,52
θ_{CO} (angle of current attack)	0,21	0,11	0,64	0,30
θ_{WO} (angle of wave attack)	0,01	0,02	0,00	0,00

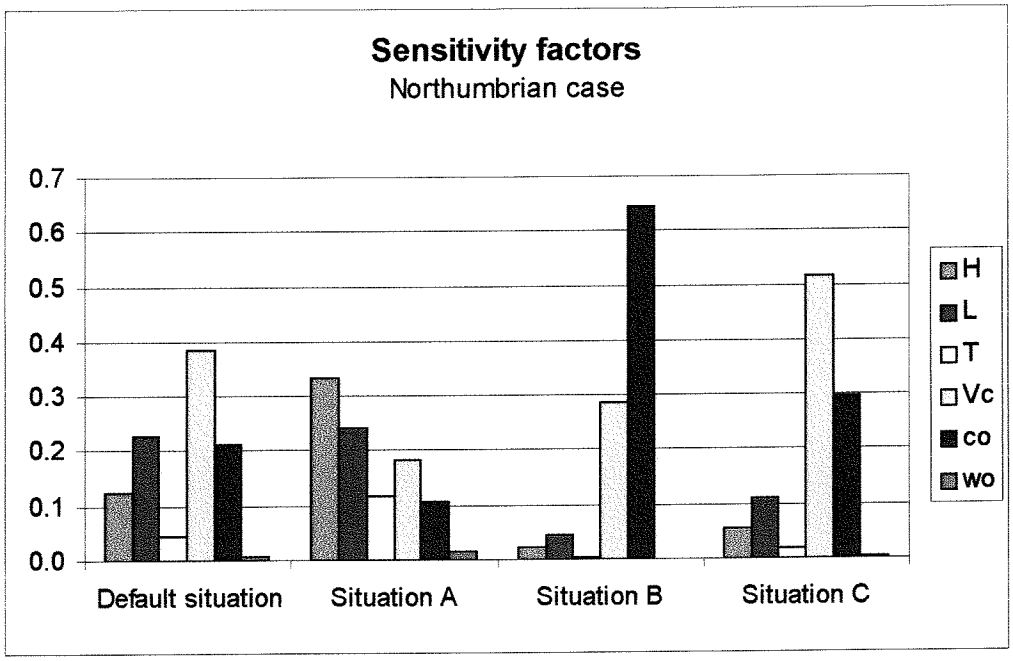

Figure 3.2 Sensitivity factors of the hydrodynamic variables (Northumbrian case)

3.3 Theoretical case

The standard deviations of the wave height, period, and indirectly the wave length, are derived from the previous two practical cases, in order to keep the theoretical case realistic.

Distribution types and values of the parameters
With the values of a default situation as starting-point, the parameters that change in three other situations are:

- Situation A: smaller water depth (which also influences the wave length)
- Situation B: higher current velocity
- Situation C: smaller outfall diameter

In table 3.7, the parameters which distribution type and values are not changed in situation A, B or C are presented. The parameters which distribution type and values are changed in situation A, B or C are presented in table 3.8.

Table 3.7 Invariable parameters (theoretical case)

Parameter	Type		Value	Unit
wave height (H)	G	μ	2.5	m
		σ	1.0	m
wave period (T)	LN	μ	6.0	s
		σ	1.5	s
angle of wave attack (θ_{wo})	N	μ	25	deg
		σ	5	deg
angle of current attack (θ_{co})	N	μ	70	deg
		σ	20	deg
Coulomb friction factor (f)	D		0.7	-
density of water (ρ)	D		1024	kg/m^3

Table 3.8 Variable parameters (theoretical case)

Parameter	Type		Default situation	Situation A	Situation B	Situation C	Unit
wave length L	LN	μ	53.0	*48.4*	53.0	53.0	m
		σ	21.7	*17.4*	21.7	21.7	m
current velocity V_C	N	μ	1.028	1.028	*2.056*	1.028	m/s
		σ	0.156	0.156	*0.156*	0.156	m/s
water depth h	DT		15	*10*	15	15	m
phase angle φ	DT		60	60	*50*	*50*	deg
outfall diameter D	DT		1.5	1.5	1.5	*0.9*	m
submerged weight W_S	DT		3787	*5249*	*8675*	*1691*	N/m
current ratio			4.99	2.94	9.98	5.00	-
KC-number			0.77	1.31	0.77	1.29	-
a'/D-ratio			4.42	3.25	14.85	7.38	-
drag coefficient C_D	DT		1.05	1.05	1.05	1.05	-
inertia coefficient C_M	DT		3.00	3.00	3.00	3.00	-
lift coefficient C_L	DT		1.30	*1.50*	*0.80*	*0.80*	-

Sensitivity factors of the hydrodynamic variables

The sensitivity factors of the hydrodynamic variables in the theoretical case, found with VaP, are presented in table 3.9 and in figure 3.3

Table 3.9 Sensitivity factors of the hydrodynamic variables (theoretical case)

	Sensitivity factors α			
	Default situation	Situation A	Situation B	Situation C
H (wave height)	0.12	0.20	0.07	0.11
L (wave length)	0.48	0.38	0.30	0.44
T (wave period)	0.16	0.24	0.08	0.12
V_c (current velocity)	0.13	0.08	0.16	0.19
θ_{CO} (angle of current attack)	0.08	0.05	0.38	0.12
θ_{WO} (angle of wave attack)	0.03	0.05	0.02	0.03

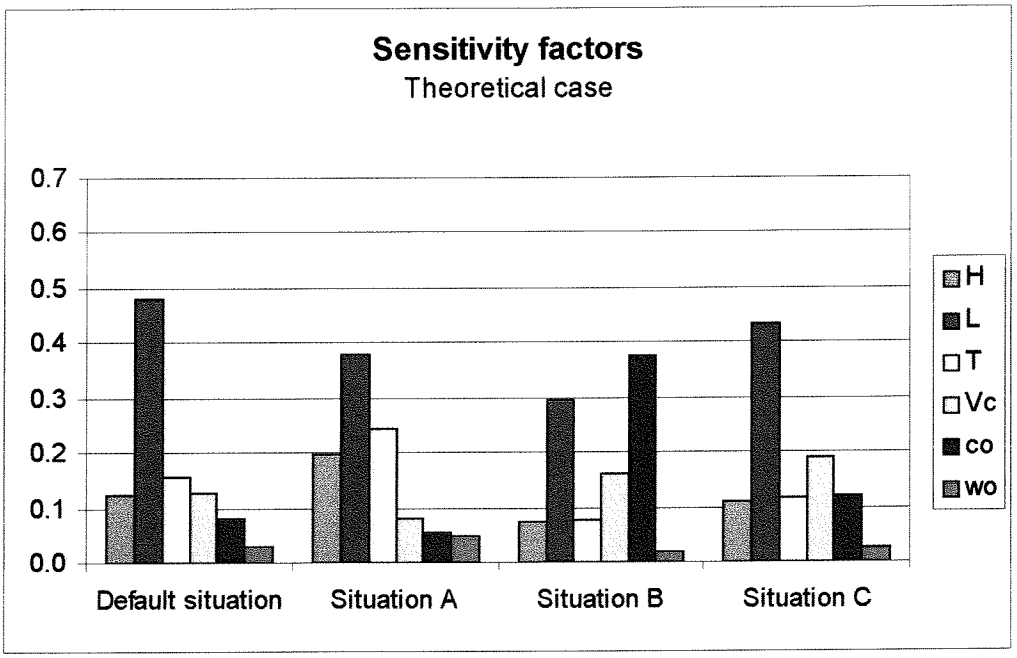

Figure 3.3 Sensitivity factors of the hydrodynamic variables (theoretical case)

4 CONCLUSIONS AND RECOMMENDATIONS

4.1 Conclusions

The extent of influence of the separate hydrodynamic variables in the equilibrium equations of outfall stability is analysed. The results give insight regarding the contribution of the hydrodynamic variables to the overall uncertainty of outfall stability:

1 In the case of a moderate current velocity, the hydrodynamic parameter which influences the stability of outfalls most is the wave period, which together with the water depth also determines the wave length. This is especially true for a wave climate that is characterised by rather high and long waves.
2 In the situation of more shallow water (cases, situation A), the wave height becomes increasingly important, compared to the default situation. Current velocity and angle of current attack decrease in importance.
3 In the situation of stronger currents (cases, situation B), the angle of current attack becomes increasingly important, compared to the default situation. Wave height and period decrease in importance.
4 In the situation of a smaller outfall diameter (cases, situation C), the angle of current attack becomes increasingly important, compared to the default situation. Wave height and period decrease in importance.
5 Small changes in the angle of wave attack are of little significance.

4.2 Recommendations

In order to reduce the overall uncertainty of outfall stability it is most important to:

- define the wave period accurate
- pay attention to the magnitude and angle of current attack.

A more thorough sensitivity analysis can be executed if the various hydrodynamic force coefficients are taken in consideration. This can be done if more information becomes available about the backgrounds the various researches and a just comparison can be made.

Further, a more advanced computer program, which has the possibility of defining and handling correlation between basic variables is recommended. With the use of such a computer program, the dependence of the wave length can be excluded.

REFERENCES

Vrouwenvelder, A.C.W.M., Vrijling, J.K., *Probalistisch ontwerpen.*
Notes on b3, Faculty of Civil Engineering, Delft University of Technology.

Groeneboom, P., et al., *Kansrekening en statistiek.*
Notes on a106, Faculty of Technical Mathematics and Informatics, Delft University of Technology, 1994.

Palmer, A.C., *Marine pipelines.*
Notes, Faculty of Civil Engineering, Delft University of Technology, 1997.

Palmer, A.C., et al., *Stability of pipelines in trenches.*
Proceedings, Offshore Oil Gas Pipeline Technology Seminar. Stavanger, 1988.

Fredsøe, J., Sumer, B.M., *Hydrodynamics around cylindrical structures.*
World Scientific, Advanced series on ocean engineering - volume12, 1997.

Mays, L.W., *Water resources handbook.*
Mc Graw-Hill, New York, 1996.

Gelder, P. van, *Software on reliability methods.*
Note, Faculty of Civil Engineering, Delft University of Technology, 1997.

PART C

STABILITY ANALYSIS OF AN OUTFALL UNDER OBLIQUE WAVE AND CURRENT ATTACK

INTRODUCTION

The final part of the graduate project 'Stability of outfalls during installation' was a stability analysis of an outfall under oblique wave and current attack.

The conservatism in the offshore technology common practice of pipeline stability applied to outfalls is among other things caused by not taking into account the hydrodynamic force variation along an outfall due to oblique wave attack. This is apparent because up to now there are no problems with stability of outfalls during installation. Therefore, a more specific approach on outfall stability that takes the hydrodynamic force variation along an outfall due to oblique wave attack into account is developed.

The structure of part C is as follows. Chapter 1 describes the hydrodynamic forces on and stability of an outfall segment. This is the conventional two-dimensional analysis of outfall stability. In chapter 2, the hydrodynamic forces and stability along an outfall are considered. This is a three-dimensional analysis of outfall stability, which takes the load variation due to oblique wave attack into account. Finally, the conclusions and recommendations are reported in chapter 3.

LIST OF SYMBOLS

η	instantaneous elevation of the water surface relative to SWL
H	wave height
k	wave number
x	horizontal co-ordinate in incoming wave direction
λ	wave length
ω	circular frequency
T	wave period
t	time
g	acceleration due to gravity
h	water depth
z	vertical co-ordinate measured from the still water level
u_m	wave-induced horizontal water particle velocity amplitude
a_m	wave-induced horizontal water particle acceleration amplitude
u_c	current velocity
f_h	horizontal hydrodynamic force per unit length
f_v	vertical hydrodynamic force per unit length
f_d	drag force per unit length
f_m	inertia force per unit length
f_l	lift force per unit length
C_D	drag coefficient
C_L	lift coefficient
C_M	inertia coefficient
θ_{wo}	angle of wave attack
θ_{co}	angle of current attack
W_S	submerged pipeline weight of outfall segment
r_c	Coulomb friction factor
D	outside diameter of outfall
ρ	density of water
ΔL	length of considered outfall segment
L	integrated part of outfall
L_P	projected wave length
$\bar{z}$	horizontal co-ordinate on outfall axis
Q	shear force
M	bending moment
EI	flexural rigidity

1 TWO-DIMENSIONAL OUTFALL STABILITY ANALYSIS

1.1 Forces due to wave cycles

The simplest and generally most useful theory for describing waves is the Airy theory. Airy presented this wave theory in which he simplified the wave profile to a linear sinusoidal wave form. His theory provides equations for the most important properties of surface gravity waves, and predicts these properties within useful limits in most practical conditions, even though real water waves are not sinusoidal. His definition sketch of a progressive, oscillatory surface gravity wave is presented in figure 1.1.

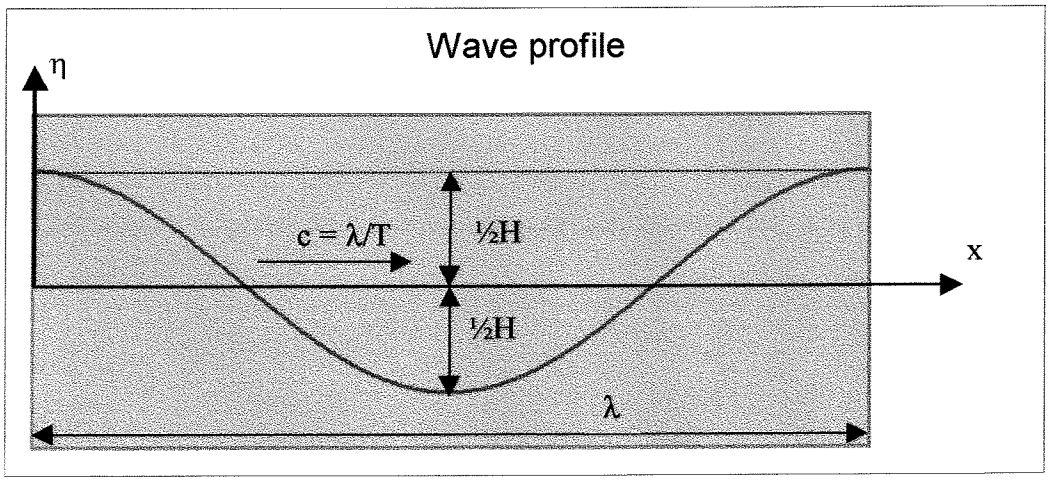

Figure 1.1 Definition sketch of a sinusoidal surface wave

This wave has the following characteristics (first order approximation):

- wave profile:

$$\eta = \frac{H}{2} \cos (kx - \omega t)$$

where:

η	instantaneous elevation of the water surface relative to SWL
H	wave height
k	wave number = $2\pi/\lambda$
x	horizontal co-ordinate in incoming wave direction
λ	wave length
ω	circular frequency = $2\pi/T$
T	wave period
t	time

- wave celerity:

$$c = \frac{\lambda}{T} = \frac{\omega}{k} = \frac{gT}{2\pi} \tanh kh$$

where:

g	acceleration due to gravity
h	water depth

- wave length:

$$\lambda = cT = \frac{gT^2}{2\pi} \tanh kh$$

- instantaneously wave-induced horizontal water particle velocity:

$$u_w = \frac{\omega H}{2} \frac{\cosh k(z+h)}{\sinh kh} \cos(kx - \omega t) = u_m \cos(kx - \omega t)$$

where:

z	vertical co-ordinate measured from the still water level
u_m	wave-induced horizontal water particle velocity amplitude

- instantaneously wave-induced horizontal water particle acceleration:

$$a_w = \frac{\omega^2 H}{2} \frac{\cosh k(z+h)}{\sinh kh} \sin(kx - \omega t) = a_m \sin(kx - \omega t)$$

where:

a_m	wave-induced horizontal water particle acceleration amplitude

The hydrodynamic drag and lift forces resulting from wave induced water particle velocities and hydrodynamic inertia forces resulting from water particle accelerations are calculated with the Morison equations. These equations are widely used in offshore engineering because it is the only reasonable straightforward theoretical model available. Figure 1.2 shows the forces on a cross-section of an exposed outfall segment on the seabed, which resists lateral movement by its own weight.

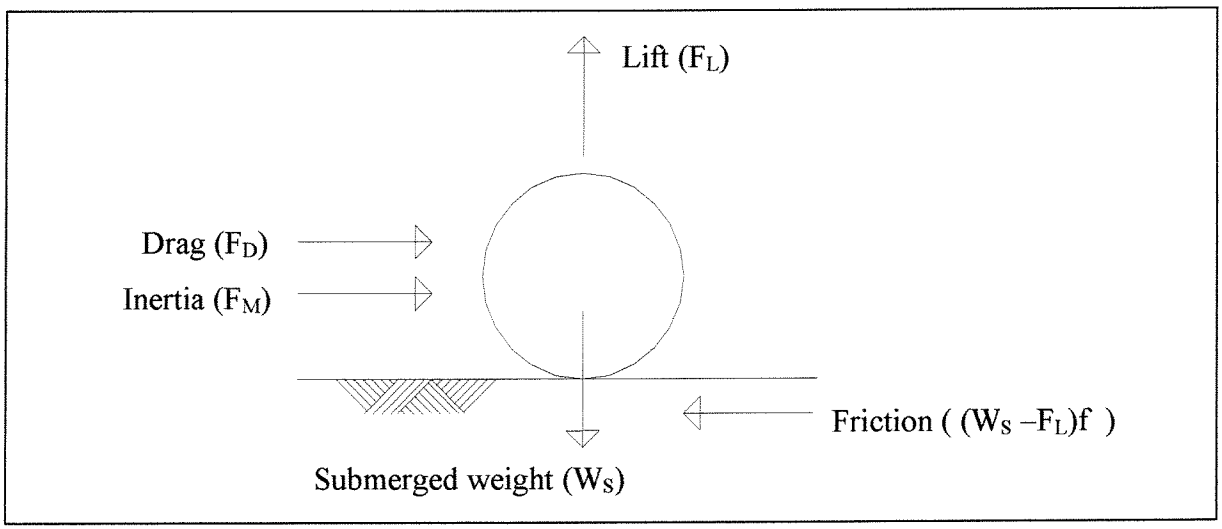

Figure 1.2 Forces on an outfall segment

For a regular, infinitely long-crested and sinusoidal wave, the hydrodynamic forces acting on a pipeline installed on the seabed during one wave cycle are illustrated in figure 1.3.

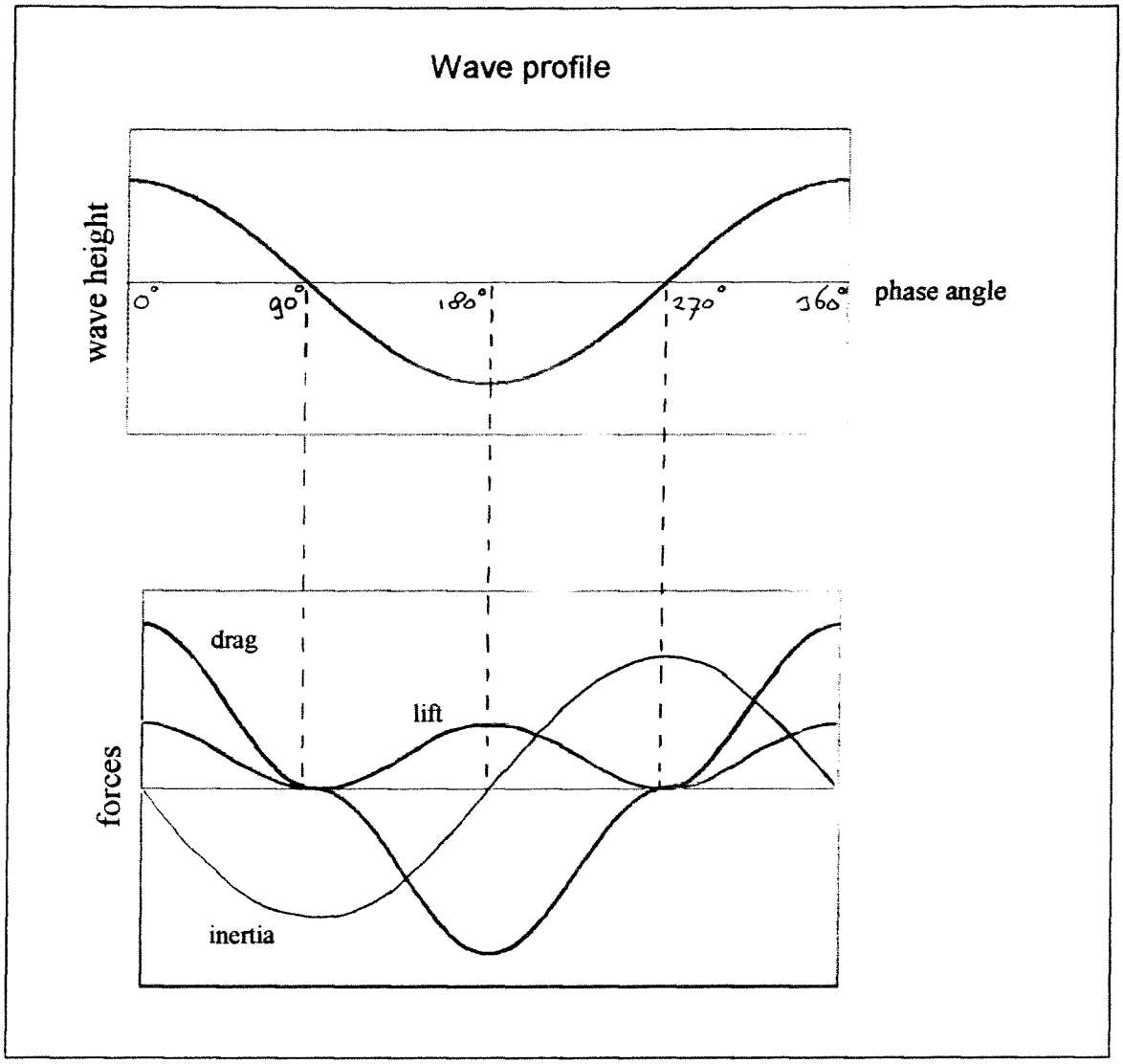

Figure 1.3 Drag, lift and inertia forces during one wave cycle

The drag, lift and inertia forces are respectively defined as:

$$F_D = \frac{1}{2} \rho C_D D u_w |u_w| \cdot \Delta L \qquad [N]$$

$$F_L = \frac{1}{2} \rho C_L D u_w^2 \cdot \Delta L \qquad [N]$$

$$F_M = \rho C_M \frac{1}{4} \pi D^2 a_w \cdot \Delta L \qquad [N]$$

where:

C_D	drag coefficient
C_L	lift coefficient
C_M	inertia coefficient
D	outside diameter of outfall
ΔL	length of considered outfall segment
ρ	density of water

1.2 Influence of oblique wave attack

When waves attack an outfall obliquely, common use is to decompose the undisturbed velocity and acceleration into components normal to the outfall axis, and then use the Morison equations with normal components of velocity and acceleration. This gives:

- instantaneously wave-induced horizontal water particle velocity component normal to outfall:

$$u_{wN} = u_m \sin\theta_{wo} \cos(kx - \omega t)$$

where:

θ_{wo} angle of wave attack (see figure 1.4)

- instantaneously wave-induced horizontal water particle acceleration component normal to outfall:

$$a_{wN} = a_m \sin\theta_{wo} \sin(kx - \omega t)$$

- hydrodynamic forces normal to outfall:

$$F_D = \frac{1}{2} \rho C_D D u_{wN} |u_{wN}| \cdot \Delta L \quad [N]$$

$$F_L = \frac{1}{2} \rho C_L D u_{wN}^2 \cdot \Delta L \quad [N]$$

$$F_M = \rho C_M \frac{1}{4} \pi D^2 a_{wN} \cdot \Delta L \quad [N]$$

The force distribution is thus perpendicular to the outfall axis. Tests have shown that the force coefficients C_D, C_L and C_M decrease slightly when the waves do not cross the outfall at a right angle due to change in cross-section and wake effect. It is therefore conservative to apply the Morison equations with the perpendicular velocity and acceleration components and the same coefficients as for perpendicular waves.

1.3 Influence of superimposed oblique current attack

When waves and currents are acting simultaneously, the combined effect should be considered. Common use is to add vectorially the wave-induced velocity and the current velocity terms of the Morison equations (the current has no acceleration component). Because of the oblique current attack, the current velocity is decomposed into a component normal to the outfall axis. This gives:

- instantaneously horizontal water particle velocity component normal to outfall:

$$u_N = u_m \sin\theta_{wo} \cos(kx - \omega t) + u_c \sin\theta_{co} = u_{wN} + u_{cN}$$

where:

u_c current velocity

θ_{co} angle of current attack (see figure 1.4)

- instantaneously horizontal water particle acceleration component normal to outfall:

$$a_N = a_m \sin\theta_{wo} \sin(kx - \omega t) = a_{wN}$$

- hydrodynamic forces normal to outfall:

$$F_D = \frac{1}{2} \rho C_D D u_N |u_N| \cdot \Delta L \qquad [N]$$

$$F_L = \frac{1}{2} \rho C_L D u_N^2 \cdot \Delta L \qquad [N]$$

$$F_M = \rho C_M \frac{1}{4} \pi D^2 a_N \cdot \Delta L \qquad [N]$$

Figure 1.4 shows a plan view and a section of an outfall with the angles of wave and current attack.

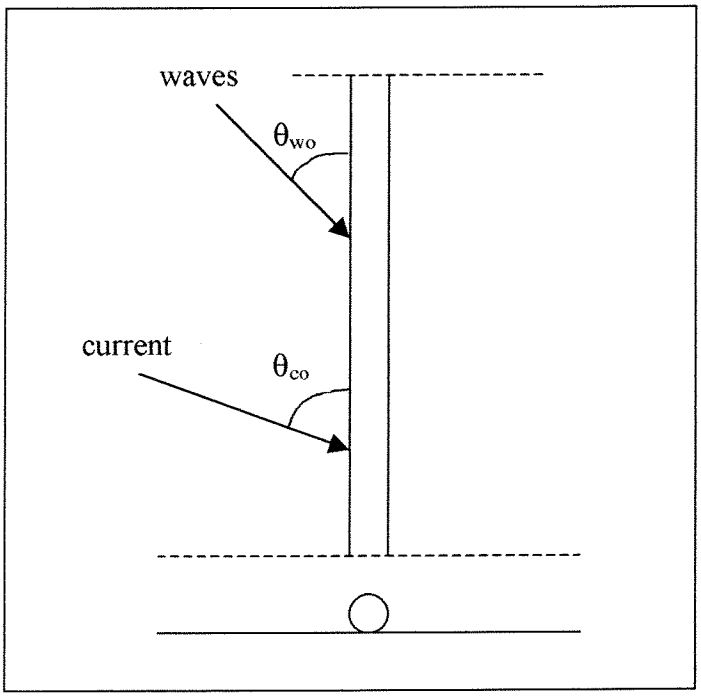

Figure 1.4 Oblique wave and current attack on an outfall

1.4 Two-dimensional stability criterion

A two-dimensional stability analysis is taking the most unfavourable combination of drag, lift and inertia forces due to wave and current attack on a segment of an outfall into account. From figure 1.2 it can be shown that for an outfall segment to remain stable:

$$W_S \geq \left(\frac{F_D + F_M}{r_c} \right) + F_L$$

where:

W_S submerged pipeline weight of outfall segment
r_c Coulomb friction factor

Thus, the stability criterion is the overall shifting of the pipeline, which is expressed with the following safety factor Sf:

$$Sf = \frac{W_S}{\left(\frac{F_D + F_M}{r_c}\right) + F_L}$$

For all phase angles of the wave profile, the hydrodynamic forces acting on an outfall segment are calculated and the matching safety factor is determined. The decisive safety factor is taken as the minimum occurring. For a segment of an outfall, this implies a phase angle that gives the combination of the drag, lift and inertia force with the least stability. Thus, the most unfortunate combination of hydrodynamic forces is considered. The submerged weight of the outfall segment is adjusted until the decisive safety factor meets the requirements.

This stability calculation and the resulting weight are performed at several locations along the outfall length.

The two-dimensional stability analysis is executed in the computer program 'Outfall stability'. This program is written in Pascal and the listing can be found in Appendix VIII.

2 THREE-DIMENSIONAL OUTFALL STABILITY ANALYSIS

2.1 Force distribution due to oblique wave attack

In the case of oblique wave attack, the wave-induced bottom velocities and accelerations vary in the direction of the outfall axis along the length of an on this axis projected wave length. In figure 2.1 an on the outfall projected wave length is sketched.

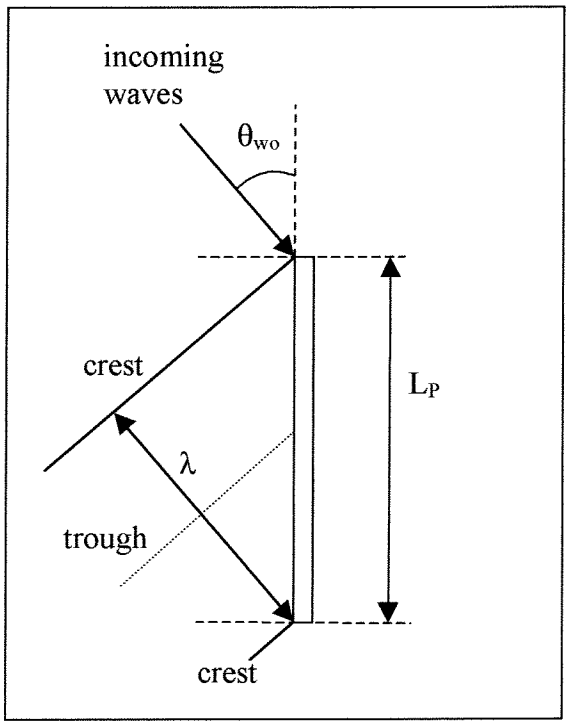

Figure 2.1 Definition sketch of the wave length projected on an outfall

The projected wave length is defined as:

$$L_P = \frac{\lambda}{\cos\theta_{wo}}$$

where

λ	wave length
θ_{wo}	angle of wave attack

Over an outfall length equal to a projected wave length, the water depth is considered constant. This implies a constant wave length and angle of wave attack.

Figure 2.2, 2.3 and 2.4 show respectively the projections of the profiles of the sinusoidal wave, the wave-induced horizontal water particle velocity and acceleration.

The projected wave profile is characterised as:

$$\eta = \frac{H}{2} \cos\left(\frac{2\pi \bar{z}}{L_P} - \frac{2\pi t}{T}\right)$$

where:

L_P projected wave length
$\bar{z}$ horizontal co-ordinate on outfall axis

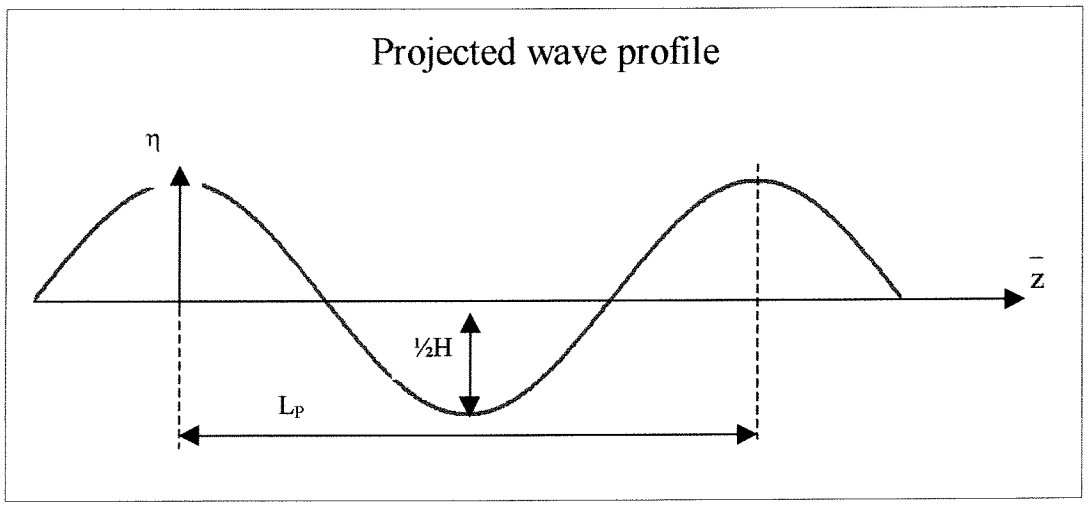

Figure 2.2 On outfall projected wave profile

The projected wave profile is characterised as:

$$u_w = u_m \sin\theta_{wo} \cos\left(\frac{2\pi \bar{z}}{L_P} - \frac{2\pi t}{T}\right)$$

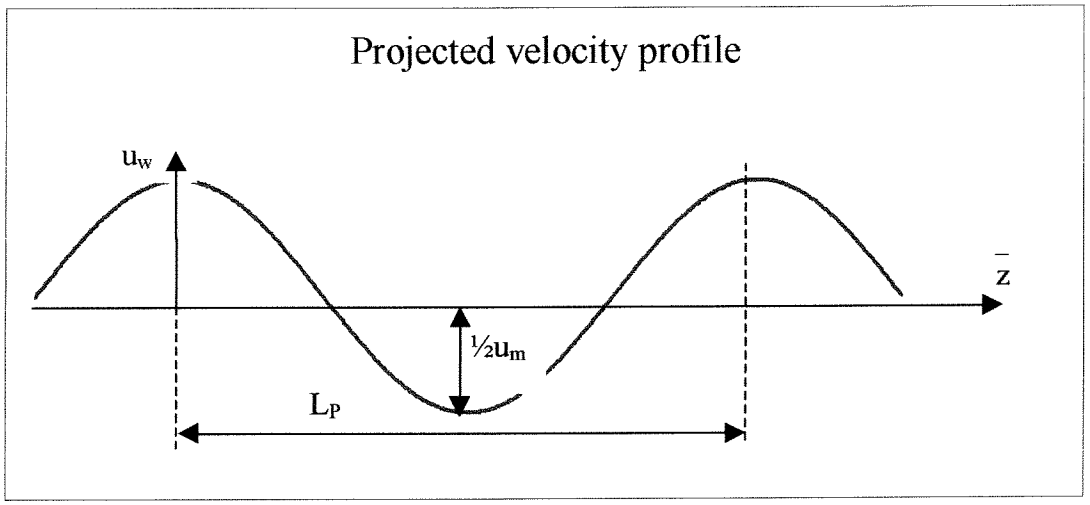

Figure 2.3 On outfall projected wave-induced velocity profile

The projected acceleration profile is characterised as:

$$a_w = a_m \sin\theta_{wo} \sin\left(\frac{2\pi \bar{z}}{L_P} - \frac{2\pi t}{T}\right)$$

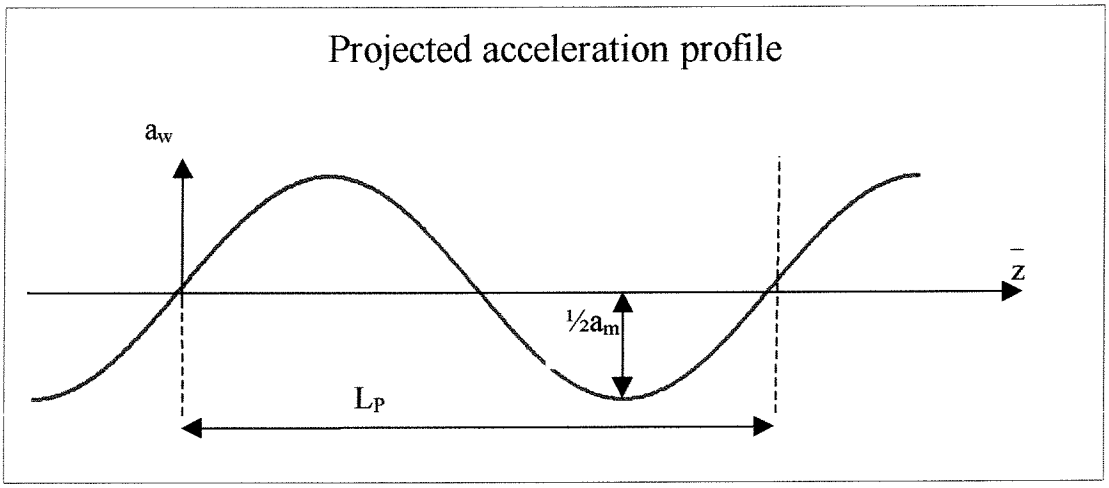

Figure 2.4 On outfall projected wave-induced acceleration profile

In the course of time, the projected wave length is translated along the outfall axis. This does not effect the absolute distribution of the wave-induced bottom velocities and accelerations.

By integrating the equations for the drag, lift and inertia forces over a defined part of an outfall at one moment in time, the resultant hydrodynamic forces acting on the considered outfall length can be determined. Because the wave-induced bottom velocities and accelerations vary repetitively over a projected wave length, the integration only has to be done over a section or the whole of an on the outfall axis projected wave length. Over the integrated length, the velocity and acceleration are decomposed into components normal to the outfall axis.

The integrands, the hydrodynamic forces per unit length respectively in horizontal and vertical direction, are:

$$f_h(\bar{z}) = \frac{1}{2}\rho C_D D u_w |u_w| + \rho C_M \frac{\pi}{4} D^2 a_w \qquad [N/m]$$

$$f_v(\bar{z}) = \frac{1}{2}\rho C_L D u_w^2 \qquad [N/m]$$

where:

$$u_w = u_m \sin\theta_{wo} \cos\left(\frac{2\pi \bar{z}}{L_P}\right)$$

$$a_w = a_m \sin\theta_{wo} \sin\left(\frac{2\pi \bar{z}}{L_P}\right)$$

Because the integrands represent the resultant horizontal and vertical forces acting on a certain outfall length at each moment in time, the variation in time of the hydrodynamic forces does not have to be regarded.

2.2 Influence of a superimposed oblique current

As already mentioned, when waves and currents are acting simultaneously, the combined effect should be considered. Common use is to add vectorially the wave-induced velocity and the current velocity terms of the Morison equations (the current has no acceleration component). Because of the oblique current attack, the current velocity is decomposed into a component normal to the outfall axis. For the hydrodynamic forces per unit length respectively in horizontal and vertical direction this gives:

$$f_h(\bar{z}) = \frac{1}{2}\rho C_D D\, u\,|u| + \rho C_M \frac{\pi}{4} D^2 a \qquad [N/m]$$

$$f_v(\bar{z}) = \frac{1}{2}\rho C_L D\, u^2 \qquad [N/m]$$

where:

$$u = u_m \sin\theta_{wo} \cos\left(\frac{2\pi\bar{z}}{L_P}\right) + u_c \sin\theta_{co}$$

$$a = a_m \sin\theta_{wo} \sin\left(\frac{2\pi\bar{z}}{L_P}\right)$$

Because the current is uniformly distributed and not accelerated, the repetitive variation over a projected wave length of the bottom velocities and accelerations is not influenced.

2.3 Additional lateral displacements and stresses of an outfall

In the two-dimensional analysis the outfall stability is determined with the most unfavourable combination of the drag, lift and inertia forces on a segment. Therefore, resultant forces acting on a near-by segment do not exceed the forces acting on the decisive segment, and will thus not cause any additional displacements and consequent stresses in the horizontal plane of an outfall. This implies that the stability criterion of an outfall in the two-dimensional approach is the overall shifting of the pipeline.

In the three-dimensional analysis the outfall stability is determined with the most unfavourable resultant hydrodynamic forces over a defined part of a projected wave length. This implies that there will be a spot on the outfall, within the defined part, where a combination of drag, lift and inertia forces results in a higher force than the average load on the considered length. In consequence, the outfall can displace locally on the seabed. As long as these additional lateral displacements and successive stresses are limited, they are acceptable and cause no obstruction for the application of the three-dimensional approach in which overall shifting of the pipeline is the stability criterion.

The additional displacements and stresses in the three-dimensional analysis will be determined with a model investigation in the following contemplation.

Because the tidal currents can be considered uniformly distributed over an outfall length equal to several wave lengths, the drag forces due to oblique current attack do not result in local bending and consequent stresses. Further, the wave-induced drag forces can be neglected, as can be seen in the Aveiro and Northumbrian cases. Therefore, in order to determine the additional displacements and stresses only the inertia forces have to be taken into account.

The outfall is modelled as a beam, supported by a pin and a roller bearing, loaded with a sinusoidal inertia force. The length of the beam is taken as half a projected wave length because this implies that the inertia forces along the beam are acting in the same direction and on the left and right side of the supports the force direction is opposite.

In figure 2.5, the beam of constant cross-section loaded with a inertia force $q(\bar{z})$ is drawn.

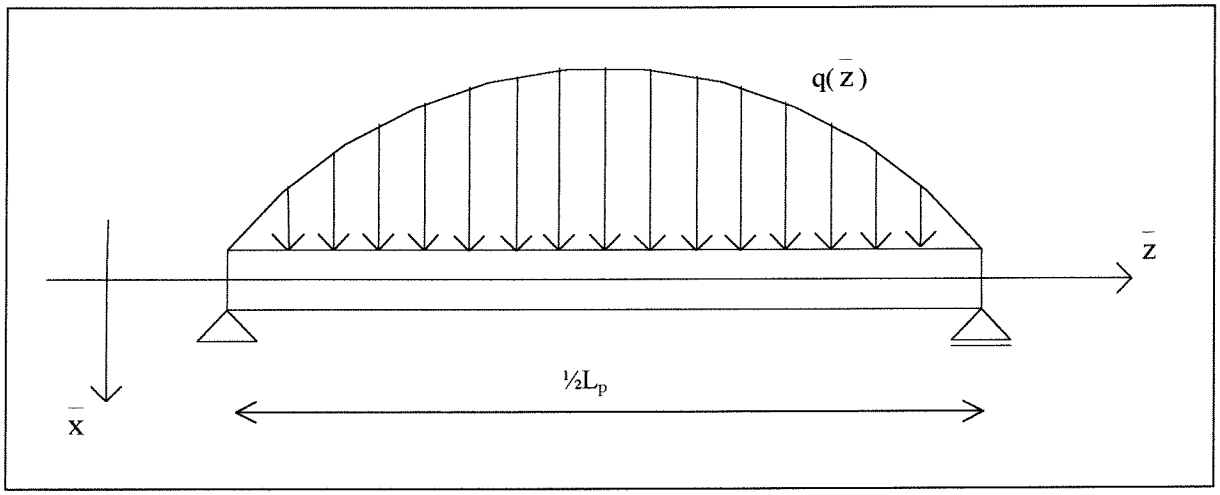

Figure 2.5 Beam loaded by a sinusoidal inertia force

Equilibrium in $\bar{x}$-direction requires that:

$$\frac{dQ}{d\bar{z}} = -q(\bar{z}) \qquad \text{where:} \quad Q \quad \text{shear force}$$

Equilibrium of moments requires that:

$$\frac{dM}{d\bar{z}} = Q \qquad \text{where:} \quad M \quad \text{bending moment}$$

These two equations of equilibrium can be combined to give the first basic equation of the theory of bending of beams:

$$\frac{d^2M}{d\bar{z}^2} = -q(\bar{z})$$

The second basic equation can be derived from a consideration of the deformations of the beam. The displacement in the $\bar{x}$-direction is denoted by w. When it is assumed that plane cross sections of the beam remain plane after deformation (Bernoulli's hypothesis), and that the rotation dw/dx is small compared to 1, one obtains:

$$EI\frac{d^2w}{d\bar{z}^2} = -M \qquad \text{where:} \quad EI \quad \text{flexural rigidity of the beam}$$

The two basic equations can be combined to give:

$$EI\frac{d^4w}{d\bar{z}^4} = q(\bar{z})$$

This is a forth order differential equation for the lateral displacement, the basic equation of the classical theory of bending of beams. This equation can be solved analytically, subject to the appropriate boundary conditions.

The load on the beam, the sinusoidal inertia force, can be written as:

$$q(\bar{z}) = \rho C_M \frac{\pi}{4} D^2 a_m \sin\theta_{wo} \sin\left(\frac{2\pi\bar{z}}{L_p}\right) = q_1 \sin\left(\frac{2\pi\bar{z}}{L_p}\right)$$

Applied to the basic forth order differential equation for the lateral displacement, this gives:

$$- EIw + \frac{L_p^4}{16\pi^4} q_1 \sin\left(\frac{2\pi\bar{z}}{L_p}\right) = \frac{1}{6}C_1 \bar{z}^3 + \frac{1}{2}C_2 \bar{z}^2 + C_3 \bar{z} + C_4$$

The appropriate boundary conditions and implications for the integration constants give for the displacements and bending moments:

- $w(\bar{z}) = \frac{L_p^4}{16\pi^4}\frac{q_1}{EI} \sin\left(\frac{2\pi\bar{z}}{L_p}\right)$

amplitude:

$$w = \frac{L_p^4}{16\pi^4}\frac{q_1}{EI} = \frac{L_p^4}{16EI\pi^4} \rho C_m \frac{\pi}{4} D^2 a_m \sin\theta_{wo} = \frac{R^2}{16\pi^3 EI} \rho C_m L_p^4 a_m \sin\theta_{wo}$$

- $M(\bar{z}) = \frac{L_p^2}{4\pi^2} q_1 \sin\left(\frac{2\pi\bar{z}}{L_p}\right)$

amplitude:

$$M = \frac{L_p^2}{4\pi^2} q_1 = \frac{L_p^2}{4\pi^2} \rho C_m \frac{\pi}{4} D^2 a_m \sin\theta_{wo} = \frac{R^2}{4\pi} \rho C_m L_p^2 a_m \sin\theta_{wo}$$

The bending stresses can be found with:

- $\sigma(\bar{z}) = \frac{M(\bar{z})\,R}{I} = \frac{L_p^2}{4\pi^2} q_1 \frac{R}{I} \sin\left(\frac{2\pi\bar{z}}{L_p}\right) = \frac{L_p^2\, q_1 R}{4\pi^2 I} \sin\left(\frac{2\pi\bar{z}}{L_p}\right)$

amplitude:

$$\sigma = \frac{L_p^2\, q_1 R}{4\pi^2 I} = \frac{R^3}{4\pi\, I} \rho C_m L_p^2 a_m \sin\theta_{wo}$$

An estimation of the amplitude of the additional displacements and bending stresses can be found by applying the Aveiro and Northumbrian case data. For the flexural rigidity of the outfall only the steel of the pipeline is taken into account, because of the discontinuity of the concrete weight coating due to joints. This is a conservative assumption.

Aveiro case

outfall characteristics

radius steel pipe:	$R = 0.75$ m
steel wall thickness:	$t = 0.0175$ m
steel elasticity modulus:	$E = 2 \cdot 10^{11}$ N/m^2
moment of inertia:	$I = \pi t R^3 = 0.023$ m^4

wave characteristics

projected wave length:	$L_p = 63.30$ m
amplitude horizontal acceleration:	$a_m = 0.32$ m/s^2
angle of wave attack:	$\theta_{wo} = 25°$
inertia coefficient:	$C_M = 3.00$
density of water:	$\rho = 1024$ kg/m^3

additional lateral displacement

$$w = \frac{R^2}{16\pi^3 EI} \rho C_m L_p^4 a_m \sin\theta_{wo} = 0.0016 \text{ m} = 1.6 \text{ mm}$$

additional lateral bending stress

$$\sigma = \frac{R^3}{4\pi I} \rho C_m L_p^2 a_m \sin\theta_{wo} = 2429814 \frac{N}{m^2} = 2.4 \frac{N}{mm^2}$$

Northumbrian case

outfall characteristics the same as for the Aveiro case

wave characteristics

projected wave length:	$L_p = 44.00$ m
amplitude horizontal acceleration:	$a_m = 0.14$ m/s^2
angle of wave attack:	$\theta_{wo} = 25°$
inertia coefficient:	$C_M = 3.00$
density of water:	$\rho = 1024$ kg/m^3

additional lateral displacement

$$w = \frac{R^2}{16\pi^3 EI} \rho C_m L_p^4 a_m \sin\theta_{wo} = 0.0002 \text{ m} = 0.2 \text{ mm}$$

additional lateral bending stress

$$\sigma = \frac{R^3}{4\pi I} \rho C_m L_p^2 a_m \sin\theta_{wo} = 513628 \frac{N}{m^2} = 0.5 \frac{N}{mm^2}$$

Compared to the outfall radius (0.75 m) and the yield stress of the pipeline steel (235 N/mm^2), the extent of the displacements and stresses are negligible. This implies that in the three-dimensional stability analysis it is superfluous to consider the additional displacements and stresses in the horizontal plane of an outfall. Thus, in the three-dimensional analysis, as in the two-dimensional approach, overall shifting of the pipeline is the stability criterion.

2.4 Three-dimensional stability criterion

A three-dimensional stability analysis is taking the variation of hydrodynamic forces along the length of an outfall, caused by oblique wave attack, into account. Figure 2.6 shows a plan view and a section of an outfall with co-ordinate system and angles of wave and current attack.

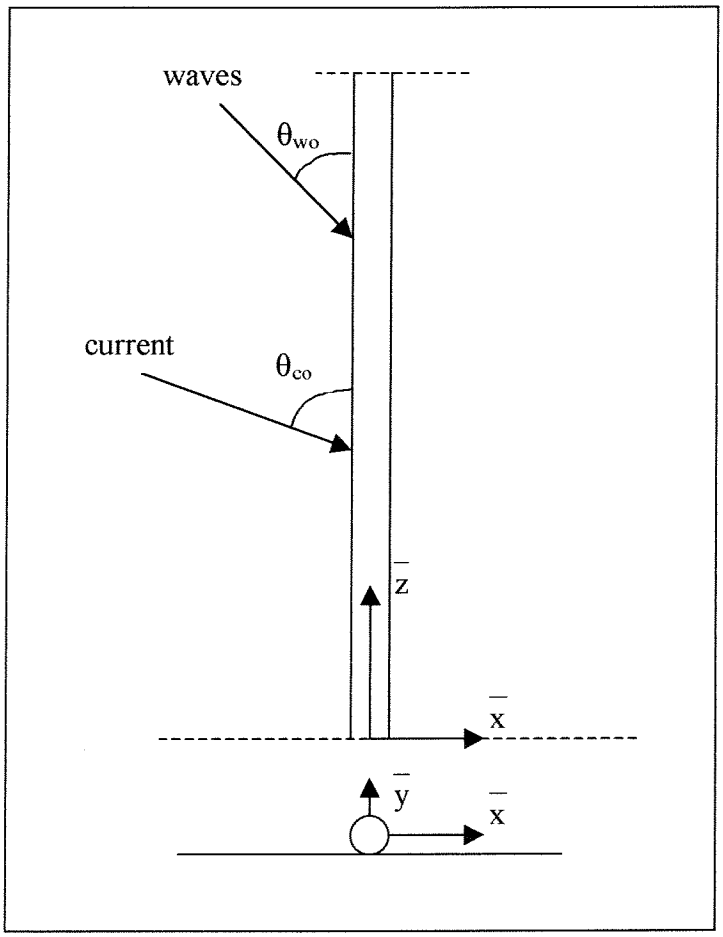

Figure 2.6 Oblique wave and current attack on an outfall

To analyse the stability of an outfall due to the force distribution, the hydrodynamic forces per unit length, in the direction of the outfall, have to be integrated over a defined part of a projected wave length. The integration can be done over a variable part of a projected wave length and with variable phase angles as the centre of the defined part. The matching safety factor Sf can be determined with the integration results and the following expression:

$$SF = \frac{W_S}{\frac{F_{\bar{x}}(\Delta\bar{z})}{r_c} + F_{\bar{y}}(\Delta\bar{z})}$$

where:

$F_{\bar{x}}(\Delta\bar{z})$ hydrodynamic force in $\bar{x}$ -direction, integrated over a defined part $\Delta\bar{z}$ of a projected wave length L_P in $\bar{z}$-direction

$F_{\bar{y}}(\Delta\bar{z})$ hydrodynamic force in $\bar{y}$-direction, integrated over a defined part $\Delta\bar{z}$ of a projected wave length L_P in $\bar{z}$-direction

The submerged weight of the outfall is adjusted until the decisive safety factor meets the requirements.

To evaluate the hydrodynamic forces and the safety factor distribution and variation in the three-dimensional stability analysis, calculations with the computer program 'Outfall stability' are executed for the Aveiro case (In Appendix IX this is done for the Northumbrian case). In 'Outfall stability', the integration of the hydrodynamic forces per unit length in the direction of the outfall, over a variable defined part of a projected wave length with variable phase angles as the centre of the defined part, is executed (Appendix VIII). This program is the numeric interpretation of the algebraic derivation of the three-dimensional stability analysis of an outfall under oblique current and wave attack (Appendix VII).

Aveiro case: ***Oblique wave and current attack***

Input:

wave height	1.597	(m)
wave period	6.293	(s)
wave length (estimation)	57	(m)
angle of wave attack	25	(deg)
current velocity	1.028	(m/s)
angle of current attack	70	(deg)
water depth	15	(m)
outfall diameter	1.5	(m)

Wave and current characteristics:

wave length	57.37	(m)
amplitude horizontal particle velocity	0.32	(m/s)
normal to outfall	0.14	(m/s)
amplitude horizontal particle acceleration	0.32	(m/s2)
normal to outfall	0.14	(m/s2)
current velocity normal to outfall	0.97	(m/s)
alpha-value	7.11	(-)
KC-number	0.57	(-)
a'/D-ratio	5.97	(-)

Cd	1.05	(-)
Cm	3.00	(-)
Cl	1.00	(-)
submerged weight	2951	(N/m)
density water	1024	(kg/m3)
Coulomb factor	0.7	(-)

The force coefficients are derived from the figure "Hydrodynamic coefficients for a pipe on the sea bed" in 'Stability of pipelines in trenches' (Palmer, 1988).

Output: Two-dimensional stability:

minimum safety factor	1.0	(-)
at phase angle	63	(deg)
horizontal particle velocity	1.03	(m/s)
horizontal particle acceleration	0.12	(m/s2)
drag force (includes current)	852	(N/m)
inertia force	656	(N/m)
lift force (includes current)	811	(N/m)

In figure 2.7 and 2.8, respectively the horizontal water particle velocity profile and the horizontal water particle acceleration profile along the outfall, over a projected wave length, have been drawn.

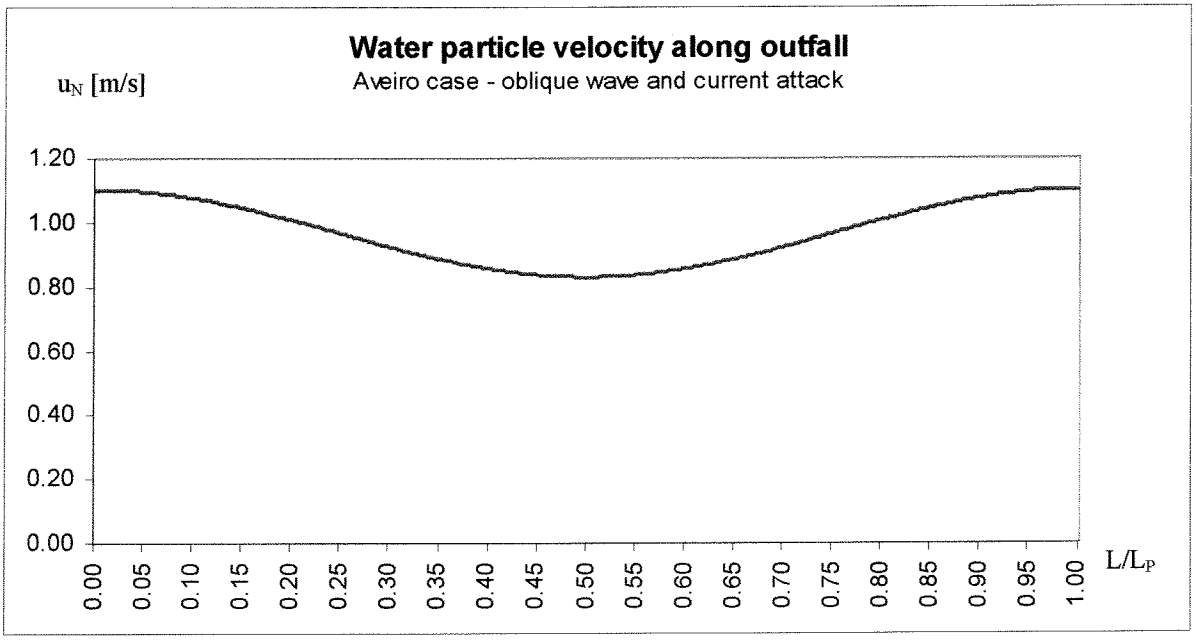

Figure 2.7

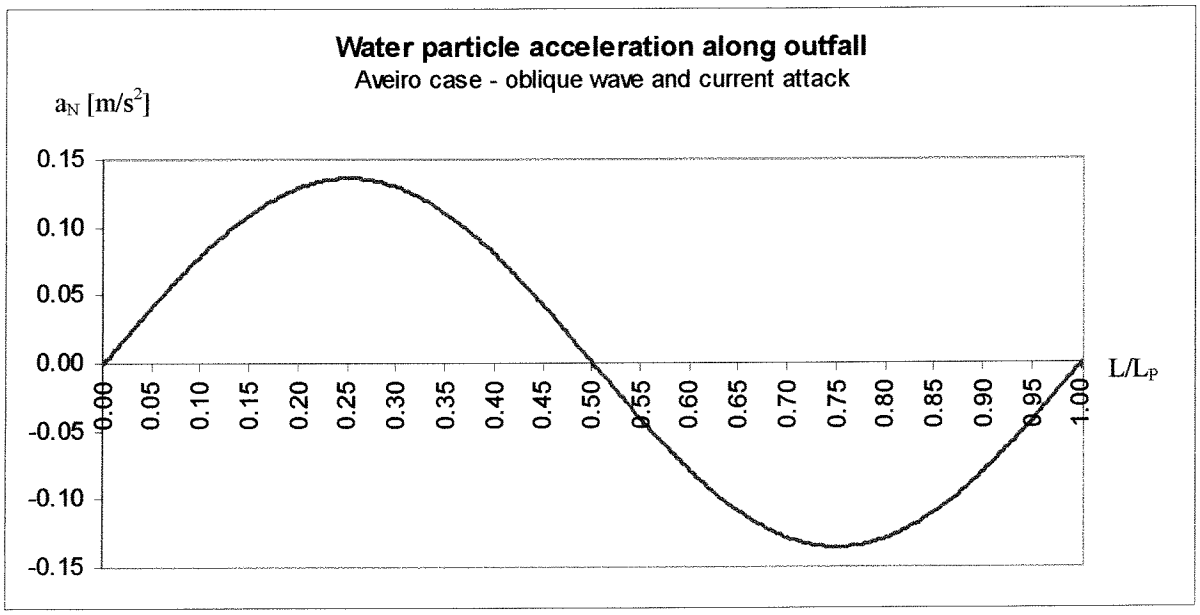

Figure 2.8

In figure 2.9, the hydrodynamic forces along the outfall, over a projected wave length, have been drawn.

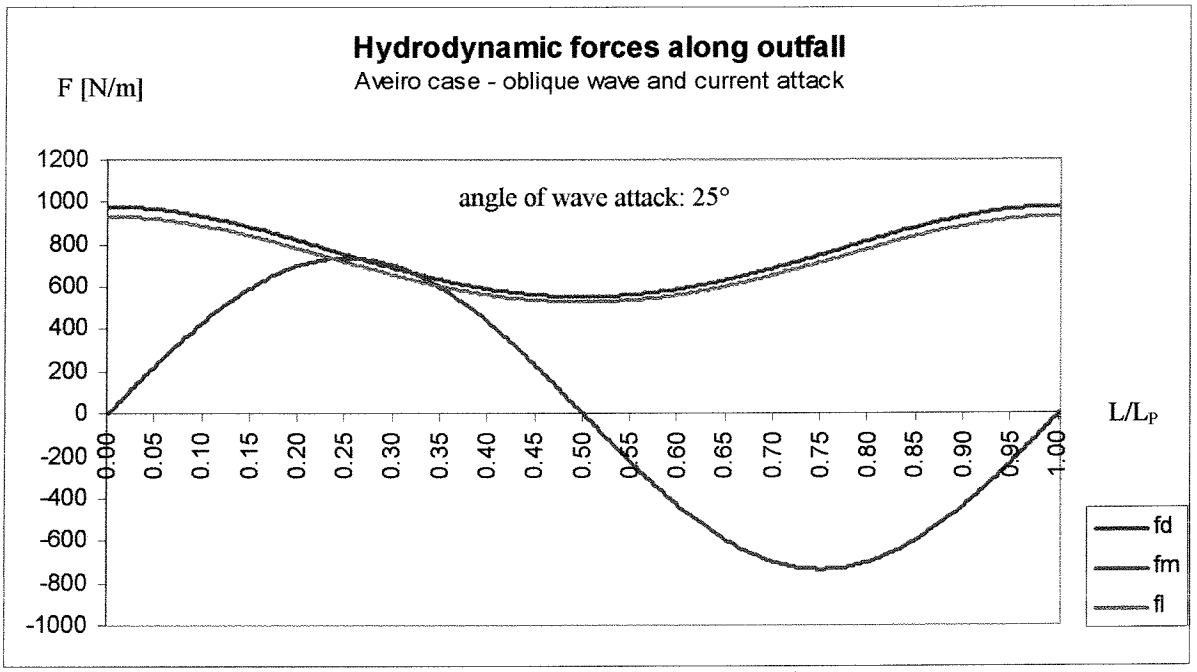

Figure 2.9

The results of the safety factor distribution and variation in the three-dimensional stability analysis of an outfall are presented in figure 2.10.

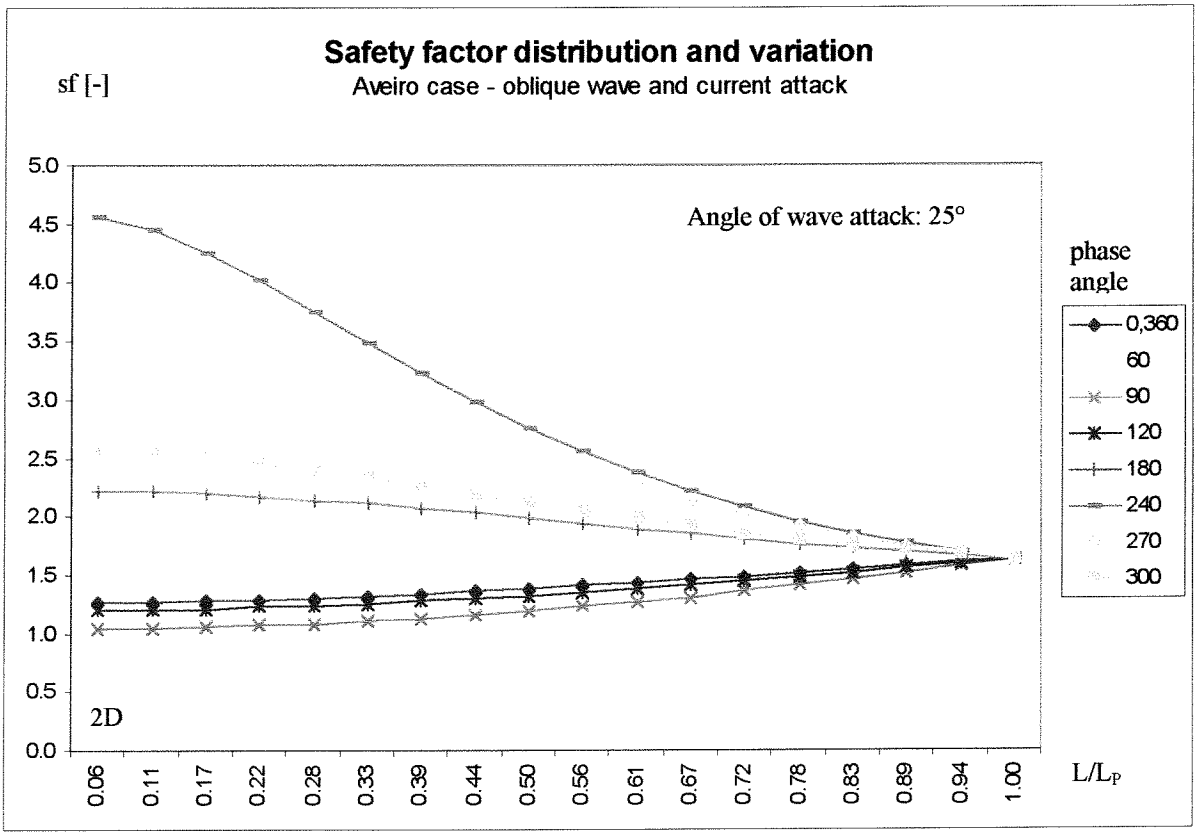

Figure 2.10

The integrated length L of the outfall is taken as the relative part of the projected wave length L_P, expressed in the factor L/L_P on the horizontal-axis. The factor L/L_P is the ratio of the considered integrated part of the projected wave length and the projected wave length. The various lines in the graphic represent the different phase angles that are taken as the centre of the defined part. The represented phase angles are shown in the legend at the right of the graphic.

From figure 2.10, it can be seen that a phase angle of 60°, represented by the bottom yellow line, gives the lowest safety factors. Thus, the minimum safety factor is found with the decisive phase angle of the two-dimensional stability analysis (63°) as the centre of the defined part.

In figure 2.11, the safety factor variation, calculated with the decisive phase angle of the two-dimensional stability analysis (63°) as the centre of the defined part and for various considered relative lengths of the outfall, has been drawn. From figure 2.11, it can be seen that with a decreasing relative length ($L/Lp \cong 0$), the three-dimensional stability factor approximates the two-dimensional safety factor.

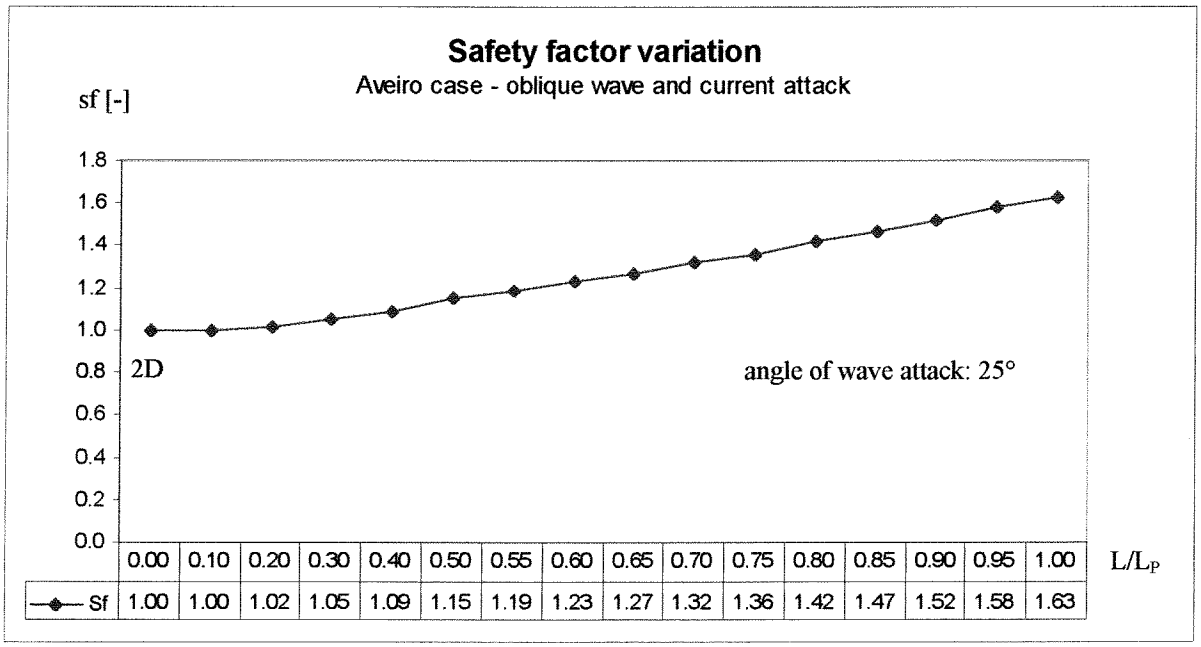

Figure 2.11

Aveiro case: *Oblique wave attack (current absent)*

Input:	wave height	1.597	(m)
	wave period	6.293	(s)
	wave length (estimation)	57	(m)
	angle of wave attack	25	(deg)
	water depth	15	(m)
	outfall diameter	1.5	(m)

Wave characteristics:	wave length	57.37	(m)
	amplitude horizontal particle velocity	0.32	(m/s)
	normal to outfall	0.14	(m/s)
	amplitude horizontal particle acceleration	0.32	(m/s2)
	normal to outfall	0.14	(m/s2)

		alpha-value		0	(-)
		KC-number		0.57	(-)
		a'/D-ratio		0.09	(-)
Input:	Cd	1.05	(-)	In comparison with the oblique wave and current attack case, only the lift coefficient is changed.	
	Cm	3.00	(-)		
	Cl	2.20	(-)		
	submerged weight	1047	(N/m)		
	density water	1024	(kg/m3)		
	Coulomb factor	0.7	(-)		
Output:	Two-dimensional stability	minimum safety factor		1.0	(-)
		at phase angle		90	(deg)
		horizontal particle velocity		0	(m/s)
		horizontal particle acceleration		0.14	(m/s2)
		drag force		0	(N/m)
		inertia force		736	(N/m)
		lift force		0	(N/m)

In figure 2.12, the horizontal water particle velocity profile along the outfall, over a projected wave length has been drawn. Because a current does not attribute to the water particle accelerations, the horizontal water particle acceleration profile along the outfall, over a projected wave length, is the same as presented in figure 2.8.

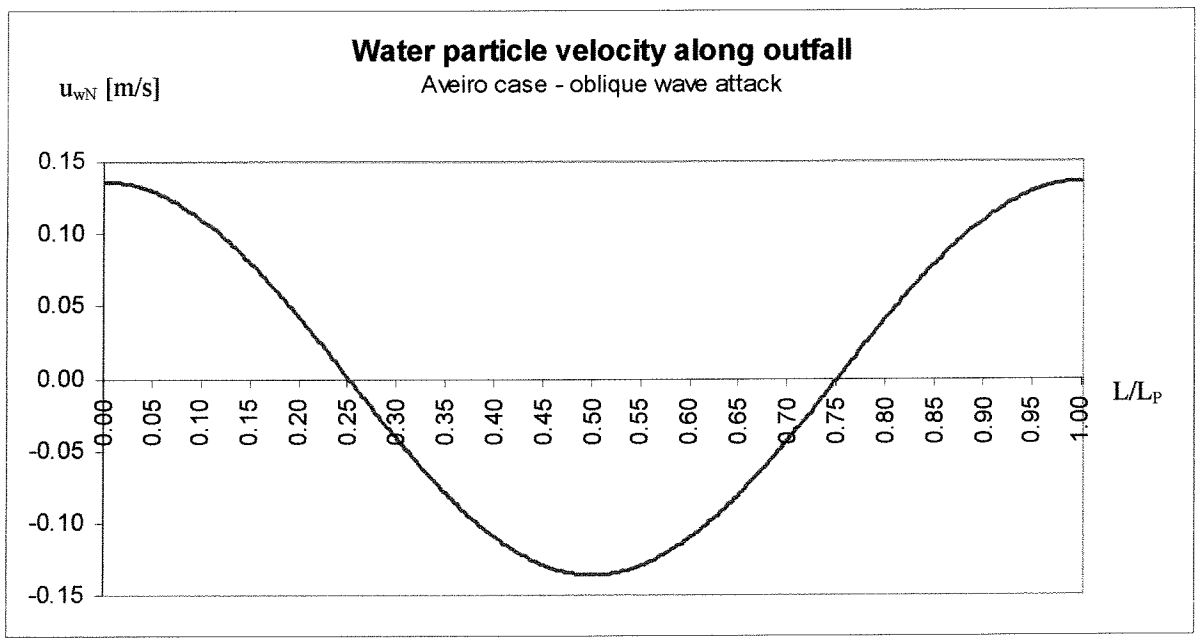

Figure 2.12

In figure 2.13, the hydrodynamic forces along the outfall, over a projected wave length have been drawn.

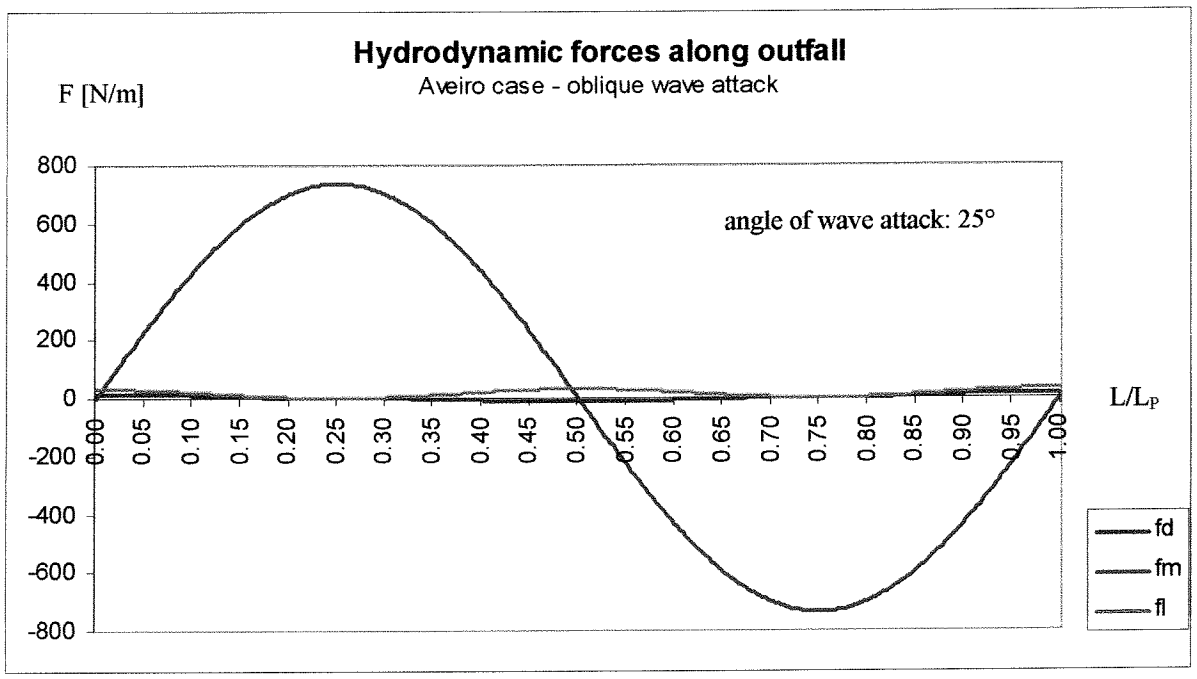

Figure 2.13

The results of the safety factor distribution and variation in the three-dimensional stability analysis of an outfall are presented in figure 2.14. From figure 2.14, it can be seen that a phase angle of 90°, represented by the bottom blue line, gives the lowest safety factors. Thus, the minimum safety factor is found with the decisive phase angle of the two-dimensional stability analysis (90°) as the centre of the defined part.

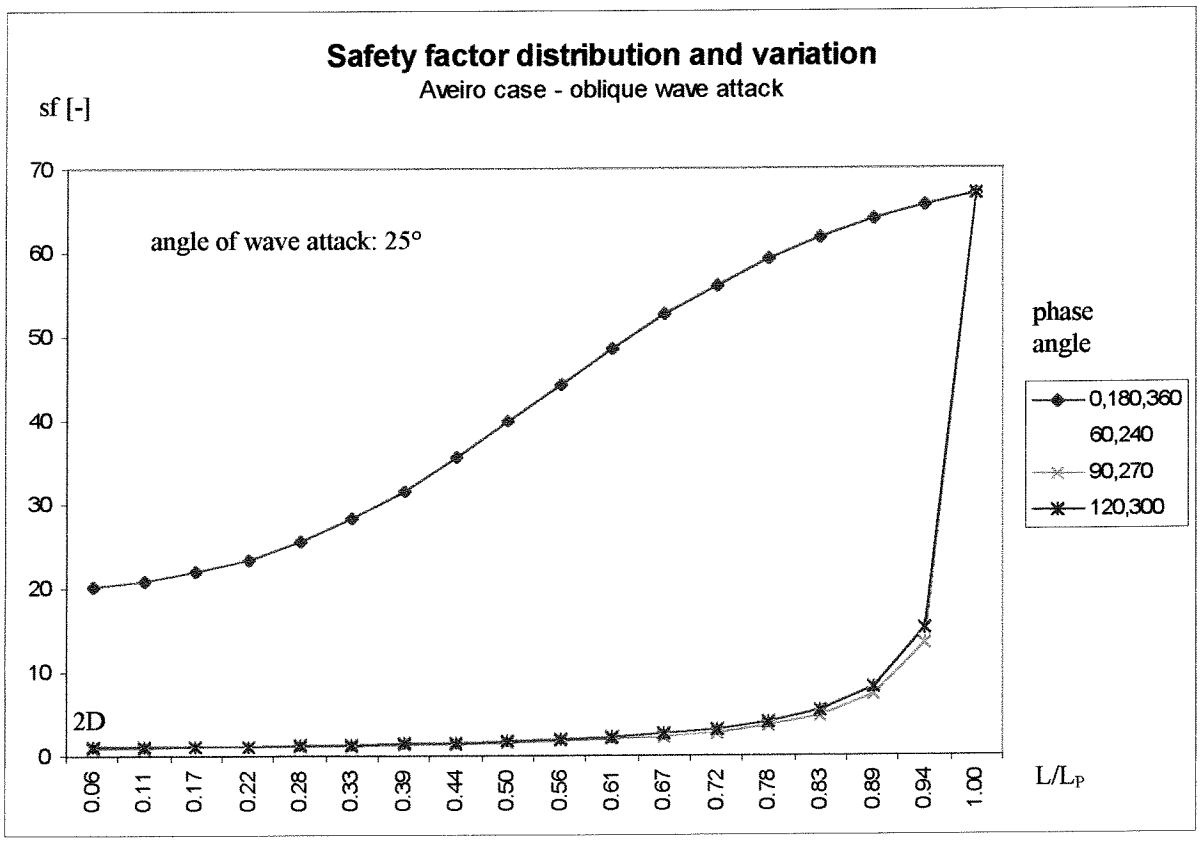

Figure 2.14

In figure 2.15, the safety factor variation, calculated with the decisive phase angle of the two-dimensional stability analysis (90°) as the centre of the defined part and for various considered relative lengths of the outfall, has been drawn. From figure 2.15, it can be seen that with a decreasing relative length (L/Lp ≅ 0), the three-dimensional stability factor approximates the two-dimensional safety factor.

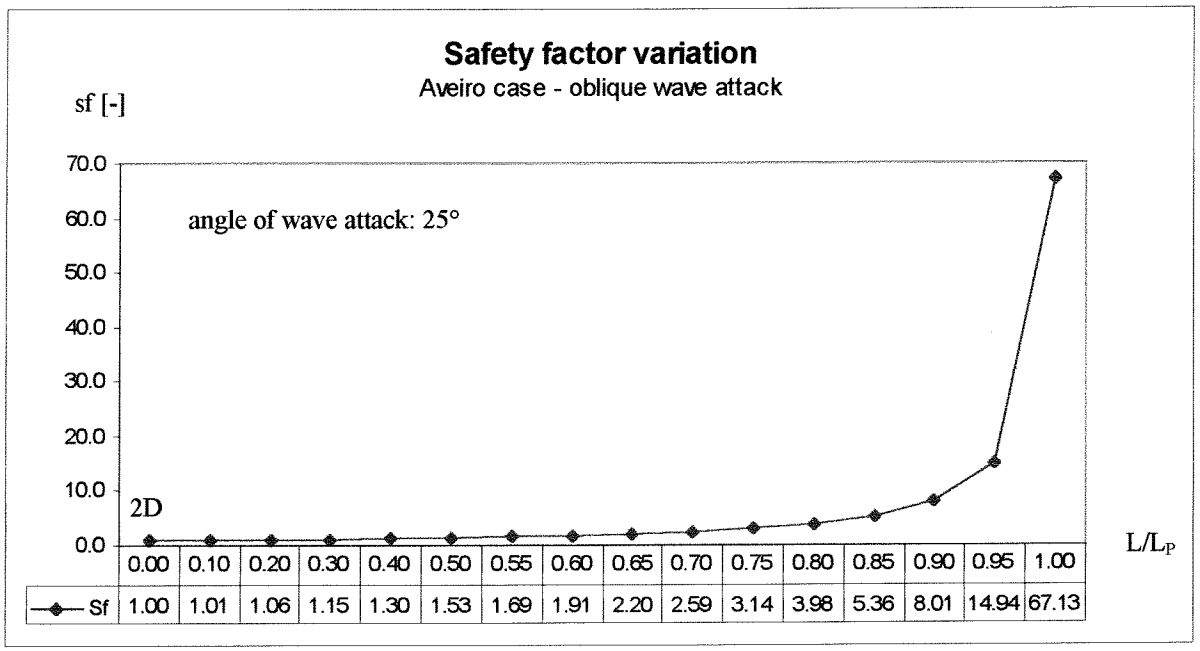

	0.00	0.10	0.20	0.30	0.40	0.50	0.55	0.60	0.65	0.70	0.75	0.80	0.85	0.90	0.95	1.00
Sf	1.00	1.01	1.06	1.15	1.30	1.53	1.69	1.91	2.20	2.59	3.14	3.98	5.36	8.01	14.94	67.13

Figure 2.15

The results of the analysis of the Aveiro case, calculated with 'Outfall stability', motivate the following considerations.

By integrating the equations for the drag, lift and inertia forces over a defined part of an outfall at one moment in time, the resultant hydrodynamic forces acting on the considered outfall length can be determined. Because the wave-induced bottom velocities and accelerations vary repetitively over a projected wave length, the integration only has to be done over a section or the whole of an on the outfall axis projected wave length. If the considered length of the outfall is taken equal to half a projected wave length, the implication is that over this length the integrated wave-induced forces, in the case of an absent current, are aligned in the same direction. Thus, the forces acting in the same direction are integrated and the stability under this resultant force is determined. Also when a current is present, the minimum stability for the defined part is still found with the decisive phase angle of the two-dimensional stability analysis as the centre of the integrated length. This execution gives plausible results in the three-dimensional analysis, also in the case of a small or even absent current.

Further, it appeared that the extent of the displacements and stresses caused by the hydrodynamic force variation due to oblique wave attack are negligible. Thus, in the three-dimensional analysis the overall shifting of the pipeline is the stability criterion, and can be determined with the described method.

From the figures 2.11 (Aveiro, oblique wave and current attack) and IX.15 in Appendix IX (Northumbrian, oblique wave and current attack) it can be seen that for a considered length of the outfall equal to half a projected wave length, the resultant forces calculated with the 3D-method are respectively 15% (Sf=1.15) and 9% (Sf=1.09) lower than if determined with the 2D-method (Sf=1.00).

3 CONCLUSIONS AND RECOMMENDATIONS

3.1 Conclusions

In the case of oblique wave attack on outfalls, a different, more specific and thus less conservative approach of calculating resulting hydrodynamic forces on outfalls during installation is the use of a three-dimensional stability analysis. This stability analysis of outfalls is taking the variation of the hydrodynamic forces along the length of an outfall, caused by the oblique wave attack, into account.

In the three-dimensional stability analysis, it is superfluous to consider the additional displacements and stresses in the horizontal plane of an outfall and thus the overall shifting of the pipeline is the stability criterion.

The resultant forces calculated with the three-dimensional method are in the order of 10% lower than if determined with the two-dimensional stability analysis.

The better predictions of resultant hydrodynamic forces on outfalls with the three-dimensional stability analysis, offer perspectives to the construction of longer outfalls and an improved economic design in general.

3.2 Recommendations

When applying this stability analysis, it is recommended to:

- consider the variation of the hydrodynamic forces, due to oblique wave attack, along the length of an outfall equal to half a projected wave length.
- take the decisive phase angle of the two-dimensional stability analysis as the centre of the defined part.

When the three-dimensional stability analysis is executed in this way, the integrated wave-induced forces, in the case of an absent current, are aligned in the same direction. Thus, the forces acting in the same direction are integrated and the stability under this resultant force is determined. Also when a current is present, the minimum stability for the defined part is still found with the decisive phase angle of the two-dimensional stability analysis as the centre of the integrated length equal to half a projected wave length.

Another recommendation is to do supplementary research on the safety contemplation used in outfall construction in general and the definition of hydrodynamic force coefficients in the different model test programs in particular.

APPENDIX I KC-NUMBER AND A'/D RATIO COMPARED

The force coefficients C_D, C_M and C_L, derived from the figure "Hydrodynamic coefficients for a pipe on the sea bed" in Palmer's 'Stability of pipelines in trenches' are plotted out against the parameter a'/D, while most of the other graphics in the literature use the KC-number. This chapter will discuss the difference and relation of these parameters.

The hydrodynamic quantities describing the flow around a smooth, circular cylinder in steady currents depend on the Reynolds number:

$$Re = \frac{U D}{\upsilon}$$

where:

U	flow velocity
D	outside diameter of the cylinder
ν	cinematic velocity

In the case where the cylinder is exposed to an oscillatory flow an additional parameter, the KC-number, appears. This KC-number is defined by:

$$KC = \frac{U_m T_w}{D}$$

where:

U_m maximum bottom velocity of the oscillating flow

If the flow is sinusoidal, the maximum velocity will be:

$$U_m = a\,\omega = \frac{2\,\pi\,a}{T_w}$$

ω	angular frequency of the motion
a	amplitude of the oscillating flow at the bottom
T_w	period of the oscillatory flow

For the sinusoidal case the KC-number will therefore be identical to:

$$KC = \frac{2\,\pi\,a}{D}$$

The ratio a/D is the oscillatory water motion in cylinder diameters, and is a measure of the development of the wake structure. When a/D is small, the wake is little developed, when a/D is large, the reverse is true.

When an oscillating flow approaches the pipeline at an angle of attack θ, the velocity and amplitude components normal to the cylinder axis have to be applied in the KC number definitions:

$$KC = \frac{U_{Nm} T_w}{D} = \frac{2\,\pi\,a_N}{D}$$

where:

U_{Nm} maximum bottom velocity of the oscillating flow normal to the cylinder axis

a_N normal component of the amplitude of the oscillating flow at the bottom

If a current coexists together with waves, the presence of the current may effect the waves. The problem of wave-current interaction is an important issue in its own right. Fredsøe has developed a model to determine the interaction between the two velocity profiles. For the sake of simplicity, we consider that the oscillatory flow remains unchanged in the presence of a superimposed current.

Let U_c be the velocity of the current. The key parameter in the case of waves and current is the current ratio α, defined as:

$$\alpha = \frac{U_{Nc}}{U_{Nm}}$$

where:

U_{Nc} current velocity normal to the cylinder axis

U_{Nm} maximum bottom velocity of the oscillating flow normal to the cylinder axis

Although there are several alternatives with regard to the definition of the Reynolds number and the Keulegan-Carpenter number in the present case, the definitions adopted in the case of pure oscillatory flow may be maintained.

The ratio a/D has to be adjusted in the case of waves and current. When a superimposed current is present, an equivalent semi-orbital movement a' is defined by:

$$a' = a\left(1 + \frac{U_{Nc}}{a\,\omega}\right)^2 = a\left(1 + \frac{2\,U_{Nc}}{a\,\omega} + \frac{U_{Nc}^2}{a^2\,\omega^2}\right)$$

with:

$$a = \frac{U_{Nw}\,T_w}{2\,\pi}, \quad \omega = \frac{2\,\pi}{T_w} \quad \text{and} \quad \alpha = \frac{U_{Nc}}{U_{Nm}}$$

this becomes:

$$a' = a\left(1 + 2\,\alpha + \alpha^2\right)$$

The relation between the KC number and the a'/D ratio, in the case of waves and currents, is thus:

$$\frac{a'}{D} = KC\left(\frac{1}{2\pi} + \frac{\alpha}{\pi} + \frac{\alpha^2}{2\pi}\right)$$

APPENDIX II SPREADSHEET CALCULATION

Wave height	2,5	(m)				
Wave period	6,0	(s)		Calculated wave length		
Wave length	53	(m)			L0	53,00 (m)
Water depth	15	(m)			L1	53,09
					L2	53,07
Circular frequency	1,0472	(1/s)			L3	53,07
Wave number	0,1184	(1/m)	(with L6)		L4	53,07
					L5	53,07
Diameter outfall	1,5	(m)			L6	53,07

Amplitude horizontal particle velocity	0,458	(m/s)
Amplitude horizontal particle acceleration	0,480	(m/s^2)
Amplitude horizontal particle displacement	0,438	(m)

Oblique waves and oblique current

Angle between waves and outfall	25	(deg)
Angle between current and outfall	70	(deg)
Current velocity	1,0	(m/s)
Amplitude horizontal particle velocity	0,194	(m/s)
Amplitude horizontal particle acceleration	0,203	(m/s^2)
Amplitude horizontal particle displacement	0,185	(m)

KC-number	0,77	(-)
Ratio alpha	4,99	(-)
Ratio a'/D	4,42	(-)
Density sea water	1024	(kg/m^3)
Drag coefficient	1,05	(-)
Inertia coefficient	3,00	(-)
Lift coefficient	1,30	(-)
Submerged weight	3791	(N/m)
Friction factor	0,7	(-)

Minimum safety factor	1,0	(-)
at phase angle	60,0	(deg)
horizontal particle velocity	1,097	(m/s)
horizontal particle acceleration	0,176	(m/s^2)
drag force	970	(N/m)
inertia force	953	(N/m)
lift force	739	(N/m)

APPENDIX III WAVE CLIMATE STUDY

Aveiro case

Data

The study is based on 12344 shipboard observations in the area 38.5-38.9 N, 9.0-9.7 W, over the period 1961-1990. The observations have been sorted and cumulated in order to obtain wave height occurrence tables in combination with wave period and wave direction distributions. The data are processed for the nearshore conditions, taking into account that the dredging site area is sheltered for waves entering from the direction sectors; 15° to 165° N. Because outfall installation is taking place during the summer period, when the wave climate is moderate, only the months July, August and September are taken into account.

Wave period (s)	
< 5	735
6 – 7	460
8 – 9	255
10 – 11	88
12 – 13	36
14 – 15	8

Wave height (m)	
0.00 – 0.25	154
0.25 – 0.75	232
0.75 – 1.25	435
1.25 – 1.75	499
1.75 – 2.25	384
2.25 – 2.75	199
2.75 – 3.25	131
3.25 – 3.75	36
3.75 – 4.25	33
4.25 – 4.75	8
4.75 – 5.25	16
5.25 – 5.75	1
5.75 – 6.25	6
6.25 – 6.75	3

Wave length (m) ; h=10m	
30.6	735
54.2	460
76.3	255
97.5	88
118.3	36
139.0	8
Wave length (m) ; h=15m	
31.5	735
60.4	460
88.7	255
115.6	88
141.7	36
167.3	8

Histograms

Wave period (s)	
lower bound	3.5
upper bound	15.5
class width	2
class midst	frequency
4.5	735
6.5	460
8.5	255
10.5	88
12.5	36
14.5	8

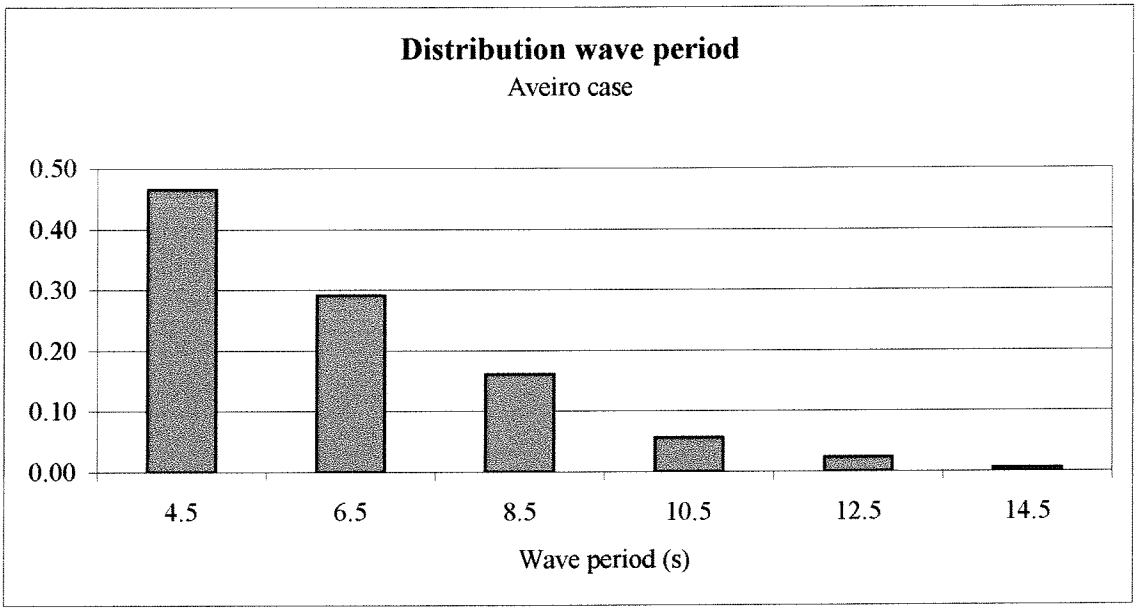

Wave height (m)	
lower bound	0.25
upper bound	6.75
class width	0.5
class midst	frequency
0.125	154
0.50	232
1.00	435
1.50	499
2.00	384
2.50	199
3.00	131
3.50	36
4.00	33
4.50	8
5.00	16
5.50	1
6.00	6
6.50	3

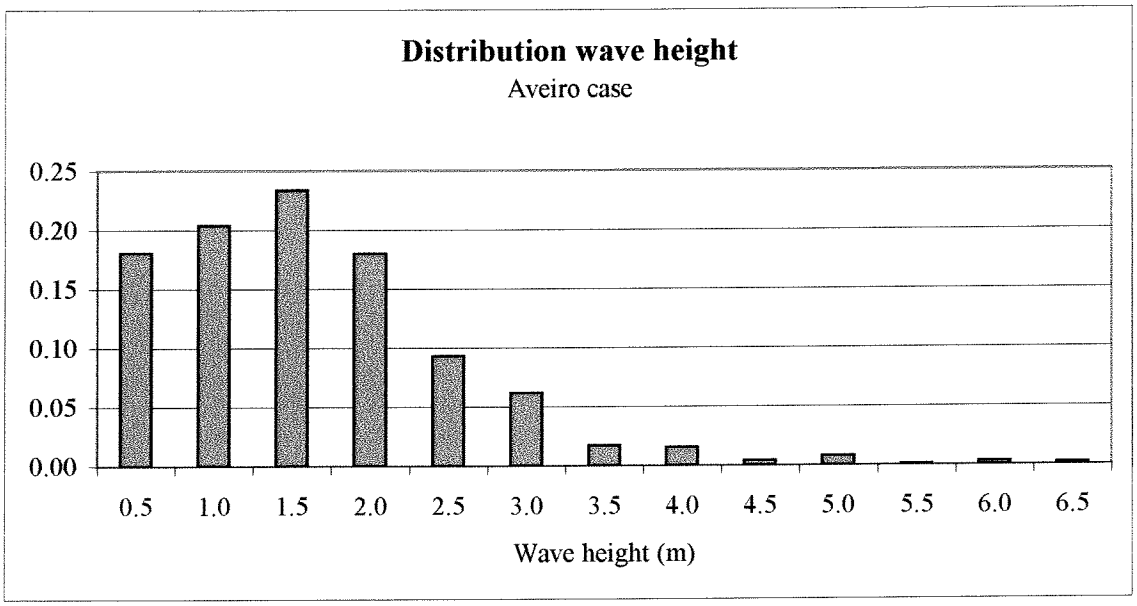

Wave length (m) ; h=10m	
lower bound	19.8
upper bound	149.8
class width	21.7
class midst	frequency
30.6	735
52.3	460
74.0	255
95.6	88
117.3	36
139.0	8

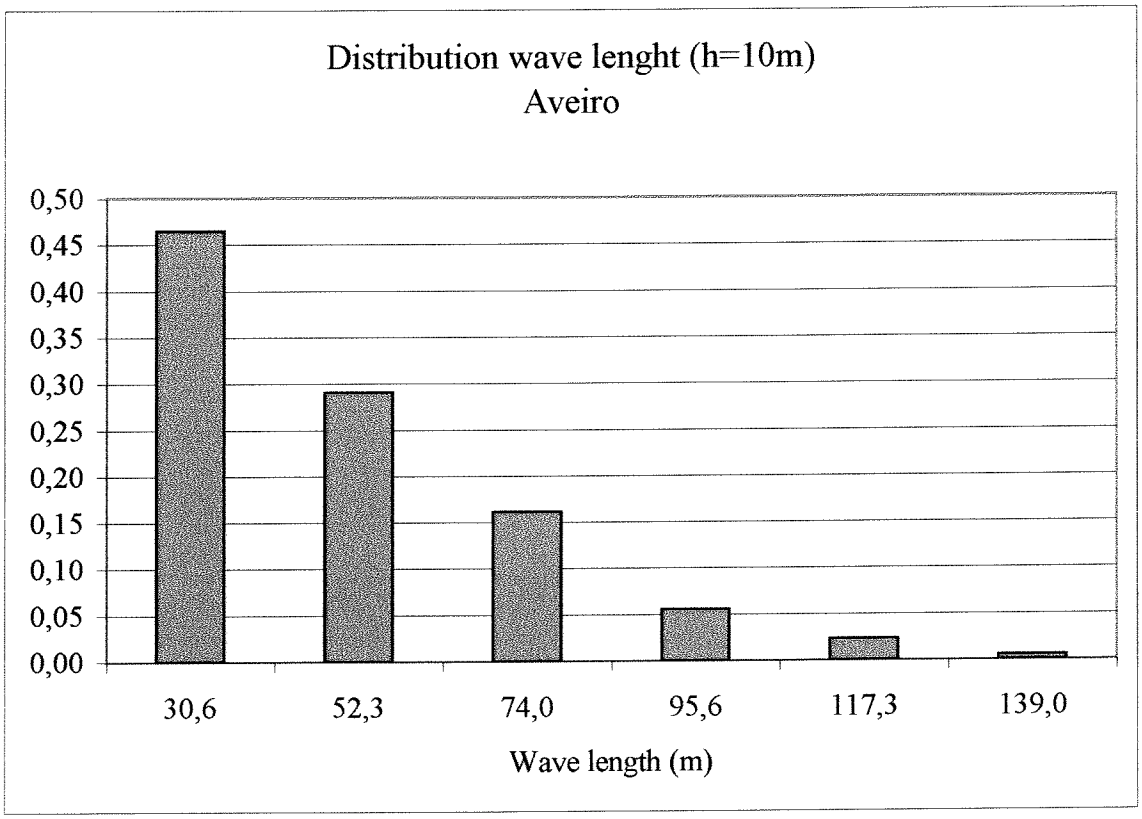

Wave length (m) ; h=15m	
lower bound	17.9
upper bound	180.9
class width	27.2
class midst	frequency
31.5	735
58.7	460
85.8	255
113.0	88
140.1	36
167.3	8

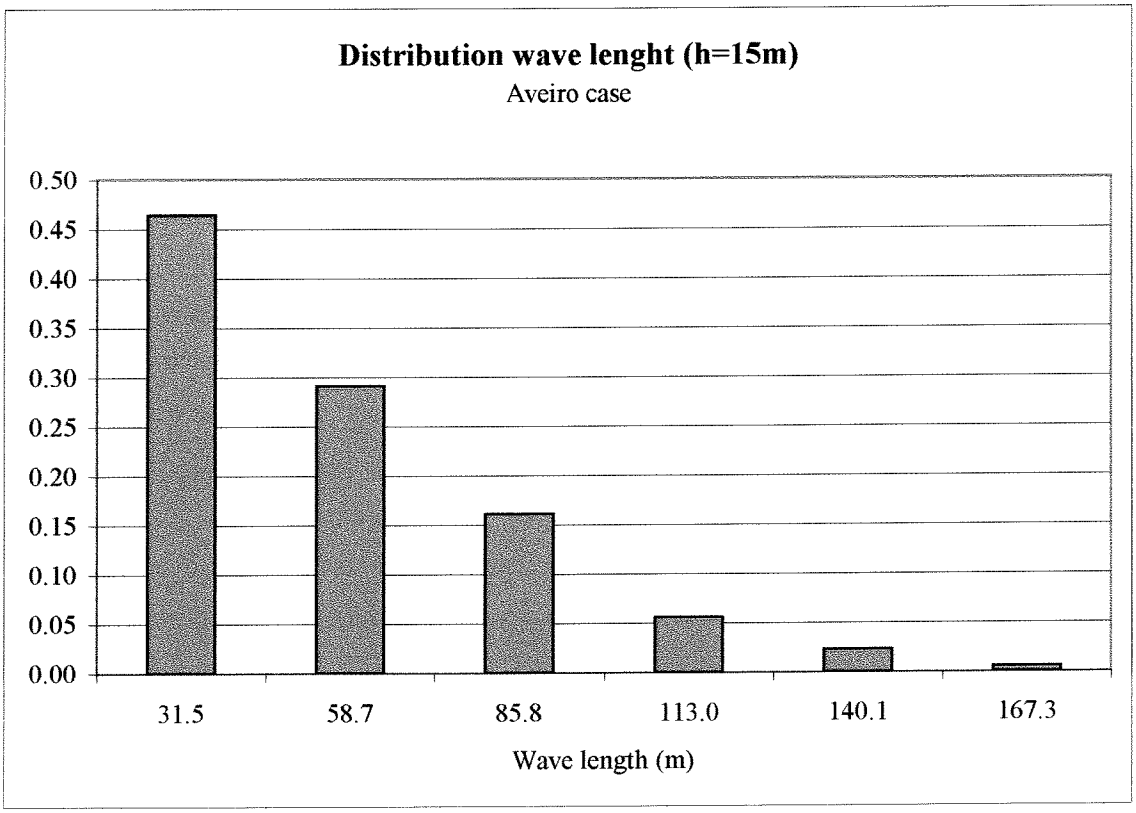

Northumbrian - England case

Data

The study is based on 6455 shipboard observations in the area 54.5-55.5 N, 0.5-1.5 W, over the period 1961-1990. The observations have been sorted and cumulated in order to obtain wave height occurrence tables in combination with wave period and wave direction distributions. The data are processed for the nearshore conditions, taking into account that the dredging site area is sheltered for waves entering from the direction sectors; 165° to 345° N. Because the wave climate data are given annually, only the yearly distributions can be taken into account.

Wave period (s)	
< 5	2344
6 – 7	383
8 – 9	145
10 – 11	50
12 – 13	4
14 – 15	5
16 – 17	1
18 – 19	0
20 – 21	0
> 22	1

Wave height (m)	
0.00 – 0.25	551
0.25 – 0.75	1804
0.75 – 1.25	472
1.25 – 1.75	324
1.75 – 2.25	220
2.25 – 2.75	85
2.75 – 3.25	101
3.25 – 3.75	31
3.75 – 4.25	34
4.25 – 4.75	8
4.75 – 5.25	19
5.25 – 5.75	12
5.75 – 6.25	14
6.25 – 6.75	0
6.75 – 7.25	2
7.25 – 7.75	4
7.75 – 8.25	1
8.25 – 8.75	0
8.75 – 9.25	1
9.25 – 9.75	1

Wave length (m) ; h=10m	
30.6	2344
54.2	383
76.3	145
97.5	50
118.3	4
139.0	5
159.3	1
179.6	0
199.3	0
217.8	1

Wave length (m) ; h=15m	
31.5	2344
60.4	383
88.7	145
115.6	50
141.7	4
167.3	5
192.4	1
217.8	0
242.3	0
267.2	1

Histograms

Wave period (s)	
lower bound	3.5
upper bound	23.5
class width	2
class midst	frequency
4.5	2344
6.5	383
8.5	145
10.5	50
12.5	4
14.5	5
16.5	1
18.5	0
20.5	0
22.5	1

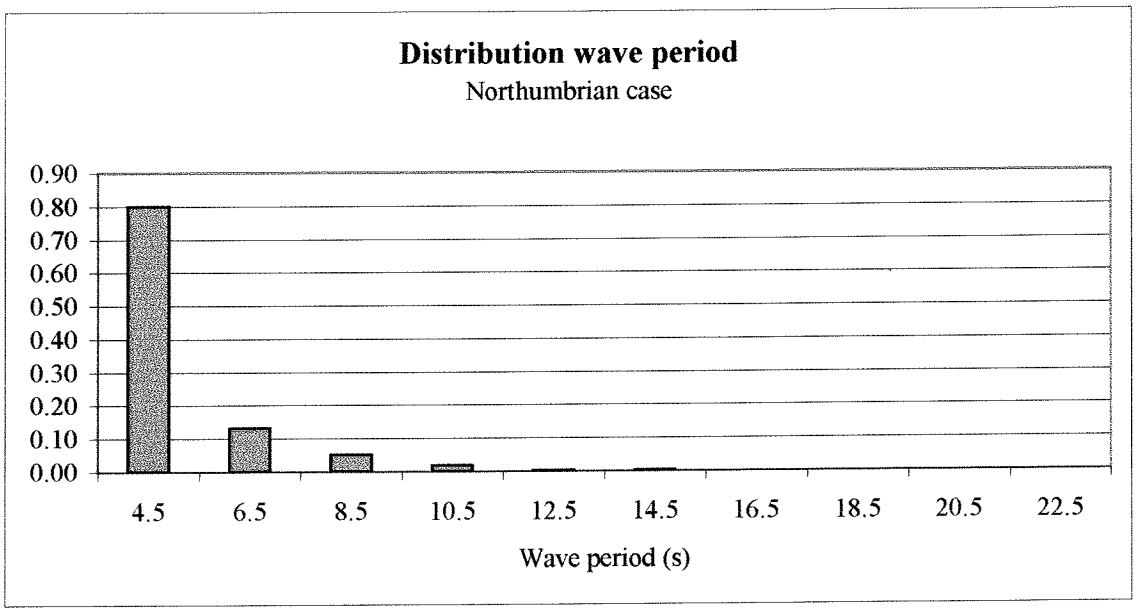

Wave height (m)	
lower bound	0.25
upper bound	9.75
class width	0.5
class midst	frequency
0.125	551
0.50	1804
1.00	472
1.50	324
2.00	220
2.50	85
3.00	101
3.50	31
4.00	34
4.50	8
5.00	19
5.50	12
6.00	14
6.50	0
7.00	2

7.50	4
8.00	1
8.50	0
9.00	1
9.50	1

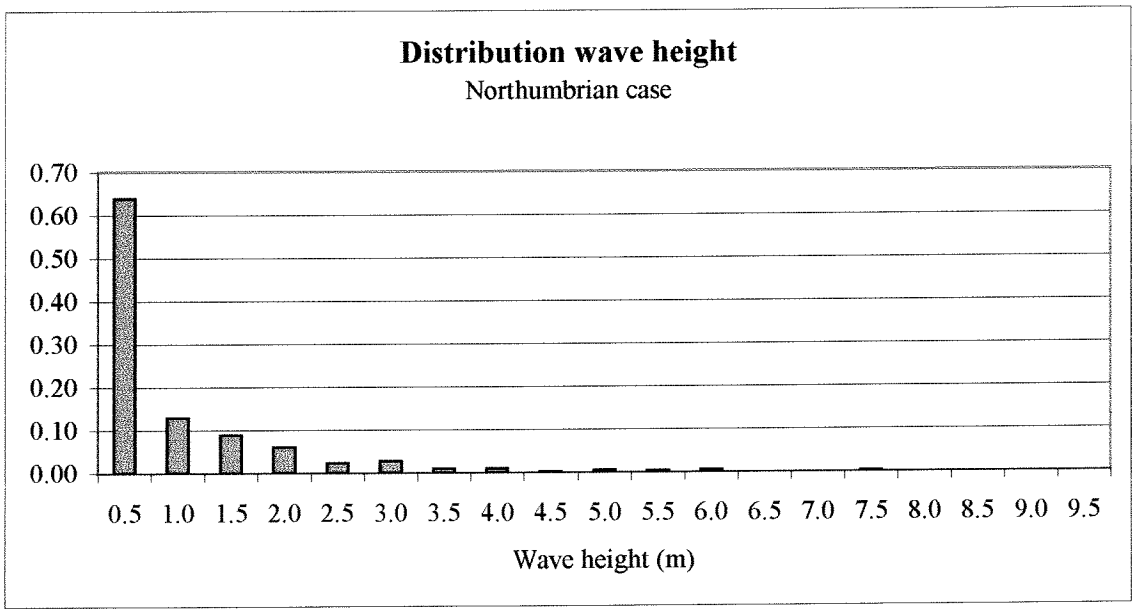

Wave length (m) ; h=10m	
lower bound	20.2
upper bound	228.2
class width	20.8
class midst	frequency
30.6	2344
51.4	383
72.2	145
93.0	50
113.8	4
134.6	5
155.4	1
176.2	0
197.0	0
217.8	1

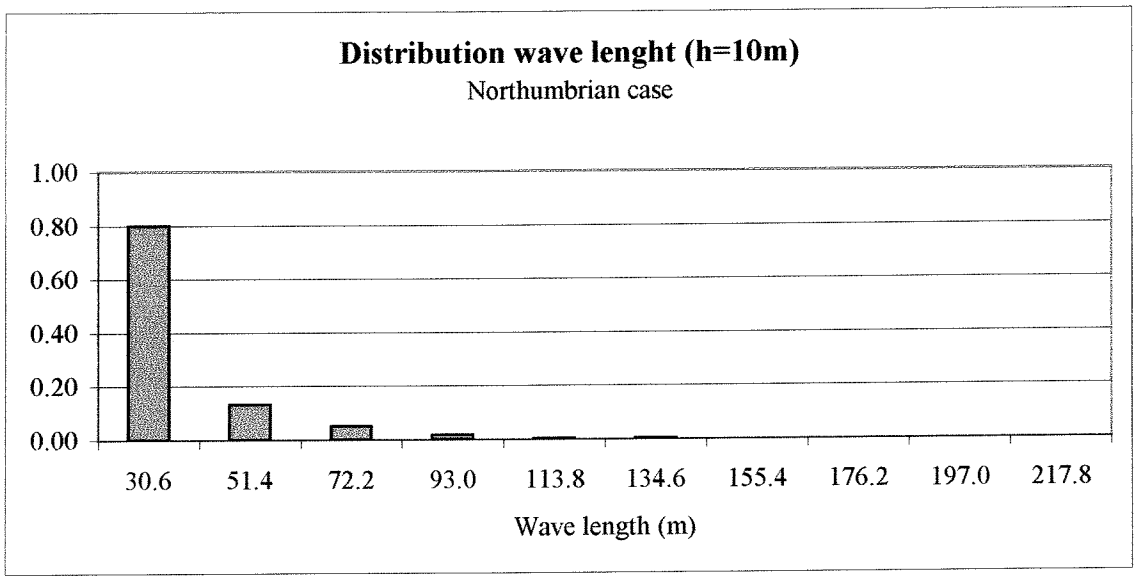

Wave length (m) ; h=15m	
lower bound	18.4
upper bound	280.3
class width	26.2
class midst	frequency
31.5	2344
57.7	383
83.9	145
110.1	50
136.3	4
162.4	5
188.6	1
214.8	0
241.0	0
267.2	1

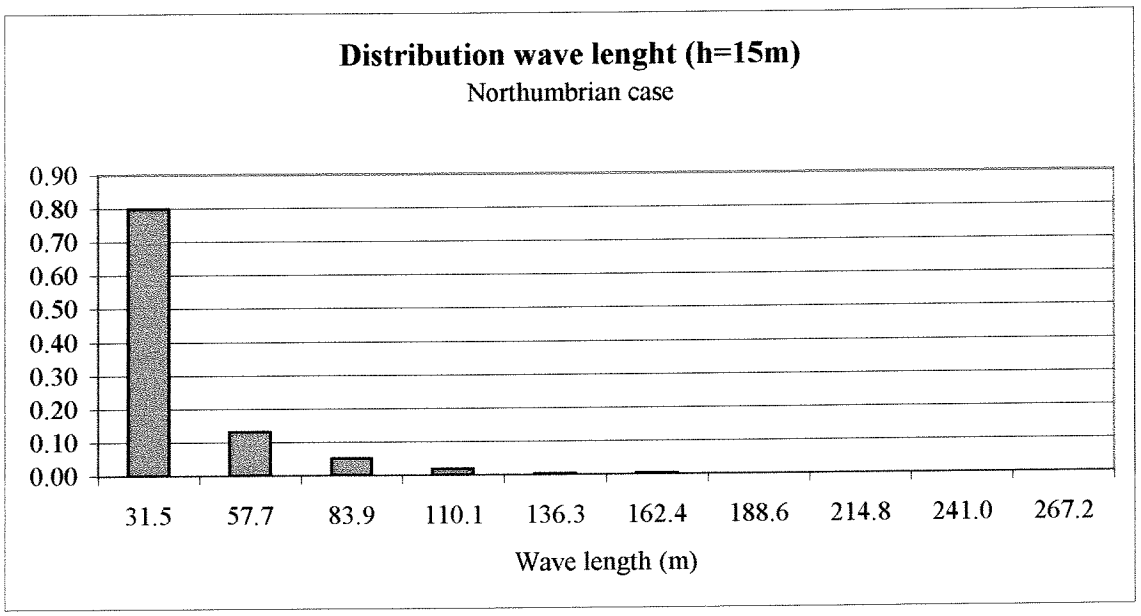

APPENDIX IV BESTFIT RESULTS

Definitions

Mean:

The mean of a set of values is the sum of all the values in the set divided by the total number of values in the set.

Standard deviation and variance:

Measurements of how widely dispersed the values are in a distribution. The variance is calculated as the average of the squared deviations about the mean. The standard deviation is calculated as the square root of the average of the squared deviations about the mean. Both values give disproportionate weight to outliners, which are values far away from the mean. The standard deviations is the square root of the variance.

Skewness:

A measure of the shape of the distribution. Skewness indicates the degree of asymmetry in a distribution. Skewed distributions have more values to one side of the peak or most likely value – one tail is much longer than the other. The higher the skewness value, the more skewed the distribution.

Kurtosis:

A measure of the shape of the distribution. Kurtosis indicates how flat or peaked the distribution is. The higher the kurtosis value, the more peaked the distribution.

Aveiro case

Because BestFit rounds off decimal numbers the wave data are converted to integers. After the curve-fitting, the output is converted to the original unit.

Wave period

Input:

x_{min} = 3.5 (s)	x_{max} = 15.5
x	p
4.5	735
6.5	460
8.5	255
10.5	88
12.5	36
14.5	8

Output:

Lognormal	(6.275, 1.964)
mean	6.293
standard deviation	2.120
variance	4.493
skewness	1.201
kurtosis	4.101

Wave height

Input:

x_{min} = 0 (m)	x_{max} = 6.75
x	p
0.125	154
0.500	232
1.000	435
1.500	499
2.000	384
2.500	199
3.000	131
3.500	36
4.000	33
4.500	8
5.000	16
5.500	1
6.000	6
6.500	3

Output:

Gamma	(2.68, 0.596)
mean	1.597
standard deviation	0.975
variance	0.951
skewness	1.061
kurtosis	5.315

Wave length (h=10m)

Input:

x_{min} = 19.8 (m)	x_{max} = 149.8
x	p
306	735
542	460
763	255
975	88
1183	36
1390	8

Output:

Lognormal	(50.9, 22.9)
mean	51.094
standard deviation	23.707
variance	561.998
skewness	1.088
kurtosis	3.708

Wave length (h=15m)

Input:

x_{min} = 17.9 (m)	x_{max} = 180.9
x	p
31.5	735
60.4	460
88.7	255
115.6	88
141.7	36
167.3	8

Output:

Lognormal	(50.9, 22.9)
mean	56.996
standard deviation	29.719
variance	883.238
skewness	1.115
kurtosis	3.763

Northumbrian case

Because BestFit rounds off decimal numbers the wave data are converted to integers. After the curve-fitting, the output is converted to the original unit.

Wave period

Input:

x_{min} = 3.5 (s)	x_{max} = 23.5
x	p
4.5	2344
6.5	383
8.5	145
10.5	50
12.5	4
14.5	5
16.5	1
18.5	0
20.5	0
22.5	1

Output:

Lognormal	(5.079, 1.095)
mean	5.099
standard deviation	1.409
variance	1.985
skewness	3.249
kurtosis	19.322

Wave height

Input:

x_{min} = 0 (m)	X_{max} = 6.75
x	P
0.125	551
0.500	1804
1.000	472
1.500	324
2.000	220
2.500	85
3.000	101
3.500	31
4.000	34
4.500	8
5.000	19
5.500	12
6.000	14
6.500	0
7.000	2
7.500	4
8.000	1

8.500	0
9.000	1
9.500	1

Output:

Lognormal	(0.950, 1.09)
mean	0.945
standard deviation	0.999
variance	0.999
skewness	2.768
kurtosis	13.625

Wave length (h=10m)

Input:

x_{min} = 20.2 (m)	x_{max} = 228.2
x	p
30.6	2344
54.2	383
76.3	145
97.5	50
118.3	4
139.0	5
159.2	1
179.6	0
199.3	0
217.8	1

Output:

Lognormal	(37.1, 11.7)
mean	37.494
standard deviation	15.902
variance	252.86
skewness	2.993
kurtosis	15.943

Wave length (h=15m)

Input:

x_{min} = 18.4 (m)	x_{max} = 280.3
x	p
31.5	2344
60.4	383
88.7	145
115.6	50
141.7	4
167.3	5
192.4	1
217.8	0
242.3	0
267.2	1

Output:

Lognormal	(39.4, 14.1)
mean	40.052
standard deviation	19.850
variance	394.014
skewness	3.042
kurtosis	16.379

APPENDIX V VaP INPUT

Limit state function

```
G =  (Ws*f)-
     (0.5*rho*Cl*D*((Vc*SIN(co))+
          ((((PI*H)/T)*((COSH((PI*D)/L))/
               (SINH((2*PI*h)/L))))*COS(ph)*SIN(wo)))^2*f)-
     (0.5*rho*Cd*D*((Vc*SIN(co))+((((PI*H)/T)*((COSH((PI*D)/L))/
          (SINH((2*PI*h)/L))))*COS(ph)*SIN(wo)))*ABS((Vc*SIN(co))+
               ((((PI*H)/T)*((COSH((2*PI*0.5*D)/L))/
                    (SINH((2*PI*h)/L))))*COS(ph)*SIN(wo))))-
     (0.25*rho*Cm*PI*D^2*((((2*PI^2*H)/T^2)*((COSH((PI*D)/L))/
          (SINH((2*PI*h)/L))))*SIN(ph)*SIN(wo)))
```

Variables of G:

Cd, Cl, Cm, D, H, L, T, Vc, Ws, Co, f, h, ph, rho, wo

Examples of distribution types

Gamma distribution

Wave height, Aveiro Case

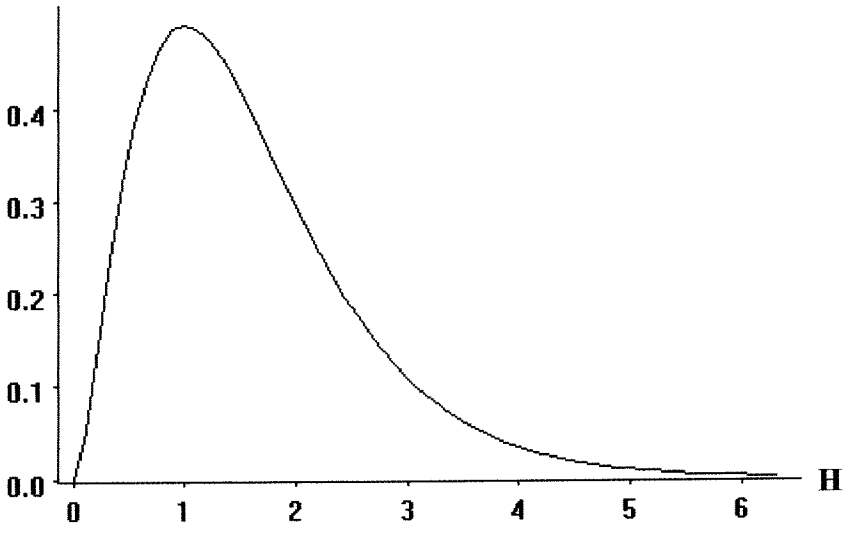

Lognormal distribution

Wave period, Aveiro Case

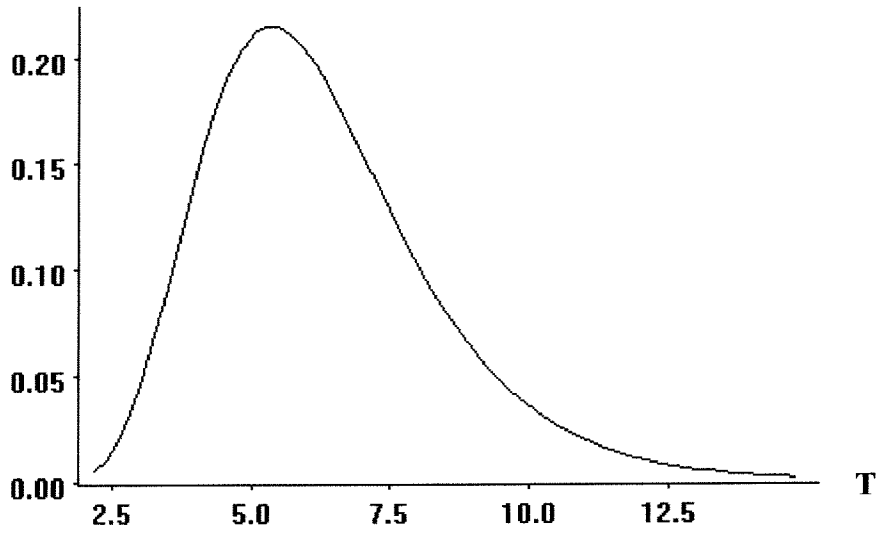

Normal distribution

Angle between current and outfall, Aveiro Case

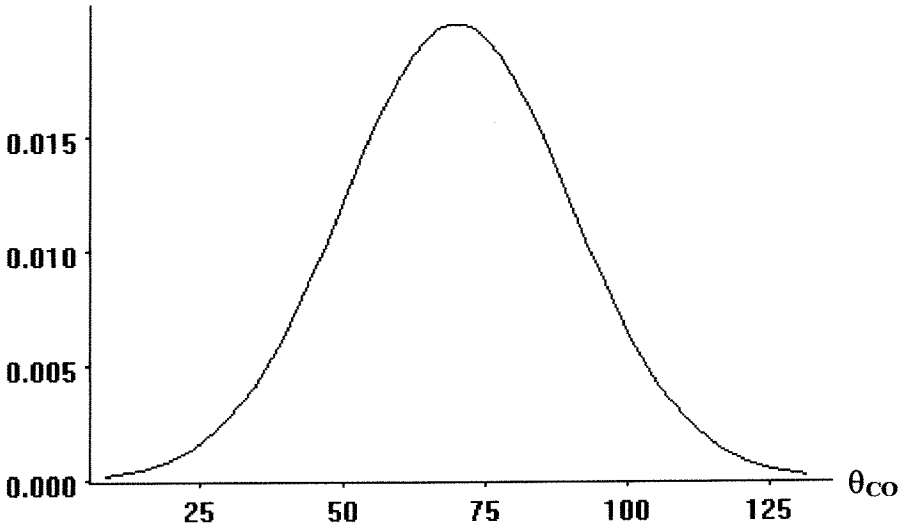

APPENDIX VI VaP OUTPUT

Aveiro Case

Default

G(E[X]) = -0.147407

FORM Analysis of G:
HL - Index = 0.259 P(G<0) = 0.398

Name	Alpha	Design Value
H	0.354	0.703
L	0.478	38.030
T	-0.209	4.843
Vc	0.619	1.053
co	0.463	72.396
wo	0.076	25.099

Option A

G(E[X]) = -0.0747376

FORM Analysis of G:
HL - Index = 0.31 P(G<0) = 0.378

Name	Alpha	Design Value
H	0.578	0.758
L	0.492	36.722
T	-0.341	4.776
Vc	0.430	1.049
co	0.328	72.028
wo	0.124	25.192

Option B

G(E[X]) = 0.3679

FORM Analysis of G:
HL - Index = 0.136 P(G<0) = 0.446

Name	Alpha	Design Value
H	0.313	1.442
L	0.457	52.098
T	-0.254	5.897
Vc	0.433	2.065
co	0.658	71.787
wo	0.091	25.062

Option C

G(E[X]) = -0.051316

FORM Analysis of G:
HL - Index = 0.193 P(G<0) = 0.423

Name	Alpha	Design Value
H	0.238	0.676
L	0.331	36.979
T	-0.130	4.881
Vc	0.719	1.050
co	0.545	72.109
wo	0.051	25.050

Northumbrian Case

Default

G(E[X]) = -0.0813659

FORM Analysis of G:
HL - Index = 0.177 P(G<0) = 0.43

Name	Alpha	Design Value
H	0.439	1.475
L	0.634	53.402
T	-0.406	5.825
Vc	0.370	1.038
co	0.295	71.048
wo	0.129	25.114

Option A

G(E[X]) = -0.0496792

FORM Analysis of G:
HL - Index = 0.151 P(G<0) = 0.44

Name	Alpha	Design Value
H	0.531	1.477
L	0.557	48.101
T	-0.483	5.823
Vc	0.301	1.035
co	0.244	70.736
wo	0.156	25.118

Option B

G(E[X]) = 0.3679

FORM Analysis of G:
HL - Index = 0.136 P(G<0) = 0.446

Name	Alpha	Design Value
H	0.313	1.442
L	0.457	52.098
T	-0.254	5.897
Vc	0.433	2.065
co	0.658	71.787
wo	0.091	25.062

Option C

G(E[X]) = 0.389926

FORM Analysis of G:
HL - Index = 0.171 P(G<0) = 0.432

Name	Alpha	Design Value
H	0.401	1.466
L	0.582	53.060
T	-0.334	5.853
Vc	0.481	1.041
co	0.380	71.296
wo	0.118	25.100

Theoretical Case

Default

G(E[X]) = 0.334854

FORM Analysis of G:

HL - Index = 0.156 P(G<0) = 0.438

Name	Alpha	Design Value
H	0.352	2.371
L	0.694	51.177
T	-0.397	5.733
Vc	0.356	1.037
co	0.286	70.890
wo	0.170	25.132

Option A

G(E[X]) = 0.307635

FORM Analysis of G:

HL - Index = 0.132 P(G<0) = 0.448

Name	Alpha	Design Value
H	0.445	2.374
L	0.615	46.852
T	-0.494	5.728
Vc	0.284	1.034
co	0.231	70.610
wo	0.215	25.141

Option B

G(E[X]) = 0.184364

FORM Analysis of G:

HL - Index = 0.126 P(G<0) = 0.45

Name	Alpha	Design Value
H	0.273	2.352
L	0.544	50.392
T	-0.275	5.771
Vc	0.399	2.064
co	0.614	71.549
wo	0.132	25.083

Option C

G(E[X]) = 0.438776

FORM Analysis of G:

HL - Index = 0.153 P(G<0) = 0.439

Name	Alpha	Design Value
H	0.333	2.367
L	0.660	51.037
T	-0.343	5.746
Vc	0.435	1.038
co	0.347	71.060
wo	0.161	25.123

APPENDIX VII ALGEBRAIC DERIVATION OF THE THREE-DIMENSIONAL STABILITY ANALYSIS

A three-dimensional stability analysis is taking the variation of hydrodynamic forces along the length of an outfall, caused by oblique wave attack into account. The measure of stability of an outfall length equal to a projected wave length can be regarded with the following safety factor Sf (see also paragraph 2.3 of part C):

$$Sf = \frac{W_S}{\frac{F_{\bar{x}}(\bar{z})}{r_c} + F_{\bar{y}}(\bar{z})}$$

where:

$F_{\bar{x}}(\bar{z})$ hydrodynamic force in the horizontal $\bar{x}$ -direction, integrated over a projected wave length in $\bar{z}$-direction

$F_{\bar{y}}(\bar{z})$ hydrodynamic force in the vertical $\bar{y}$ -direction, integrated over a projected wave length in $\bar{z}$-direction

The variation of the hydrodynamic forces along the length of an outfall is completely regarded when the integration of the forces is done over a projected wave length. A more conservative approach is to integrated over a defined part of a projected wave length and determine the matching safety factor. In this case, the centre of the defined part has to be varied on the interval of a projected wave length to find the decisive safety factor.

In the case of an outfall loaded with waves only, the contribution of the drag force in the hydrodynamic force equation is divided three parts (respectively [0,¼L] where the wave-induced horizontal water particle velocity u_w is positive, [¼L ,¾L] where u_w is negative and [¾L ,L] where u_w is positive again). When a current is superimposed on the waves, it is laborious to determine where on the interval [0,L] the vectorially added wave-induced and current velocity is positive or negative. The direction of the velocity has to be known before the hydrodynamic force equation in horizontal plane can be elaborated any further, with a considered defined part [a,b], located on the interval [0,L]. This problem can be disposed of when the wave and current contributions to the drag force are determined separately. The inertia (the presence of a current is has no influence on the acceleration term) and lift (no absolute value in the velocity term) forces can be determined by vectorially adding the wave-induced velocity and the current velocity.

The integrands, the hydrodynamic forces per unit length, in $F_{\bar{x}}(\bar{z})$ and $F_{\bar{y}}(\bar{z})$ are:

$$f_{\bar{x}}(\bar{z}) = \frac{1}{2}\rho C_{D_C} D u_{N_C} \left|u_{N_C}\right| + \frac{1}{2}\rho C_{D_W} D u_{N_W} \left|u_{N_W}\right| + \rho C_M \frac{\pi}{4} D^2 a_N \qquad [N/m]$$

$$f_{\bar{y}}(\bar{z}) = \frac{1}{2}\rho C_L D u_{N_{cw}}^2 \qquad [N/m]$$

where:

$$u_{N_c} = u_c \sin\theta_{co}$$

$$u_{N_w} = u_m \sin\theta_{wo} \cos(\frac{2\pi\bar{z}}{L})$$

$$u_{N_{cw}} = u_c \sin\theta_{co} + u_m \sin\theta_{wo} \cos(\frac{2\pi\bar{z}}{L})$$

$$a_N = a_m \sin\theta_{wo} \sin(\frac{2\pi\bar{z}}{L})$$

The subscript c and w denote respectively current and waves. This distinction is not made for a_N (by definition only waves), C_M and C_L (the combined effect of current and waves is always taken into account. The integrands thus become:

$$f_{\bar{x}}(\bar{z}) = \frac{1}{2}\rho C_{D_c} D \left\{u_c \sin\theta_{co} \cos\left(\frac{2\pi\bar{z}}{L}\right)\right\}^2 + \frac{1}{2}\rho C_{D_w} D \left\{u_m \sin\theta_{wo} \cos\left(\frac{2\pi\bar{z}}{L}\right) \cdot \left|u_m \sin\theta_{wo} \cos\left(\frac{2\pi\bar{z}}{L}\right)\right|\right\} + \rho C_M \frac{\pi}{4} D^2 a_m \sin\theta_{wo} \sin\left(\frac{2\pi\bar{z}}{L}\right)$$

$$f_{\bar{y}}(\bar{z}) = \frac{1}{2}\rho C_L D \left\{u_c \sin\theta_{co} + u_m \sin\theta_{wo} \cos\left(\frac{2\pi\bar{z}}{L}\right)\right\}^2$$

The expression of $f_{\bar{x}}(\bar{z})$ can be written without the absolute value if the following distribution is used:

- if $u_{N_w} > 0$:

$$f_{\bar{x}}(\bar{z}) = \frac{1}{2}\rho C_{D_c} D \left\{u_c \sin\theta_{co} \cos\left(\frac{2\pi\bar{z}}{L}\right)\right\}^2 + \frac{1}{2}\rho C_{D_w} D \left\{u_m \sin\theta_{wo} \cos\left(\frac{2\pi\bar{z}}{L}\right)\right\}^2 + \rho C_M \frac{\pi}{4} D^2 a_m \sin\theta_{wo} \sin\left(\frac{2\pi\bar{z}}{L}\right)$$

- if $u_{N_w} < 0$:

$$f_{\bar{x}}(\bar{z}) = \frac{1}{2}\rho C_{D_c} D \left\{u_c \sin\theta_{co} \cos\left(\frac{2\pi\bar{z}}{L}\right)\right\}^2 - \frac{1}{2}\rho C_{D_w} D \left\{u_m \sin\theta_{wo} \cos\left(\frac{2\pi\bar{z}}{L}\right)\right\}^2 + \rho C_M \frac{\pi}{4} D^2 a_m \sin\theta_{wo} \sin\left(\frac{2\pi\bar{z}}{L}\right)$$

With $\bar{z}_1 = 0$, $\bar{z}_2 = \frac{1}{4}L$, $\bar{z}_3 = \frac{3}{4}L$, and $\bar{z}_4 = L$, the integrals over the considered defined part ($\Delta\bar{z}$) on the interval [0,L] of an outfall are:

$$F_x(\Delta\bar{z}) = \frac{1}{2}\rho C_{D_C} D\left\{\int_{\bar{z}_1}^{\bar{z}_4}\left(u_{N_C}{}^2\right)d\bar{z}\right\}$$
$$+ \frac{1}{2}\rho C_{D_W} D\left\{\int_{\bar{z}_1}^{\bar{z}_2}\left(u_{N_W}{}^2\right)d\bar{z} - \int_{\bar{z}_2}^{\bar{z}_3}\left(u_{N_W}{}^2\right)d\bar{z} + \int_{\bar{z}_3}^{\bar{z}_4}\left(u_{N_W}{}^2\right)d\bar{z}\right\}$$
$$+ \rho C_M \frac{\pi}{4} D^2\left\{\int_{\bar{z}_1}^{\bar{z}_4}\left(a_N\right)d\bar{z}\right\} \qquad [N]$$

$$F_y(\Delta\bar{z}) = \frac{1}{2}\rho C_L D\int_{\bar{z}_1}^{\bar{z}_4}\left(u_{N_{CW}}{}^2\right)d\bar{z} \qquad [N]$$

In general, there is valid:

- $$\int_a^b \left(u_{N_C}{}^2\right)d\bar{z} = \frac{1}{2}u_c{}^2 \sin^2\theta_{co}\left[\frac{4\pi(b-a)}{L} + \left\{\sin\left(\frac{4\pi b}{L}\right) - \sin\left(\frac{4\pi a}{L}\right)\right\}\right]$$
- $$\int_a^b \left(u_{N_W}{}^2\right)d\bar{z} = \frac{1}{2}u_m{}^2 \sin^2\theta_{wo}\left[\frac{4\pi(b-a)}{L} + \left\{\sin\left(\frac{4\pi b}{L}\right) - \sin\left(\frac{4\pi a}{L}\right)\right\}\right]$$
- $$\int_a^b \left(u_{N_{CW}}{}^2\right)d\bar{z} = \int_a^b \left(\left\{u_c \sin\theta_{co} + u_m \sin\theta_{wo}\cos\left(\frac{2\pi\bar{z}}{L}\right)\right\}^2\right)d\bar{z}$$
$$= \int_a^b \left(u_c{}^2 \sin^2\theta_{co} + 2u_c \sin\theta_{co} u_m \sin\theta_{wo}\cos\left(\frac{2\pi\bar{z}}{L}\right) + u_m{}^2 \sin^2\theta_{wo}\cos^2\left(\frac{2\pi\bar{z}}{L}\right)\right)d\bar{z}$$
$$= \int_a^b \left(u_c{}^2 \sin^2\theta_{co} + 2u_c \sin\theta_{co} u_m \sin\theta_{wo}\cos\left(\frac{2\pi\bar{z}}{L}\right) + \frac{1}{2}u_m{}^2 \sin^2\theta_{wo} + \frac{1}{2}u_m{}^2 \sin^2\theta_{wo}\cos\left(2\,\frac{2\pi\bar{z}}{L}\right)\right)d\bar{z}$$
$$= \left[u_c{}^2 \sin^2\theta_{co}\bar{z} + \frac{L}{\pi}u_c \sin\theta_{co} u_m \sin\theta_{wo}\sin\left(\frac{2\pi\bar{z}}{L}\right) + \frac{1}{2}u_m{}^2 \sin^2\theta_{wo}\bar{z} + \frac{L}{8\pi}u_m{}^2 \sin^2\theta_{wo}\sin\left(\frac{4\pi\bar{z}}{L}\right) + c\right]_a^b$$

$$= \left[u_c^2 \sin^2\theta_{co} b + \frac{L}{\pi} u_c \sin\theta_{co} u_m \sin\theta_{wo} \sin\left(\frac{2\pi b}{L}\right) + \frac{1}{2} u_m^2 \sin^2\theta_{wo} b + \frac{L}{8\pi} u_m^2 \sin^2\theta_{wo} \sin\left(\frac{4\pi b}{L}\right) \right]$$

$$- \left[u_c^2 \sin^2\theta_{co} a + \frac{L}{\pi} u_c \sin\theta_{co} u_m \sin\theta_{wo} \sin\left(\frac{2\pi a}{L}\right) + \frac{1}{2} u_m^2 \sin^2\theta_{wo} a + \frac{L}{8\pi} u_m^2 \sin^2\theta_{wo} \sin\left(\frac{4\pi a}{L}\right) \right]$$

$$= u_c^2 \sin^2\theta_{co}(b-a) + \frac{L}{\pi} u_c \sin\theta_{co} u_m \sin\theta_{wo} \left\{ \sin\left(\frac{2\pi b}{L}\right) - \sin\left(\frac{2\pi a}{L}\right) \right\} + \frac{1}{2} u_m^2 \sin^2\theta_{wo}(b-a) + \frac{L}{8\pi} u_m^2 \sin^2\theta_{wo} \left\{ \left(\frac{4\pi b}{L}\right) - \sin\left(\frac{4\pi a}{L}\right) \right\}$$

- $$\int_a^b (a_N)\, d\bar{z} = a_m \sin\theta_{wo} \left[\frac{L}{2\pi} \left\{ \cos\left(\frac{2\pi a}{L}\right) - \cos\left(\frac{2\pi b}{L}\right) \right\} \right]$$

with use of: proposition $f(x) = \cos^2 x = \frac{1}{2} + \frac{1}{2}\cos 2x$

integration constant c taken as 0

If the defined part ($\Delta\bar{z}$) has the begin and end co-ordinates (a,b) on the interval [0,L] of an outfall, the integrated forces in $\bar{x}$ and $\bar{y}$-direction, over the interval [0,L] become:

$$F_{\bar{x}}(\Delta\bar{z}) = \frac{1}{2}\rho C_{D_c} D \left\{ \frac{1}{2} u_c^2 \sin^2\theta_{co} \left[\frac{4\pi(b-a)}{L} + \left(\sin\left\langle \frac{4\pi b}{L} \right\rangle - \sin\left\langle \frac{4\pi a}{L} \right\rangle \right) \right] \right\}$$

$$+ \frac{1}{2}\rho C_{D_w} D \left\{ \int_{\bar{z}_1}^{\bar{z}_2} \left(u_{N_w}^2\right) d\bar{z} - \int_{\bar{z}_2}^{\bar{z}_3} \left(u_{N_w}^2\right) d\bar{z} + \int_{\bar{z}_3}^{\bar{z}_4} \left(u_{N_w}^2\right) d\bar{z} \right\}$$

$$+ \rho C_M \frac{\pi}{4} D^2 \left\{ a_m \sin\theta_{wo} \left[\frac{L}{2\pi} \left(\cos\left\langle \frac{2\pi a}{L} \right\rangle - \cos\left\langle \frac{2\pi b}{L} \right\rangle \right) \right] \right\}$$

$$F_{\bar{y}}(\Delta\bar{z}) = \frac{1}{2}\rho C_L D \left\{ u_c^2 \sin^2\theta_{co}(b-a) + \frac{L}{\pi} u_c \sin\theta_{co} u_m \sin\theta_{wo} \left[\sin\left\langle \frac{2\pi b}{L} \right\rangle - \sin\left\langle \frac{2\pi a}{L} \right\rangle \right] + \frac{1}{2} u_m^2 \sin^2\theta_{wo}(b-a) + \frac{L}{8\pi} u_m^2 \sin^2\theta_{wo} \left[\sin\left\langle \frac{4\pi b}{L} \right\rangle - \sin\left\langle \frac{4\pi a}{L} \right\rangle \right] \right\}$$

The contribution of the waves in the drag force part of the hydrodynamic force equation is divided three parts. Respectively [0,¼L] where u_w is positive, [¼L ,¾L] where u_w is negative and [¾L ,L] where u_w is positive again. Because it is not known beforehand where the considered defined part [a,b] is located on the interval [0,L], it is not possible to elaborate the hydrodynamic force equation in horizontal plane any further.

The safety factor:

$$SF = \frac{W_s}{\frac{F_x(\Delta z)}{r_c} + F_y(\Delta z)}$$

over a defined part (Δz), with co-ordinates (a,b) on the interval [0,L]] of an outfall, can be determined with the previous results. The position and length of the defined part can be varied on the interval [0,L]. The two-dimensional stability analysis can be used to determine the phase angle that gives the combination of the drag, inertia and lift force with the least stability. This phase angle can be taken as the centre of the defined part. Further, with the fixed centre, the length of the defined part can be increased step by step on the interval [0,L].

Because only the interval of the projected wave length is taken into account, it is possible to consider a discontinue defined part. For example, if the safety factor of a projected wave crest interval has to be determined, this implies (due to the cosines shaped definition of the wave profile) an integration over the intervals [0,¼L] and [¾L,L].

APPENDIX VIII PROGRAM LISTING 'OUTFALL STABILITY'

The program 'Outfall stability' is written in the computer language Pascal.

In 'Outfall stability' the following wave climate data and outfall characteristics are required:

- wave height
- wave period
- wave length (estimation)
- angle of wave attack
- current velocity
- angle of current attack
- water depth
- diameter outfall

With the linear Airy wave theory, the following wave characteristics and hydrodynamic quantities are determined:

- wave length
- amplitude of horizontal orbit velocity
  component normal to outfall
- amplitude of horizontal orbit acceleration
  component normal to outfall
- current velocity component normal to outfall
- alpha-value
- KC-number
- a'D-ratio

Further, for the derivation of the hydrodynamic forces on the outfall, and with this also for the calculation of the two-dimensional stability, values have to be assigned to the following variables:

- drag coefficient
- inertia coefficient
- lift coefficient
- submerged weight outfall
- density water
- coulomb friction factor

In a two-dimensional stability analysis, the following is calculated:

- minimum two-dimensional stability factor
  decisive phase angle
- hydrodynamic quantities the phase angle of minimum stability:
  - velocity
  - acceleration
  - drag force
  - inertia force
  - lift force
  - resultant horizontal force
  - resultant vertical force

For the numerical calculation of the three-dimensional stability, the considered length of the outfall, which is equal to the projected wave length, is divided in 360 segments. For each segment the drag, lift and inertia forces and the matching stability factor are determined.

To evaluate the effect of integrating over a defined part of a projected wave length, an extended three-dimensional stability analysis is executed. In this the length and centre of the defined part can be varied.

The listing of 'Outfall stability' is:

```
program outfall (input, output, outfile);
 uses crt;
  const
    pi=3.141593;
    g=9.81;
  var
   {input}
    H,T,L0,Awo,Vc,Aco,hd,D,Ws,rho,rc,Cd,Cm,Cl:real;
    ph_min2D,rlo:real;
    n,m,i, nsc1,nec1,nsc2,nec2:integer;
   {calculation parameters}
    L1,L2,L3,L4,L5,L6,kh0,kh1,kh2,kh3,kh4,kh5,kh6:real;
    Um,Umn,am,amn,Vcn,alpha,KC,aD:real;
    Fdmax,Fmmax,Flmax,Umnph,amnph,Fdph,Fmph,Flph,Fhph,Fvph,SF,SFmin,phmin:real;
    Umnphmin,amnphmin,VcnUmnphmin,Fdphmin,Fmphmin,Flphmin,Fhphmin,Fvphmin:real;
    Lp,z,Ws_Lp,Ws_Lc,dLp,Uncw,ancw,fd,fd_i,fm,fm_i,fl,fl_i,Fd_Lp,Fm_Lp,Fl_Lp:real;
    Fx_Lp,Fy_Lp,SF_Lp:real;
    Lp_min2D,dLp_3D,dLp_3Dh,Lp_3Dsc1,Lp_3Dsc2,absent:real;
    Lp_3Dm,Lp_3Doe,Lp_3Dos,Lp_3Dec1,Lp_3Dec2:real;
    ph:integer;
   {others}
    outfile:text;name:string;c:char;

procedure title;
 begin
   clrscr;textbackground(0);textcolor(2);
   writeln('Graduate project: Stability of outfalls during installation');
   writeln; writeln('Erwin de Jong'); writeln('December 1997');
   gotoxy(15,10);textcolor(4);
   write('STABILITY FACTOR CALCULATION OF AN OUTFALL');
   gotoxy(18,12);textcolor(4);
   write('UNDER OBLIQUE CURRENT AND WAVE ATTACK');
   gotoxy(25,23);textcolor(6);
   write('Press a key to continue');
   c:=readkey;
 end;

procedure input1;
 begin
   clrscr;textbackground(0);textcolor(2);
   writeln('For the derivation of the wave and current charecteristics at the location');
   writeln('of the outfall, values have to be assigned to the following variables:');
   writeln;writeln;
   write('Wave height.....[m]      '); readln(H);
   write('Wave period.....[t]      ');readln(T);
   write('Wave length (estimation)...[m]      ');readln(L0);
   write('Angle of wave attack.....[deg]      ');readln(Awo);
   write('Current velocity.....[m/s]      ');readln(Vc);
   write('Angle of current attack....[deg]      ');readln(Aco);
   write('Water depth.....[m]      ');readln(hd);
```

```
  write('Diameter outfall.....[m]      ');readln(D);
  gotoxy(5,23);textcolor(6);
  write('Press a key to examine the computed wave and current characteristics');
  c:=readkey;
 end;

procedure wavecharacteristics;
 begin
  kh0:=2*pi*hd/L0;
  L1:=(((g*sqr(T))/(2*pi))*((exp(kh0)-exp(-kh0))/(exp(kh0)+exp(-kh0))));
  kh1:=2*pi*hd/L1;
  L2:=(((g*sqr(T))/(2*pi))*((exp(kh1)-exp(-kh1))/(exp(kh1)+exp(-kh1))));
  kh2:=2*pi*hd/L2;
  L3:=(((g*sqr(T))/(2*pi))*((exp(kh2)-exp(-kh2))/(exp(kh2)+exp(-kh2))));
  kh3:=2*pi*hd/L3;
  L4:=(((g*sqr(T))/(2*pi))*((exp(kh3)-exp(-kh3))/(exp(kh3)+exp(-kh3))));
  kh4:=2*pi*hd/L4;
  L5:=(((g*sqr(T))/(2*pi))*((exp(kh4)-exp(-kh4))/(exp(kh4)+exp(-kh4))));
  kh5:=2*pi*hd/L5;
  L6:=(((g*sqr(T))/(2*pi))*((exp(kh5)-exp(-kh5))/(exp(kh5)+exp(-kh5))));
  kh6:=2*pi*hd/L6;
  Um:=(pi*H/T)*(exp(pi*D/L6)+exp(-1*pi*D/L6))/(exp(kh6)-exp(-kh6));
  Umn:=Um*sin(Awo*pi/180);
  am:=(2*sqr(pi)*H/sqr(T))*(exp(pi*D/L6)+exp(-1*pi*D/L6))/(exp(kh6)-exp(-kh6));
  amn:=am*sin(Awo*pi/180);
  Vcn:=Vc*sin(Aco*pi/180);
  alpha:=Vcn/Umn;
  KC:=Umn*T/D;
  aD:=KC*((1/(2*PI))+(alpha/pi)+(sqr(alpha)/(2*pi)));
 end;

procedure output1;
 begin
  clrscr;textbackground(0);textcolor(2);
  writeln('    The computed wave and current characteristics are:');
  writeln('Wave length:                              ',L6:3:2,' [m]');
  writeln('Amplitude of horizontal orbit velocity:          ',Um:3:2,' [m/s]');
  writeln('    component normal to outfall:              ',Umn:3:2,' [m/s]');
  writeln('Amplitude of horizontal orbit acceleration:      ',am:3:2,' [m2/s]');
  writeln('    component normal to outfall:              ',amn:3:2,' [m2/s]');
  writeln('Current velocity:                         ',Vc:3:2,' [m/s]');
  writeln('    component normal to outfall:              ',Vcn:3:2,' [m/s]');
  writeln;writeln;writeln;
  writeln('    The hydrodynamic quantities are:');
  writeln('alpha-value:        ',alpha:3:2,' [-]');
  writeln('KC-number:          ',KC:3:2,' [-]');
  writeln('aD-ratio:           ',aD:3:2,' [-]');
  gotoxy(20,23);textcolor(6);
  write('Press a key to continue');
  c:=readkey;
 end;

procedure input2;
 begin
  clrscr;textbackground(0);textcolor(2);
  writeln('For the derivation of the hydrodynamic forces at the location of the outfall,');
  writeln('and with this the calculation of the two-dimensional stability, values have');
  writeln('to be assigned to the following variables:');
  writeln;writeln;
  write('Drag coefficient.....[-]      ');readln(Cd);
```

```
  write('Inertia coefficient.....[-]       ');readln(Cm);
  write('Lift coefficient.....[-]       ');readln(Cl);
  write('Submerged weight outfall...[N/m]   ');readln(Ws);
  write('Density water.....[kg/m3]   ');readln(rho);
  write('Coulomb friction factor....[-]       ');readln(rc);
  gotoxy(10,23);textcolor(6);
  write('Press a key to exam the two-dimensional stability');
  c:=readkey;
 end;

procedure TwoDstability;
 begin
  Fdmax:=0.5*rho*Cd*D*(Vcn+Umn)*abs(Vcn+Umn);
  Fmmax:=rho*Cm*0.25*pi*sqr(D)*amn;
  Flmax:=0.5*rho*Cl*D*sqr(Vcn+Umn);
  SFmin:=1000000;   {infinitly large}
   for ph:=0 to 360 do
     begin
      Umnph:=Umn*cos(ph*pi/180);
      amnph:=amn*sin(ph*pi/180);
      Fdph:=0.5*rho*Cd*D*(Vcn+Umnph)*abs(Vcn+Umnph);
      Fmph:=rho*Cm*0.25*pi*sqr(D)*amnph;
      Flph:=0.5*rho*Cl*D*sqr(Vcn+Umnph);
      Fhph:=Fdph+Fmph;
      Fvph:=Flph;
      SF:=Ws/((abs(Fhph)/rc)+Flph);
       if SF<SFmin
         then
          begin
           SFmin:=SF;
           phmin:=ph;
          end;
     end;
  Umnphmin:=Umn*cos(phmin*pi/180);
  amnphmin:=amn*sin(phmin*pi/180);
  VcnUmnphmin:=Vcn+Umnphmin;
  Fdphmin:=0.5*rho*Cd*D*(VcnUmnphmin)*abs(VcnUmnphmin);
  Fmphmin:=rho*Cm*0.25*pi*sqr(D)*amnphmin;
  Flphmin:=0.5*rho*Cl*D*sqr(VcnUmnphmin);
  Fhphmin:=Fdphmin+Fmphmin;
  Fvphmin:=Flphmin;
 end;

procedure output2;
 begin
  clrscr;textbackground(0);textcolor(2);
  writeln('The computed hydrodynamic forces are:');
  writeln;
  writeln('  Maximum occuring drag force:    ',Fdmax:5:0,' [N/m]');
  writeln('  Maximum occuring inertia force: ',Fmmax:5:0,' [N/m]');
  writeln('  Maximum occuring lift force:    ',Flmax:5:0,' [N/m]');
  writeln;
  writeln('The minimum two-dimensional stability factor is:  ',SFmin:3:2);
  writeln('This stability factor occurs at a phase angle of:  ',phmin:3:0,' deg');
  writeln;
  writeln('The hydrodynamic forces at the phase angle of minimum stability are:');
  writeln;
  writeln('  Velocity:                ',VcnUmnphmin:5:2,' [m/s]');
  writeln('  Acceleration:              ',Amnphmin:5:2,' [m/s2]');
  writeln;
```

```
  writeln('  Drag force:                ',Fdphmin:5:0,' [N/m]');
  writeln('  Inertia force:             ',Fmphmin:5:0,' [N/m]');
  writeln('  Lift force:                ',Flphmin:5:0,' [N/m]');
  writeln('  Resultant horizontal force:  ',Fhphmin:5:0,' [N/m]');
  writeln('  Resultant vertical force:    ',Fvphmin:5:0,' [N/m]');
  gotoxy(20,23);textcolor(6);
  write('Press any key to continue');
  c:=readkey;
 end;

procedure ThreeDstability;
 begin
  {name:='a:dat3DLp.txt';
  assign(outfile,name);
  rewrite(outfile);}
  clrscr;textbackground(0);textcolor(2);
  writeln('For the numerical calculation of the three-dimensional stability, the');
  writeln('considered length of the outfall, which is equal to the projected wave');
  writeln('length, is divided in 360 segments.');
  Lp:=L6/cos(Awo*pi/180);
  Ws_Lp:=Ws*Lp;
  m:=360;
  dLp:=Lp/m;
  Fd_Lp:=0;
  Fm_Lp:=0;
  Fl_Lp:=0;
   for i:=0 to m do
    begin
     z:=i*dLp;
     Uncw:=(Vc*(sin(Aco*pi/180)))+((Um*sin(Awo*pi/180)*cos(2*pi*z/Lp)));
      begin
       if Uncw>=0 then
        begin
         if (i=0) or (i=m) then
          begin
           fd:=0.5*rho*Cd*D*sqr(Uncw);
           fd_i:=fd*0.5*dLp
          end
         else
          begin
           fd:=0.5*rho*Cd*D*sqr(Uncw);
           fd_i:=fd*dLp
          end
        end
       else
        begin
         if (i=0) or (i=m) then
          begin
           fd:=-0.5*rho*Cd*D*sqr(Uncw);
           fd_i:=fd*0.5*dLp
          end
         else
          begin
           fd:=-0.5*rho*Cd*D*sqr(Uncw);
           fd_i:=fd*dLp
          end
        end
      end;
      begin
       if (i=0) or (i=m) then
```

```
          begin
            fl:=0.5*rho*Cl*D*sqr(Uncw);
            fl_i:=fl*0.5*dLp
          end
        else
          begin
            fl:=0.5*rho*Cl*D*sqr(Uncw);
            fl_i:=fl*dLp
          end
      end;
    ancw:=am*sin(Awo*pi/180)*sin(2*pi*z/Lp);
      begin
        if (i=0) or (i=m) then
          begin
            fm:=rho*Cm*0.25*pi*sqr(D)*ancw;
            fm_i:=fm*0.5*dLp
          end
        else
          begin
            fm:=rho*Cm*0.25*pi*sqr(D)*ancw;
            fm_i:=fm*dLp
          end
      end;
    Fd_Lp:=Fd_Lp+fd_i;
    Fm_Lp:=Fm_Lp+fm_i;
    Fl_Lp:=Fl_Lp+fl_i;
    {writeln(outfile,z:7:2,Uncw:7:2,ancw:7:2,fd:7:2,fm:7:2,fl:7:2);}
  end;
 Fx_Lp:=Fd_Lp+Fm_Lp;
 Fy_Lp:=Fl_Lp;
 SF_Lp:=Ws_Lp/((abs(Fx_Lp)/rc)+Fy_Lp);
 {close(outfile);}
end;

procedure output3;
 begin
  writeln;
  writeln('The projected wave length (Lp) is:    ',Lp:4:2,' [m]');
  writeln('The length of each segment is:        ',dLp:4:2,' [m]');
  writeln;
  writeln('The computed hydrodynamic forces over Lp are:');
  writeln;
  writeln('  Total drag force:    ',Fd_Lp:5:0,' [N]');
  writeln('  Total inertia force: ',Fm_Lp:5:0,' [N]');
  writeln('  Total lift force:    ',Fl_Lp:5:0,' [N]');
  writeln;
  writeln('  Resultant horizontal force:  ',Fx_Lp:5:0,' [N]');
  writeln('  Resultant vertical force:    ',Fy_Lp:5:0,' [N]');
  writeln('  Submerged weight:            ',Ws_Lp:5:0,' [N]');
  writeln;
  writeln('The three-dimensional stability factor is:  ',SF_Lp:3:2);
  gotoxy(20,23);textcolor(6);
  write('Press any key to continue');
  c:=readkey;
 end;

procedure input3;
 begin
   clrscr;textbackground(0);textcolor(2);
   writeln('For the calculation of the extended three-dimensional stability, values have');
```

```
  writeln('to be assigned to the following variables:');
  writeln;
  write('phase angle of minimum two-dimensional stability.....[deg]  ');
  readln(ph_min2D);
  write('considered relative length of outfall (L/Lp).....[-]  ');
  readln(rlo);
 end;

procedure ThreeDstabilityX1;
 begin
  n:=360;
  dLp:=Lp/n;
  Lp_min2D:=((round(ph_min2D))/360)*Lp;
  dLp_3D:=round((rlo*Lp)/dLp)*dLp;
  dLp_3Dh:=round(((rlo/2)*Lp)/dLp)*dLp;
  Lp_3Dm:=Lp_min2D;
  Lp_3Dos:=0;
  Lp_3Doe:=0;
  begin
   if (rlo=1) then
    begin
     Lp_3Dsc1:=0;
     Lp_3Dec1:=Lp;
     Lp_3Dsc2:=0;
     Lp_3Dec2:=0;
    end
   else
    begin
     if (Lp_3Dm-dLp_3Dh) >= 0 then
      begin
       if (Lp_3Dm+dLp_3Dh) <= Lp then
        begin
         Lp_3Dsc1:=Lp_3Dm-dLp_3Dh;
         Lp_3Dec1:=Lp_3Dm+dLp_3Dh;
         Lp_3Dsc2:=absent;
         Lp_3Dec2:=absent;
        end
       else
        begin
         Lp_3Dsc1:=Lp_3Dm-dLp_3Dh;
         Lp_3Dec1:=Lp;
         Lp_3Doe:=Lp_3Dm+dLp_3Dh-Lp;
          begin
           if (Lp_3Doe<(dLp/2)) then
            begin
             Lp_3Dsc2:=0;
             Lp_3Dec2:=0;
            end
           else
            begin
             Lp_3Dsc2:=0;
             Lp_3Dec2:=Lp_3Doe;
            end
           end
         end
       end
      else
       begin
        Lp_3Dsc1:=0;
        Lp_3Dec1:=Lp_3Dm+dLp_3Dh;
```

```
          Lp_3Dos:=dLp_3Dh-Lp_3Dm;
           begin
            if (Lp_3Dos<(dLp/2)) then
             begin
              Lp_3Dsc2:=0;
              Lp_3Dec2:=0;
             end
            else
             begin
              Lp_3Dsc2:=Lp-Lp_3Dos;
              Lp_3Dec2:=Lp;
             end
           end
         end
       end;
     end;
     begin
      nsc1:=round(Lp_3Dsc1/dLp);
      nec1:=round(Lp_3Dec1/dLp);
      begin
       if (Lp_3Dsc2 <> absent) and (Lp_3Dec2 <> absent) then
        begin
         nsc2:=round(Lp_3Dsc2/dLp);
         nec2:=round(Lp_3Dec2/dLp);
        end
       else
        begin
         nsc2:=0;
         nec2:=0;
        end
      end;
     end;
    end;

procedure output4;
 begin
  writeln('The projected wave length is:              ',Lp:4:2,' [m]');
  writeln('The two-dimensional stability is minimum at:  ',Lp_min2D:4:2,' [m]');
  writeln('The three-dimensional stability analysis will be executed with this point');
  writeln('as the center of the considered length.');
  writeln('The considered length is:   ',dLp_3D:4:2,' [m]');
  writeln('first start coordinate:  ',Lp_3Dsc1:4:2,' [m], first begin segment:'  ,nsc1:3);
  writeln('first end coordinate:   ',Lp_3Dec1:4:2,' [m], first end segment:'   ,nec1:3);
  writeln('second start coordinate: ',Lp_3Dsc2:4:2,' [m], second begin segment:' ,nsc2:3);
  writeln('second end coordinate:  ',Lp_3Dec2:4:2,' [m], second end segment:'  ,nec2:3);
  gotoxy(20,23);textcolor(6);
  write('Press any key to continue');
  c:=readkey;
 end;

procedure ThreeDstabilityX2;
 begin
  {name:='a:dat3DdLp.txt';
  assign(outfile,name);
  rewrite(outfile);}
  Fd_Lp:=0;
  Fm_Lp:=0;
  Fl_Lp:=0;
  SF_Lp:=0;
   begin
```

```
for i:=nsc1 to nec1 do
 begin
  z:=i*dLp;
   Uncw:=(Vc*(sin(Aco*pi/180)))+((Um*sin(Awo*pi/180)*cos(2*pi*z/Lp)));
    begin
     if Uncw>=0 then
      begin
       if (i=nsc1) or (i=nec1) then
        begin
         fd:=0.5*rho*Cd*D*sqr(Uncw);
         fd_i:=fd*0.5*dLp
        end
       else
        begin
         fd:=0.5*rho*Cd*D*sqr(Uncw);
         fd_i:=fd*dLp
        end
      end
     else
      begin
       if (i=nsc1) or (i=nec1) then
        begin
         fd:=-0.5*rho*Cd*D*sqr(Uncw);
         fd_i:=fd*0.5*dLp
        end
       else
        begin
         fd:=-0.5*rho*Cd*D*sqr(Uncw);
         fd_i:=fd*dLp
        end
      end
    end;
    begin
     if (i=nsc1) or (i=nec1) then
      begin
       fl:=0.5*rho*Cl*D*sqr(Uncw);
       fl_i:=fl*0.5*dLp
      end
     else
      begin
       fl:=0.5*rho*Cl*D*sqr(Uncw);
       fl_i:=fl*dLp
      end
    end;
   ancw:=am*sin(Awo*pi/180)*sin(2*pi*z/Lp);
    begin
     if (i=nsc1) or (i=nec1) then
      begin
       fm:=rho*Cm*0.25*pi*sqr(D)*ancw;
       fm_i:=fm*0.5*dLp
      end
     else
      begin
       fm:=rho*Cm*0.25*pi*sqr(D)*ancw;
       fm_i:=fm*dLp
      end
    end;
   Fd_Lp:=Fd_Lp+fd_i;
   Fm_Lp:=Fm_Lp+fm_i;
   Fl_Lp:=Fl_Lp+fl_i;
```

```
        {writeln(outfile,z:7:2,Uncw:7:2,ancw:7:2,fd:7:2,fm:7:2,fl:7:2);}
    end;
end;
begin
 if (nsc2<>0) or (nec2 <> 0) then
  begin
   for i:=nsc2 to nec2 do
    begin
     z:=i*dLp;
     Uncw:=(Vc*(sin(Aco*pi/180)))+((Um*sin(Awo*pi/180)*cos(2*pi*z/Lp)));
      begin
       if Uncw>=0 then
        begin
         if (i=nsc2) or (i=nec2) then
          begin
           fd:=0.5*rho*Cd*D*sqr(Uncw);
           fd_i:=fd*0.5*dLp
          end
         else
          begin
           fd:=0.5*rho*Cd*D*sqr(Uncw);
           fd_i:=fd*dLp
          end
        end
       else
        begin
         if (i=nsc1) or (i=nec1) then
          begin
           fd:=-0.5*rho*Cd*D*sqr(Uncw);
           fd_i:=fd*0.5*dLp
          end
         else
          begin
           fd:=-0.5*rho*Cd*D*sqr(Uncw);
           fd_i:=fd*dLp
          end
        end
      end;
      begin
       if (i=nsc1) or (i=nec1) then
        begin
         fl:=0.5*rho*Cl*D*sqr(Uncw);
         fl_i:=fl*0.5*dLp
        end
       else
        begin
         fl:=0.5*rho*Cl*D*sqr(Uncw);
         fl_i:=fl*dLp
        end
      end;
     ancw:=am*sin(Awo*pi/180)*sin(2*pi*z/Lp);
      begin
       if (i=nsc1) or (i=nec1) then
        begin
         fm:=rho*Cm*0.25*pi*sqr(D)*ancw;
         fm_i:=fm*0.5*dLp
        end
       else
        begin
         fm:=rho*Cm*0.25*pi*sqr(D)*ancw;
```

```
                fm_i:=fm*dLp
              end
            end;
          Fd_Lp:=Fd_Lp+fd_i;
          Fm_Lp:=Fm_Lp+fm_i;
          Fl_Lp:=Fl_Lp+fl_i;
          {writeln(outfile,z:7:2,Uncw:7:2,ancw:7:2,fd:7:2,fm:7:2,fl:7:2);}
        end;
      end;
    end;
    begin
    Fx_Lp:=Fd_Lp+Fm_Lp;
    Fy_Lp:=Fl_Lp;
    Ws_Lc:=dLp_3D*Ws;
    SF_Lp:=Ws_Lc/((abs(Fx_Lp)/rc)+Fy_Lp);
    end;
    {close(outfile);}
 end;

procedure output5;
 begin
  clrscr;textbackground(0);textcolor(2);
  writeln;
  writeln('The computed hydrodynamic forces over the considered length are:');
  writeln('  Total drag force:    ',Fd_Lp:5:0,' [N]');
  writeln('  Total inertia force: ',Fm_Lp:5:0,' [N]');
  writeln('  Total lift force:    ',Fl_Lp:5:0,' [N]');
  writeln('  Resultant horizontal force:  ',Fx_Lp:5:0,' [N]');
  writeln('  Resultant vertical force:    ',Fy_Lp:5:0,' [N]');
  writeln('  Submerged weight:            ',Ws_Lp:5:0,' [N]');
  writeln('The three-dimensional stability factor is:  ',SF_Lp:3:2);
  gotoxy(20,23);textcolor(6);
  write('Press any key to continue');
  c:=readkey;
 end;

begin
 title;
 input1;
 wavecharacteristics;
 output1;
 input2;
 TwoDstability;
 output2;
 ThreeDstability;
 output3;
 input3;
 ThreeDstabilityX1;
 output4;
 ThreeDstabilityX2;
 output5;
end.
```

APPENDIX IX NORTHUMBRIAN CASE - STABILITY ANALYSIS

The integration of the hydrodynamic forces per unit length, in the direction of the outfall, can be done over a variable part of a projected wave length, and with variable phase angles as the centre of the defined part. To get insight in the distribution of the safety factor on an outfall with these variations, the execution is written in a Pascal program. The wave climate data of the practice cases in Northumbrian (England), supplied by Van Oord ACZ, is used as input. The wave climate in Northumbrian is moderate.

Oblique wave and current attack

Input:	Wave height	0.945	(m)
	Wave period	5.099	(s)
	Wave length (estimation)	40	(m)
	Angle of wave attack	25	(deg)
	Current velocity	1.028	(m/s)
	Angle of current attack	70	(deg)
	Water depth	15	(m)
	Outfall diameter	1.5	(m)

Wave and current characteristics:	Wave length	39.88	(m)
	Amplitude horizontal particle velocity	0.11	(m/s)
	Normal to outfall	0.05	(m/s)
	Amplitude horizontal particle acceleration	0.14	(m/s2)
	Normal to outfall	0.06	(m/s2)
	Current velocity normal to outfall	0.970	(m/s)
	Alpha-value	20.53	(-)
	KC-number	0.16	(-)
	a'/D-ratio	11.80	(-)

	Cd	1.05	(-)
	Cm	3.00	(-)
	Cl	0.80	(-)
	Submerged weight	2131	(N/m)
	Density water	1024	(kg/m3)
	Coulomb factor	0.7	(-)

Output:	Two-dimensional stability:	Minimum safety factor	1.0	(-)
		at phase angles	70	(deg)
		Horizontal particle velocity	0.98	(m/s)
		Horizontal particle acceleration	0.05	(m/s2)
		drag force	778	(N/m)
		Inertia force	296	(N/m)
		lift force	593	(N/m)

For the Northumbrian – oblique wave and current attack – case, the results of the safety factor distribution and variation in the three-dimensional stability analysis of an outfall are presented in figure IX.1. The integrated length of the outfall L is taken as the relative part of the projected wave length L_P, expressed in the factor L/L_P on the x-axis. The factor L/L_P is the ratio of the projected wave length and the considered integrated defined part of the projected

wave length. The various lines in the graphic represented the different phase angles that are taken as the centre of the defined part. The represented phase angles are shown in the legend at the right of the graphic.

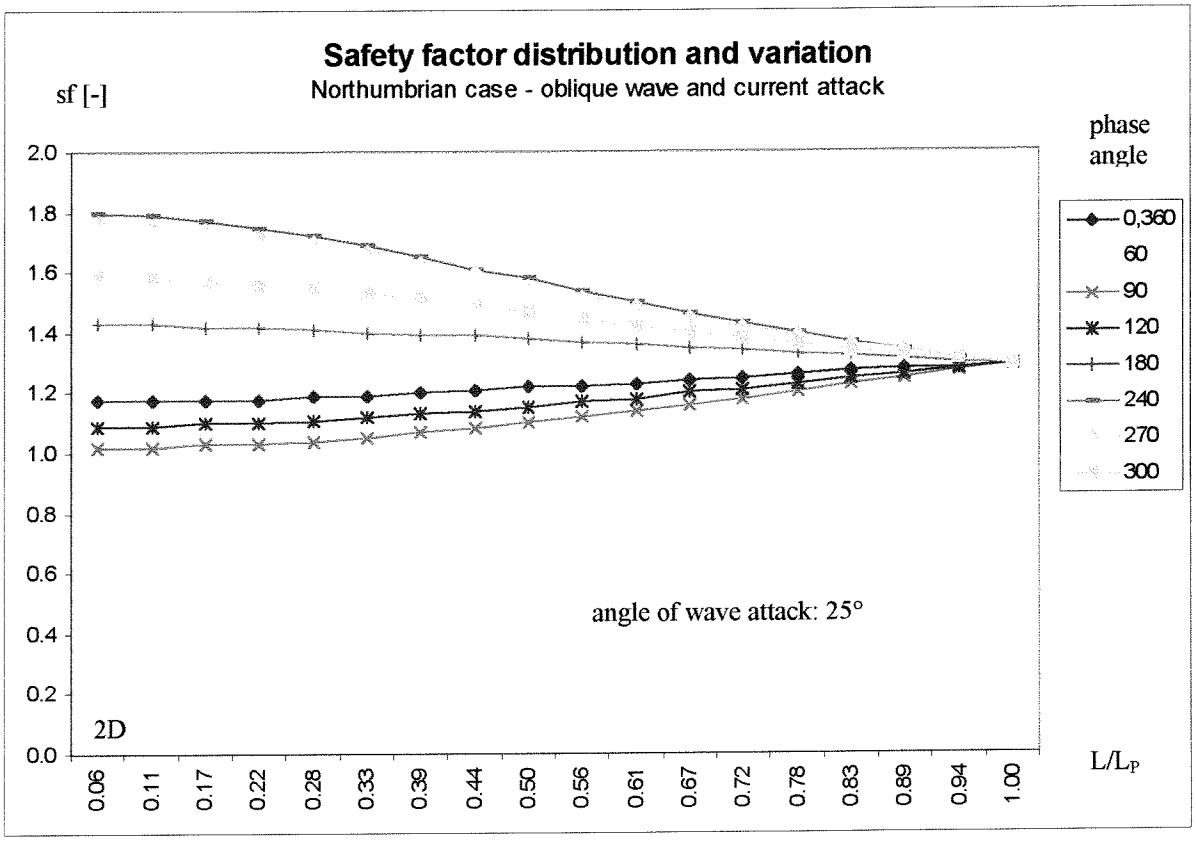

Figure IX.1

From figure IX.1, it can be seen that the minimum safety factor is found with the decisive phase angle of the two-dimensional stability analysis as the centre of the defined part. With a fixed centre of a variable defined part as starting-point, the following results have been derived.

Output:	Three-dimensional stability:	projected wave length	44.00	(m)
		rl	1	(-)
		safety factor	1.29	(-)
		drag force	33152	(N)
		inertia force	0	(N)
		lift force	25259	(N)
		submerged weight	93772	(N)

In figure IX.2, the velocity profile along the outfall, over a projected wave length has been drawn for the Northumbrian – oblique wave and current attack – case.

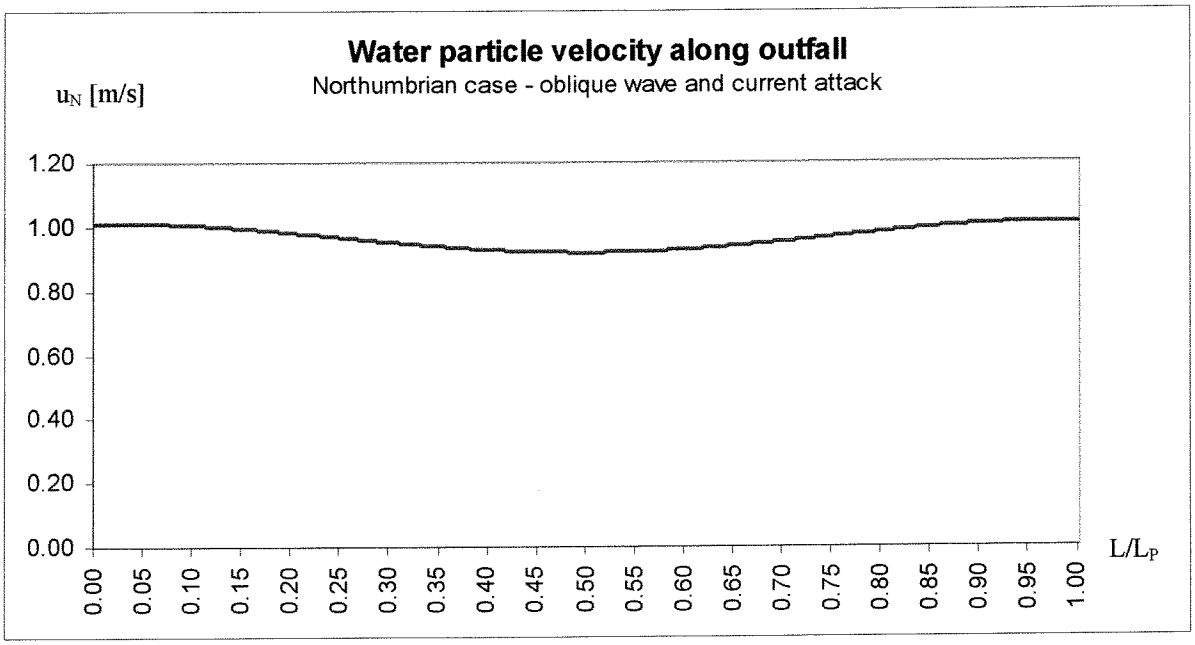

Figure IX.2

In figure IX.3, the acceleration profile along the outfall, over a projected wave length has been drawn for the Northumbrian – oblique wave and current attack – case.

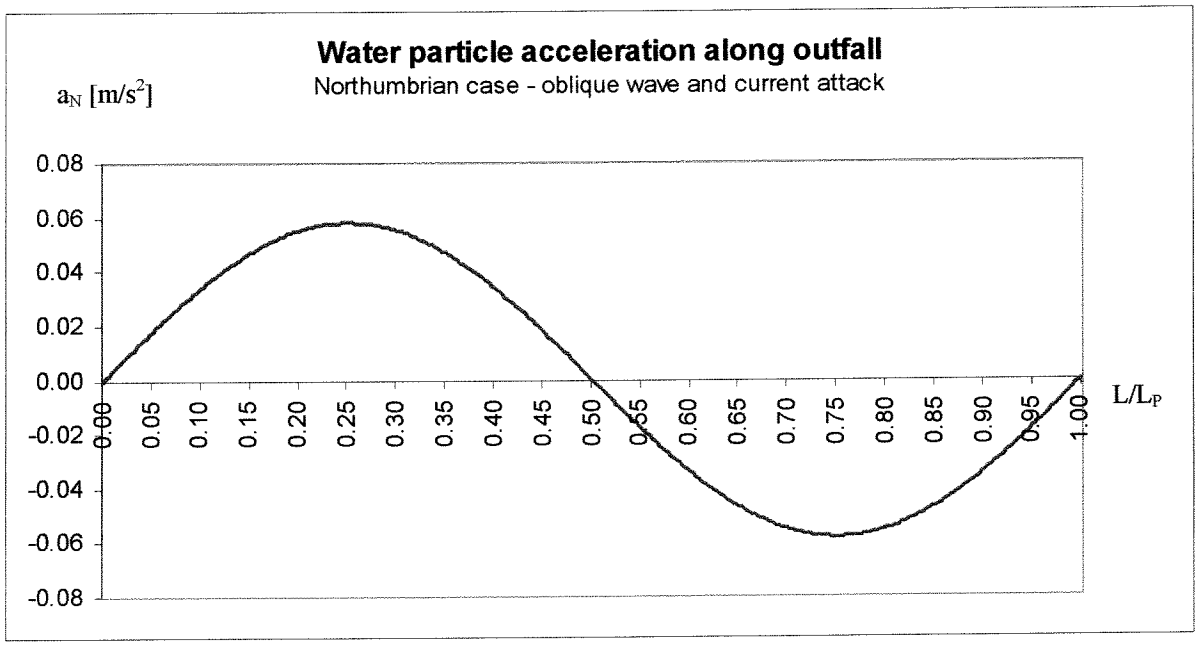

Figure IX.3

In figure IX.4, the hydrodynamic forces along the outfall, over a projected wave length has been drawn for the Northumbrian – oblique wave and current attack – case.

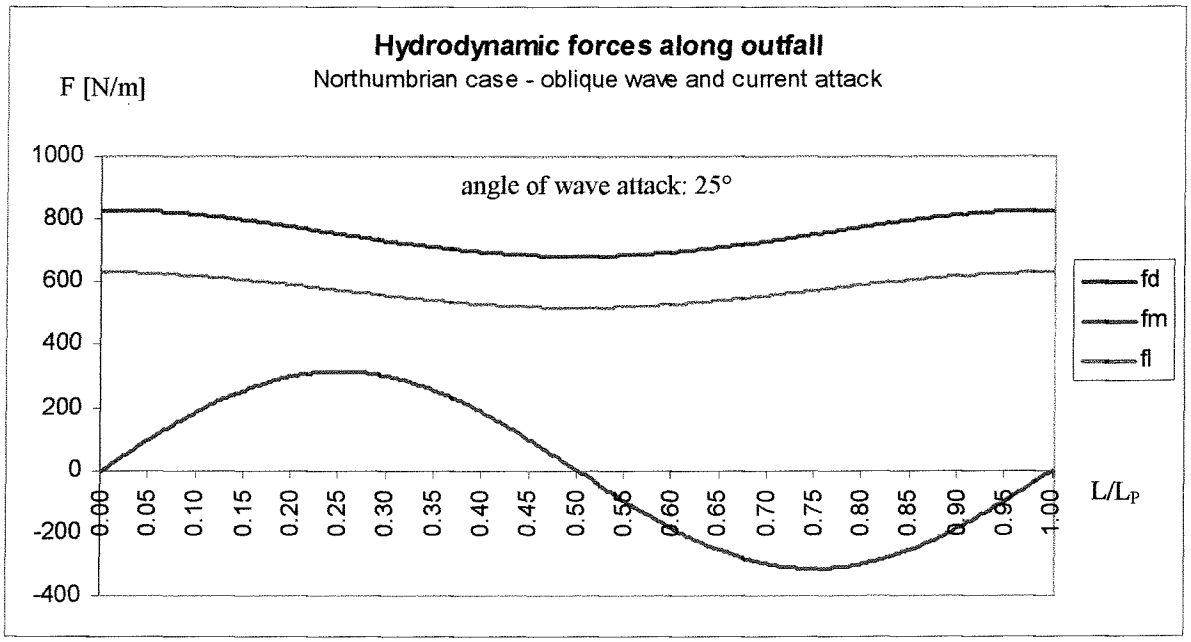

Figure IX.4

In figure IX.5, the course of the safety factor along the outfall, over a projected wave length has been drawn for the Northumbrian – oblique wave and current attack – case.

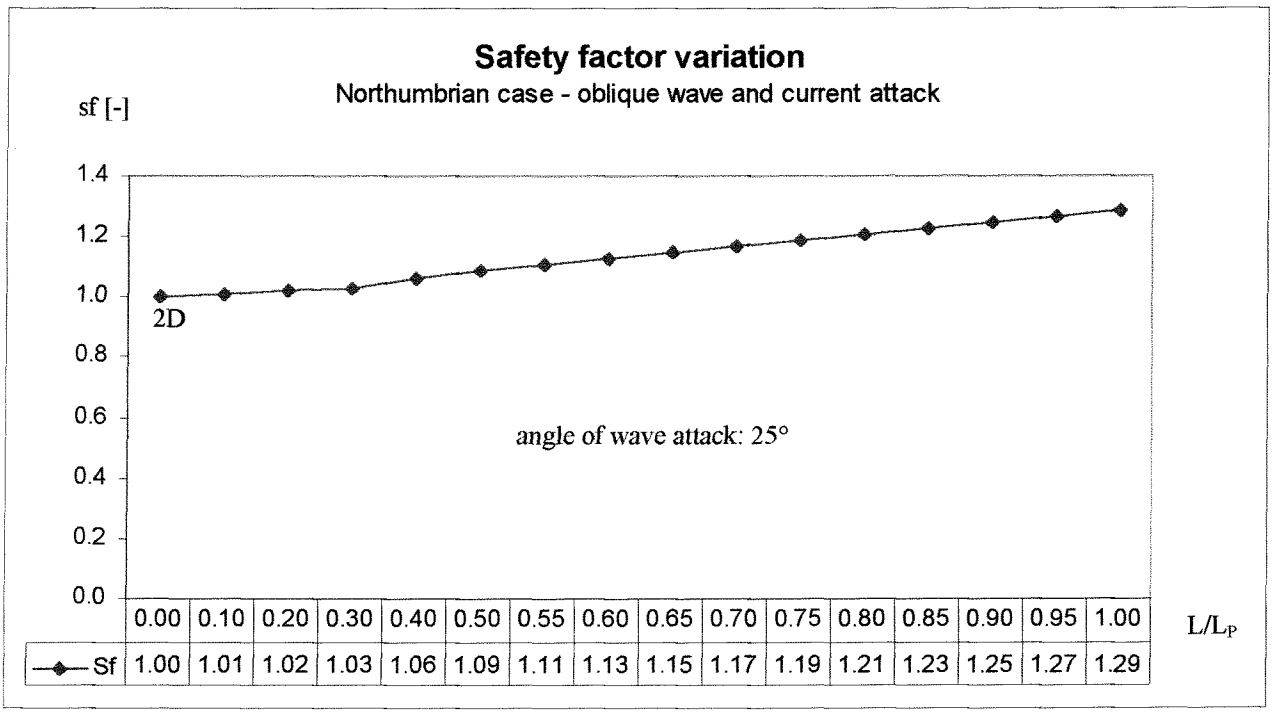

	0.00	0.10	0.20	0.30	0.40	0.50	0.55	0.60	0.65	0.70	0.75	0.80	0.85	0.90	0.95	1.00
Sf	1.00	1.01	1.02	1.03	1.06	1.09	1.11	1.13	1.15	1.17	1.19	1.21	1.23	1.25	1.27	1.29

Figure IX.5

With a decreasing relative length (L/Lp ≅ 0), the three-dimensional stability factor approximates the two-dimensional safety factor.

Oblique wave attack

Input:	Wave height	0.945	(m)
	Wave period	5.099	(s)
	Wave length (estimation)	40	(m)
	Angle of wave attack	25	(deg)
	Water depth	15	(m)
	Outfall diameter	1.5	(m)

Wave characteristics:	Wave length	39.88	(m)
	Amplitude horizontal particle velocity	0.11	(m/s)
	Normal to outfall	0.05	(m/s)
	Amplitude horizontal particle acceleration	0.14	(m/s2)
	Normal to outfall	0.06	(m/s2)
	Alpha-value	0	(-)
	KC-number	0.16	(-)
	a'/D-ratio	0.03	(-)

Input:	Cd	1.05	(-)
	Cm	3.00	(-)
	Cl	2.20	(-)
	Submerged weight	448	(N/m)
	Density water	1024	(kg/m3)
	Coulomb factor	0.7	(-)

Output:	Two-dimensional stability	Minimum safety factor	1.0	(-)
		At phase angles	90	(deg)
		Horizontal particle velocity	0	(m/s)
		Horizontal particle acceleration	0.06	(m/s2)
		Drag force	0	(N/m)
		Inertia force	315	(N/m)
		Lift force	0	(N/m)

For the Northumbrian – oblique wave attack – case, the results of the safety factor distribution and variation in the three-dimensional stability analysis of an outfall are presented in figure IX.6.

From figure IX.6, it can be seen that the minimum safety factor is found with the decisive phase angle of the two-dimensional stability analysis as the centre of the defined part. With a fixed centre of a variable defined part as starting-point, the following results have been derived.

Output:	Three-dimensional stability	Projected wave length	44.00	(m)
		rl	1	(-)
		Safety factor	239.48	(-)
		drag force	0	(N)
		inertia force	0	(N)
		Lift force	82	(N)
		Submerged weight	19714	(N)

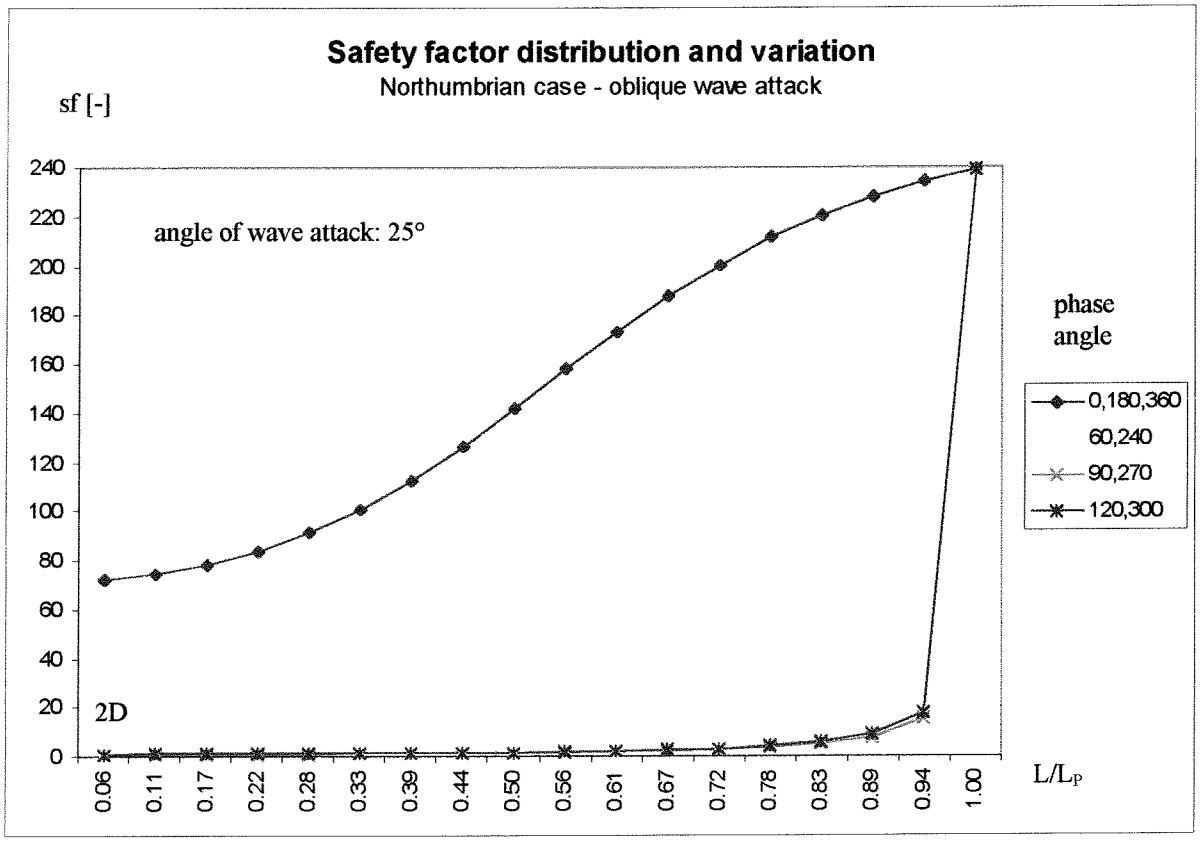

Figure IV.6

In figure IX.7, the velocity profile along the outfall, over a projected wave length has been drawn for the Northumbrian – oblique wave attack – case.

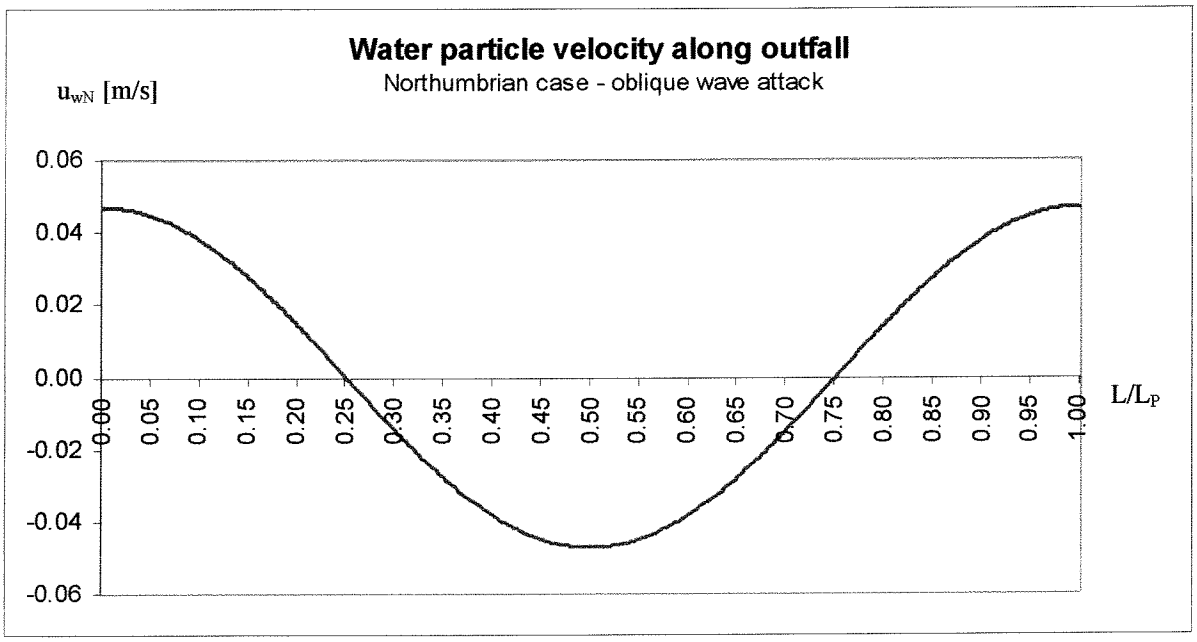

Figure IX.7

The acceleration profile along the outfall, over a projected wave length for the Aveiro – oblique wave attack – case, is the same as drawn in figure IX.3 for the Northumbrian – oblique wave and current attack case.

In figure IX.8, the hydrodynamic forces along the outfall, over a projected wave length has been drawn for the Northumbrian – oblique wave attack – case.

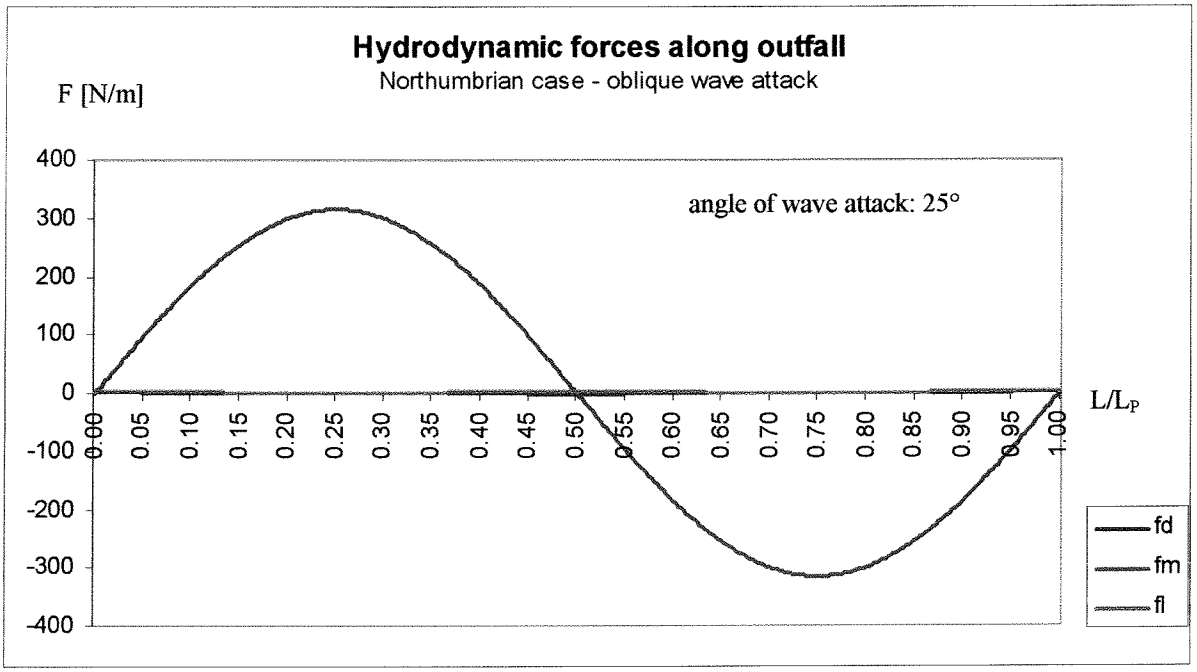

Figure IX.8

In figure IX.9, the course of the safety factor along the outfall, over a projected wave length has been drawn for the Northumbrian – oblique wave attack – case.

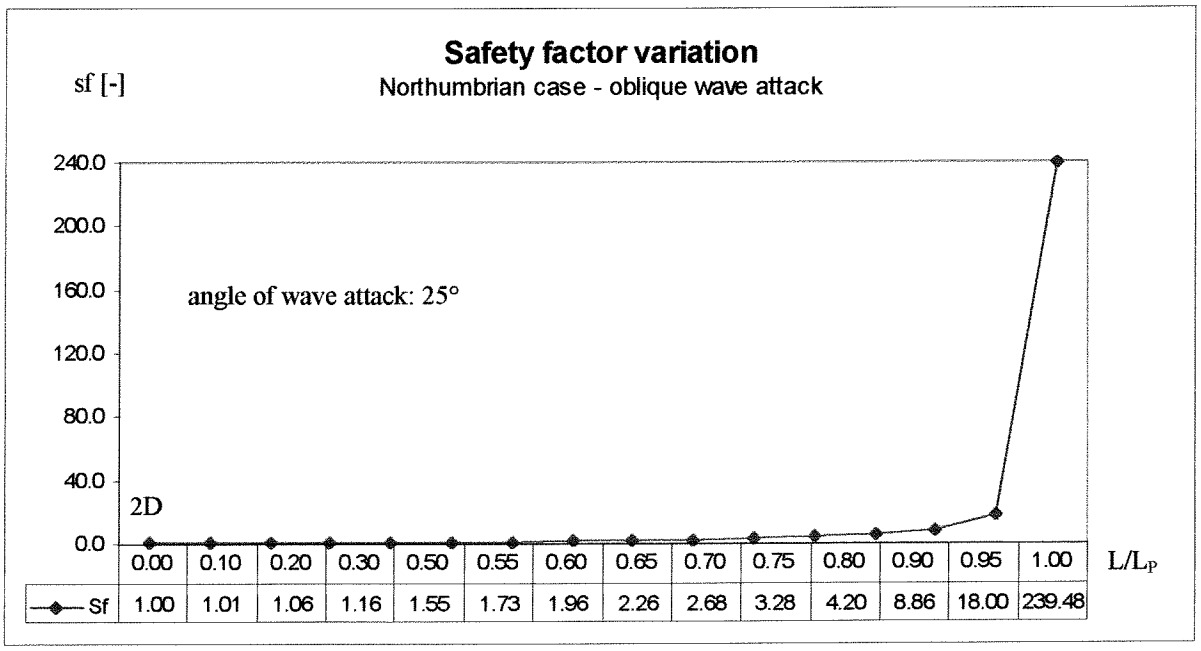

Figure IX.9

With a decreasing relative length (L/Lp ≅ 0), the three-dimensional stability factor approximates the two-dimensional safety factor.